Glucotoxic and Lipotoxic Consequences for Human β Cell Function *In Vivo*

By

Nora Kayton Bryant

Dissertation

Submitted to the Faculty of the

Graduate School of Vanderbilt University

in partial fulfillment of the requirements

for the degree of

DOCTOR OF PHILOSOPHY

in

Molecular Physiology and Biophysics

December, 2015

Nashville, Tennessee

Approved:

Roger Colbran, Ph.D., Chair

Richard O'Brien, Ph.D.

Wenbiao Chen, Ph.D.

William E. Russell, M.D.

Brian E. Wadzinski, Ph.D.

To my grandfather, David Kayton,

an immigrant to this country who knew and espoused the value of education

as the only thing that can be carried anywhere but cannot be taken away.

This understanding has permeated my family, for which I am deeply grateful.

To my parents, Irving and Karyl Kayton,

who encourage me to enjoy the power of my mind

and to look for ways to wield it for the betterment of the world.

To my God,

who makes me a more fearless scientist

and anchors me in my identity as His Beloved.

ACKNOWLEDGEMENTS

An initial and fundamental thank you is due to the designers and administrators of the Interdisciplinary Graduate Program, particularly Roger Chalkley and Michelle Grundy. The IGP year of coursework and rotations exceeded my expectations and provided a firm foundation for my subsequent efforts at Vanderbilt.

The Department of Molecular Physiology and Biophysics has been a wonderful community for me within Vanderbilt. I am proud to graduate from a department with such elevated academic expectations, excellent programming, and great care for the graduate student experience. Thank you to Danny Winder, Chuck Cobb, and Alyssa Hasty for their efforts during their tenures as Director of Graduate Studies for the department. Thank you to the magnificent Angie Pernell, whose logistical and administrative support provided reassurance related to many committee meetings, moments of student account confusion, and generally made the students feel cared for. Thank you also to Karen Gieg, who has ably filled this important role in recent years. A very important thank you is due to Richard O'Brien, for selecting me for a training grant through the Molecular Endocrinology Training Program (5T32 DK07563), which funded my first two years of laboratory work. The work in this dissertation was also supported by the National Institutes of Health, multiple grants from the National Institute of Diabetes and Digestive and Kidney Diseases, the Juvenile Diabetes Research Foundation, and the U.S. Department of Veterans Affairs.

My graduate school experience has been most profoundly and positively influenced by my Ph.D. mentor, Dr. Alvin Powers. The day I elected to join his lab was, in retrospect, the most fortunate of my graduate career. Al epitomizes true mentorship, and I could not be more

grateful. He has consistently espoused that one must “always follow the data,” indicating that he is a true scientist. My writing has improved beyond recognition, as a result of his thoughtful and time-consuming editing of my work. Al, I thank you for taking excellent care of me scientifically and personally, a combination that is rare and inestimably valuable. I have thoroughly enjoyed coming to know you as a scientist, as a physician, and as a person. I consider myself blessed to henceforth always call you my mentor and colleague.

Sometimes, getting ahold of Al in person is a challenge! Thank you to Terri Ray and Laurie Hembree, who always know where Al is and when he will be back. Your tireless efforts to schedule and re-schedule meetings, book room space, and generally answer urgent questions from Al’s lab members has been much appreciated.

The Powers laboratory has been a happy professional home, and each member has contributed, directly or indirectly, to the success of my work. Thank you to former lab members Lara Nyman, Joe Henske, Qing Cai, Ioannis Papagiannis, and Ana Robledo Padgett, for filling my hours in lab with laughter, understanding, and valuable perspective, as well as for providing valuable technical expertise and collaboration. Our current postdoctoral fellows, Neil Phillips, Nathaniel Hart, and Danielle Dean, have provided diverse examples to me of how to do science well. Neil, in particular, I would like to thank for many important coffee breaks, his ready ear, and his loyal friendship. Kristie Aamodt, with whom I sat back-to-back for 4 very eventful years, is a treasure, whose friendship and example I take with me as I leave Vanderbilt. Thank you, Kristie, for your smile, laughter, perspective, and willingness to watch a bunny video anytime things go awry. The lab’s current graduate students, Rachana Haliyur and Daine Saunders, have been delightful additions to our lab group and to my experience. Thank you Diane, for the time and effort that went into the making of countless gluten-free baked goods. Rachana, my neighbor, thank you for making me feel that I have something to offer you as you begin and I end this

process. To whatever extent I have been of use to you, it is an honor. Radhika Aramandla, Alena Shostak, and Courtney Thompson, your excellent work is the foundation for so much of what I have been able to accomplish and envision. Thank you for your incredible work ethic and for so generously sharing your technical knowledge with me. Given the number of human islet transplantations involved in my dissertation work, the technical assistance of Greg Poffenberger, world-class islet transplant surgeon, has been fundamental to my research. In addition, Greg has been a source of limitless general expertise, excellent company, and true friendship.

The majority of the work in this document would not have been possible without the magical benchwork, staunch support, and persistence of Chunhua Dai. I thank her for her commitment to my training, her excellent technical assistance, and her delightful friendship. Her office has unfailingly been a place of refuge, where I gain direction, understanding, and renewed determination.

A special thanks is due to Dr. Rachel Reinert, who has been a role model since my first day in the lab. As a senior graduate student, she trained me in my first techniques, reassured me as I encountered early confusions, and gave a quiet example of intellectual rigor, technical excellence, and professionalism. Rachel, thank you for helping a young graduate student find her feet and aspire to greatness.

The work in this document has depended significantly on the technical assistance of Vanderbilt's core facilities. In particular, Anastasia Coldren and Marcela Brissova of the Islet Procurement & Analysis Core, Susan Hajizadeh of the Hormone Assay & Analytical Services Core, Carlo Malabanan in the Mouse Metabolic Phenotyping Center, and Janice Williams and Mary Dawes of the Cell Imaging Shared Resource have been invaluable in assisting with experimental execution and data collection. In addition, the Division of Animal Care has been fundamental to the success and quality of our in vivo studies, providing excellent care for our animals and

collaborating on appropriate ways to implement proposed protocols, particularly in Vanderbilt's Barrier Facility.

I am grateful to have had the opportunity to collaborate with very accomplished scientists during the course of my graduate work. Thank you to Dale Greiner (University of Massachusetts Medical School), Lenny Shultz (The Jackson Laboratory), Pedro Herrera (The University of Geneva), Roland Stein (VUMC), William Russell (VUMC), and Larry Scheving (VUMC). I have learned much from observing how you think, write, mentor, and generally conduct your research programs. Thank you for your time, effort, and for treating a graduate student like a burgeoning colleague. A special thank you is due to Will Bush, whose statistical and bioinformatics expertise made it possible to sophisticatedly and comprehensively perform our analyses of human islet perifusion data. Will, thank you for teaching me as thoroughly and generously as I could have hoped for. It was a pleasure to become a colleague after having been your friend for multiple years. Barbara Olack, of the Integrated Islet Distribution Program, was also instrumental in this project by providing critical insight into history of human islet distribution in this country and much appreciated feedback on our analyses and on our manuscript.

A large portion of my scientific development has resulted from interaction with my dissertation committee members, who have been exemplary in every way. Thank you to my excellent dissertation committee chair, Roger Colbran. Your thoughtful and fair nature has enabled me to successfully navigate moments of difficulty. I appreciate that your office has always been open to me and that I always leave it with greater clarity and purpose. Thank you no less to my other committee members, Richard O'Brien, Wenbiao Chen, Bill Russell, and Brian Wadzinski. Your scientific rigor, high expectations, and dedication to my success have impressed me at every stage and inspired me to improve and progress.

I do not know how I would have successfully navigated or completed graduate school without the steadfast friendship and inspiration of fellow student, and now Ph.D.-holder, Elizabeth Conrad. Her resilience, competence, kindness, and incredibly hard work have been examples to me in moments of frustration and uncertainty. Her love, care, and support have sustained me through the direst of challenges, both scientific and personal.

It is difficult to overstate the degree of comfort, reassurance, and understanding that I have received from my brilliant, kind, and thoughtful husband, Nathan Bryant. His familiarity with the rigors and stressors of academic research in general, and of the pursuit of a Ph.D., specifically, has enabled many moments of graciousness on his part. Thank you, Nathan, for being a guide and a cheerleader during this demanding process.

To my parents, I express my astonished appreciation for the care and fortitude you brought to my graduate school experience. Your confidence in my ability, commiseration with my experiences, and joy in my successes were the underpinnings of my years at Vanderbilt. Thank you for every moment spent on the phone and every other moment of prayer and care. Your opinion has always and will always mean the most, for good reason, and to my great benefit.

TABLE OF CONTENTS

LIST OF TABLES

Page

LIST OF FIGURES

Page

LIST OF ABBREVIATIONS

ADAM	a disintegrin and metalloproteinase
Akt	protein kinase B
ANOVA	analysis of variance
AUC	area under the curve
BMI	body mass index
BSA	bovine serum albumin
cAMP	cyclic adenosine monophosphate
Cav-1	caveolin-1
CDK	cyclin-dependent kinase
Cre	Cre recombinase
DAPi	4’6-diamidino-2-phenylindole
DM	diabetes mellitus
DMEM	Dulbecco’s modified Eagle’s medium
DT	diphtheria toxin
DTR	diphtheria toxin receptor

E	embryonic day
EPC	endocrine progenitor cell
FBS	fetal bovine serum
fl	flox, flanked by loxP sites
Gcg	glucagon
GTT	glucose tolerance test
HBSS	Hanks balanced salt solution
HFD	high fat diet
IBMX	3-isobutyl-1-methylxanthine
Ins	insulin
IP	intraperitoneal
MAPK	mitogen-activated protein kinase
NGN3	neurogenin3
NOD	non-obese diabetic mouse model
NKX6.1	NK6 homeobox 1
NSG	NOD-SCID-gamma
ob	*obese* gene mutation (leptin deficiency)

PCR	polymerase chain reaction
Pdx1	pancreatic and duodenal homeobox 1
PECAM1	platelet endothelial cell adhesion molecule 1
PP	pancreatic polypeptide
PI3K	phosphoinositide 3-kinase
Ptf1a	pancreas-specific transcription factor 1a
RIA	radioimmunoassay
RIP	rat insulin promoter
rpm	rotations per minute
RPMI	Roswell Park Memorial Institute (medium)
SCID	severe combined immunodeficiency
STZ	streptozotocin
VAChT	vesicular acetylcholine transporter

CHAPTER I

BACKGROUND AND SIGNIFICANCE

The Pancreas

Tissue compartments

The pancreas, located against the curve of the duodenum (Figure 1A) and posterior to the stomach, is an organ composed of two anatomically and functionally distinct compartments: the exocrine pancreas, which is responsible for production of digestive enzymes, and the endocrine pancreas, which produces multiple hormones that collaborate to regulate glucose metabolism and homeostasis. The exocrine pancreas is central to proper gastrointestinal function, digesting almost all categories of macromolecules to forms that are absorbable across the intestinal wall. The enzymes trypsin, chymotrypsin, pancreatic lipase, and amylase are produced in the pancreatic acinar cells and are transported to the gut via an extensive network of pancreatic ducts (Figure 1B). The endocrine pancreas makes up only 1-2% of total pancreatic mass and is organized into mini-organs

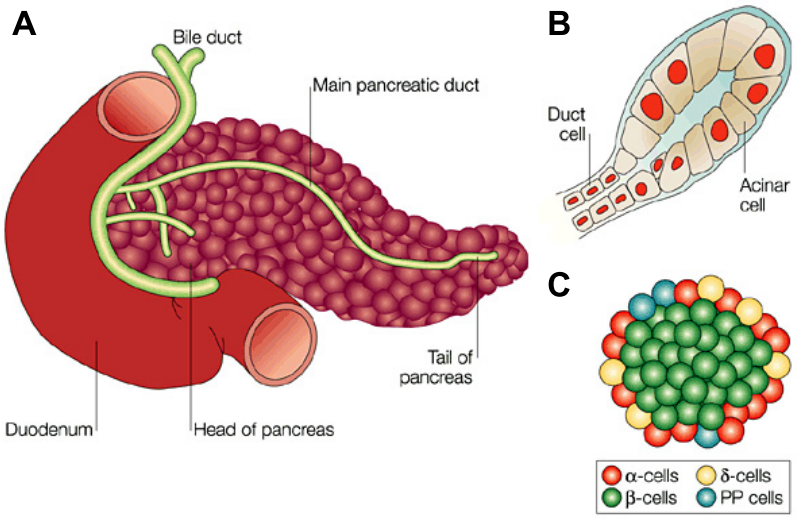

Figure 1. Pancreas anatomy and tissue compartments. A. The pancreas sits against the duodenum and is connected to the bile duct by the main pancreatic duct, which runs the length of the organ. B. Digestive enzymes are secreted into the ducts by the exocrine acinar cells. C. Five types of endocrine cells are arranged into the islets of Langerhans, each of which secretes a distinct hormone into the bloodstream (not pictured are ghrelin-producing ε-cells). Images from Edlund et al. (2002).

called the islets of Langerhans. The islets are clusters of approximately 100-1000 hormone-producing cells, and these clusters are spatially distributed throughout the exocrine pancreas. Islets are composed of five endocrine cell types, each of which produces a distinct hormone. They are the α cell (glucagon), β cell (insulin), δ cell (somatostatin), PP cells (pancreatic polypeptide), and ε cell (ghrelin) (Figure 1C). In proper coordination, the regulated secretion of these hormones into the blood stream responds to and manages changes in blood glucose in an exquisitely precise manner.[1]

Islet vascularization and innervation

Control of glucose metabolism by the endocrine pancreas is dependent on extensive vascularization, which not only allows the endocrine cells to accurately sense the prevailing blood glucose level, but also allows delivery of secreted hormones from the islet into the blood stream. For this reason, islets are highly vascularized, receiving 10-20% of pancreatic blood flow, about 10-fold higher than the exocrine tissue.[2] In addition, islet-associated vessels are denser and thicker than those in the surrounding tissue (Figure 2). The endothelial cells of islet vasculature are critical for proper pancreatic and islet development, both morphologically and transcriptionally, which is orchestrated by a delicate cooperation between islet cell and endothelial cell secreted factors.[3]

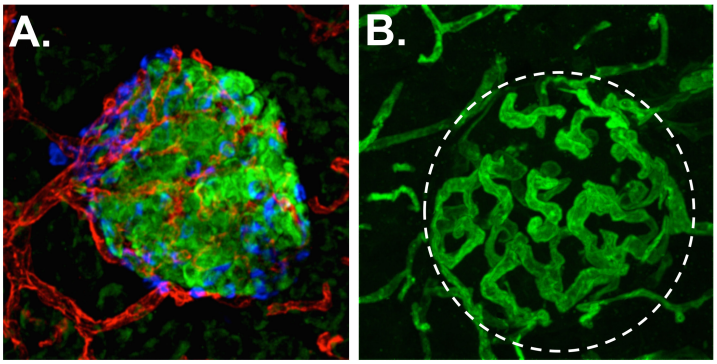

Figure 2. Islets are extensively vascularized. A. Mouse pancreatic islet immunolabeled for endothelial cell marker CD31 (red), insulin (green), and glucagon (blue), showing vessels around and penetrating the islet. B. Mouse islet with vasculature labeled by infused tomato lectin, conjugated to FITC fluorophore, showing dense and tortuous islet capillaries within the islet (defined by white dashed line). Images courtesy of Marcela Brissova, Vanderbilt University.

Closely associated with the islet vessels are parasympathetic,

sympathetic, and sensory nerve fibers. Similar to the islet vasculature, nerve fibers and neurons are specifically denser around and in the islets. Acetylcholine-releasing parasympathetic fibers originate from the vagus and penetrate the pancreas along the vessels, and the nerves ultimately project directly upon individual endocrine cells (Figure 3A). Acetylcholine has a general stimulatory effect on hormone secretion from all islet endocrine cell types, as a result of signaling through endocrine cell muscarinic receptors. Norepinephrine-expressing sympathetic nerve fibers originate in the hypothalamus and similarly enter the pancreas in tight spatial association with vessels (Figure 3B). Norepinephrine can either suppress glucose-stimulated insulin secretion by hyperpolarizing β cells downstream of α-adrenoreceptors or stimulate secretion through β adrenoreceptor-mediated cAMP generation. Thus, norepinephrine's net effect may depend on the relative abundance of receptor types.[4] Glucagon secretion is stimulated by sympathetic nerve activity, but somatotstatin is suppressed. The presence of peri-islet sensory nerve fibers has been well established, and although their role in islet physiology is not well understood, there is evidence that they could also impact hormone secretion.[4-7]

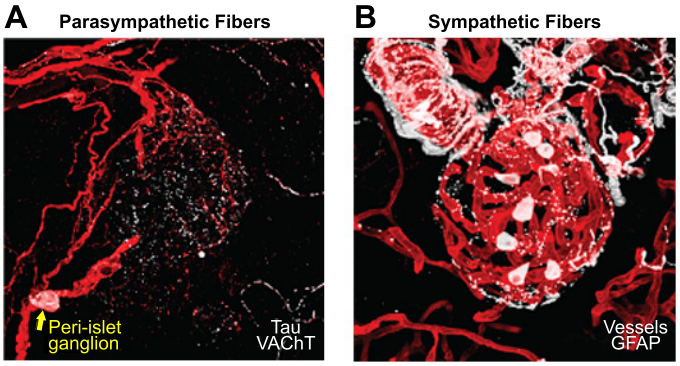

Figure 3. Islets are innervated by multiple nerve types. A. Parasympathetic nerve fibers entering a mouse islet. Image stained for vesicular acetylcholine transporter (VAChT) to mark cholinergic neurons (white) and with Tau, an axonal marker (red). The peri-islet ganglion is shown by the arrow. Image depth: 60 um. B. Sympathetic nerve fibers entering a mouse islet. Staining for sympathetic nerve marker tyrosine hydroxylase (TH) in white and for blood vessels in red. Close alignment of sympathetic nerve fibers along arterioles and other vessels is demonstrated. Image depth: 75 um. Images from Tang et al. (2014).[5]

Organ morphogenesis and specification of endocrine cells

The process of pancreas development has been intensely studied in mouse models, and many aspects of morphogenesis and transcriptional control in the developing mouse pancreas are now understood. All references to embryonic timing in the following descriptions thus refer to mouse embryogenesis (Figure 4).[8]

Pancreas morphogenesis begins at e9.5 and e10, with the formation of two distinct buds, dorsal and ventral, from a portion of foregut endoderm between the stomach and the duodenum. At this stage, the burgeoning pancreas is composed of multipotent progenitor cells. Separation subsequently begins between the tip and trunk epithelia, as the tip domain grows via protrusions at the tissue edges, whereas trunk cells grow and rearrange rapidly into a single layer of polarized epithelial cells that branch into the primitive duct. Dedication to the pancreatic lineage and budding from the foregut endoderm is specified and enabled by the transcription factors

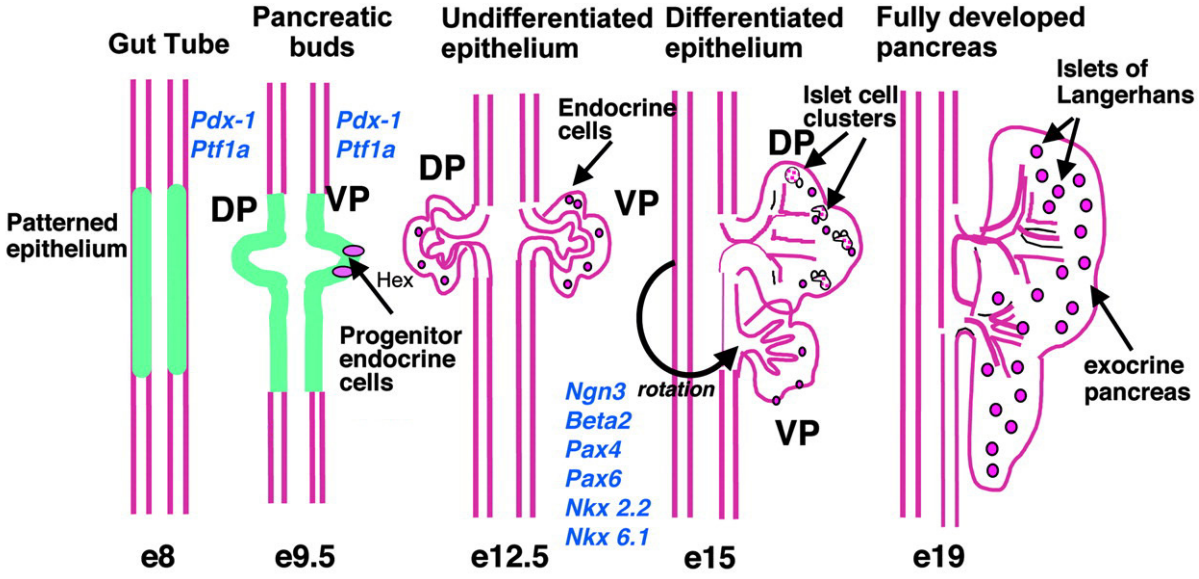

Figure 4. Morphogenesis during mouse pancreas and islet development. Schematic depicting stages of pancreas development. A portion of patterned epithelium on the gut tube expresses Pdx1 and Ptf1a around e8, leading to the budding of the dorsal and ventral pancreas (DP and VP). Endocrine progenitor cells within the buds, expressing ngn3, produce endocrine cells that cluster into proto-islets by e15. The fully formed pancreas contains discrete endocrine and exocrine tissue by e19 in the mouse. Image adapted from Habener et al. (2005).[8]

Pdx1 (Pancreatic duodenal homeobox1) and Ptf1a (Pancreas-specific transcription factor 1a), which are jointly capable of also directing other endodermal lineages to a pancreatic fate (Figures 4 and 5).[8-11]

As the gut grows and rotates, the ventral and dorsal pancreatic buds are brought into spatial proximity to fuse into a single organ, with a continuous central duct. A morphological rearrangement then occurs, separating outer tip cells, which express Ptf1a, from the inner trunk cells, which express Nkx6.1. Tip cells then further differentiate to become acinar cells, and continued growth of the exocrine pancreas occurs via extensive branching morphogenesis. In contrast, the inner trunk cells develop in a highly branched network of single-layer ductal epithelium and are the progenitors of all ductal and endocrine cells. Ptf1a expression remains critical for development of the tip domain, whereas Nkx6.1 (NK6 Homeobox 1) and Nkx6.2 (NK6 Homeobox 2) mediate trunk growth and arrangement.[10-13]

A subset of duct epithelial cells begin to express the transcription factor Neurogenin 3 (ngn3) and are referred to as endocrine precursor cells (Figure 5), as Ngn3 expression is both requisite and sufficient to specify endocrine cell fate. Upon expression of Ngn3, ductal cells stop proliferating and delaminate from the ductal epithelium at e14.5, slowly moving into the surrounding acinar tissue. The

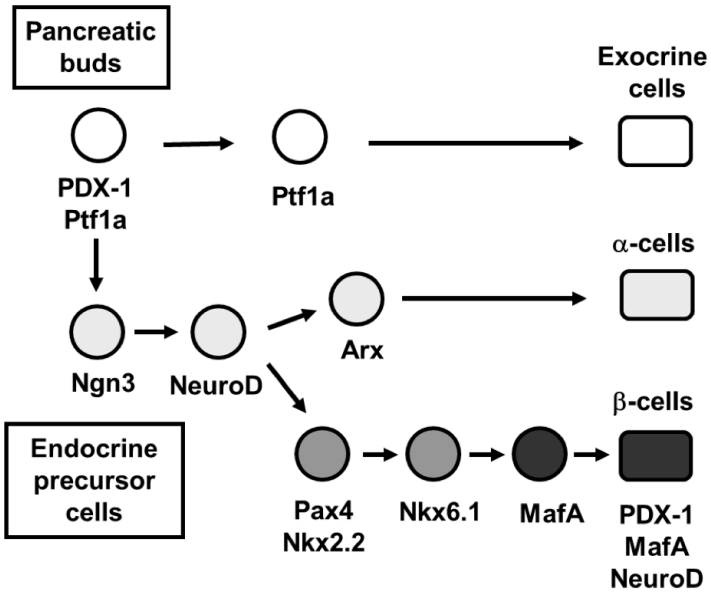

Figure 5. Transcription factor specification of pancreatic cell types. Pancreatic buds are patterned by Pdx1 and Ptf1a. Ngn3 expression defines endocrine precursor cells. Arx and Pax4 specify the α and β cell lineages, specifically. Image from Kaneto et al. (2015).[15]

mutually repressive transcription factors Pax4 (Paired box gene 4) and Arx (Aristaless-related homeobox), both targets of Ngn3, then designate cells to the β/ δ cell or α cell fate, respectively (Figure 5). As hormone expression begins in these cells, they rearrange into proto-islet clusters by e17.5, abandoning the peri-ductal, cord-like structures from which they migrated. After embryonic development, there is little new generation of endocrine precursors from the ductal epithelium, although intense investigation continues to determine if ductal cells can be induced to generate new endocrine cells after various types of pancreatic injury or aging-related phenomena. The development of fully functional islets occurs around postnatal day 8.[8,14-18]

Development of the human pancreas is, for experimental reasons, less defined. It appears that PDX1, PTF1A, NKX6.1, NGN3, PAX4, and ARX are similarly important in human development to the roles defined in mouse studies. The timing of expression (based on morphogenic stage, rather than gestational period) for PDX1 is slightly different in human pancreata, but the order of events is similar, based on transcriptional analysis of whole fetal pancreata. Bud formation begins at 4 weeks of gestation, with NKX6.1 appearing in multipotent progenitor cells quickly thereafter. NGN3 appears as early as 8 weeks, with full expression by 11 weeks and reduced expression at 19 weeks. PAX4, insulin, and glucagon all are expressed around 9 weeks.[10,19,20]

Maturation and adult function of β cells

At the time of birth, late stages of mouse islet development are ongoing. Importantly, the functional competence of β cells remains incomplete. To yield glucose-sensitive cells that appropriately regulate insulin secretion, a cast of critical, islet-enriched transcription factors is required to work in concert. The transcriptional profile of the mature β cell is generally considered to include, among other factors, Pdx1, Nkx6.1, MafA, and MafB (Figure 6).[21-23]

The levels of Pdx1 are carefully orchestrated throughout pancreas and β cell development. Despite the critical role of Pdx1 in pancreas development as a whole (discussed above), the adult pancreas shows Pdx1 expression is restricted to β cells, with little or no expression in other islet cells, and only low levels in acinar cells. Models of Pdx1 loss, either late in development or in adult β cells, have diabetic phenotypes. Although this effect is certainly related to Pdx1 as a transcriptional regulator of the *Insulin* gene, Pdx1 also controls genes related to glucose sensing, insulin secretion, and maintenance of β cell mass. Unlike in the mouse, human PDX1 seems to be also expressed in ductal cells, but the importance of this is not yet understood.[24-27]

Nkx6.1 is essential for maturation along the β cell lineage, but it is also fundamental to adult β cell identity and function. Nkx6.1 directly suppresses transcription of the *Glucagon* gene, contributes to insulin biosynthesis, and mediates expression of critical β cell genes involved in glucose flux and granule fusion. Removal of Nxk6.1 from adult β cells results in glucose intolerance, reduced insulin secretion, reduced insulin content, and the appearance insulin-positive cells co-expressing ngn3 and somatostatin, suggesting changes in cell identity.[28-31]

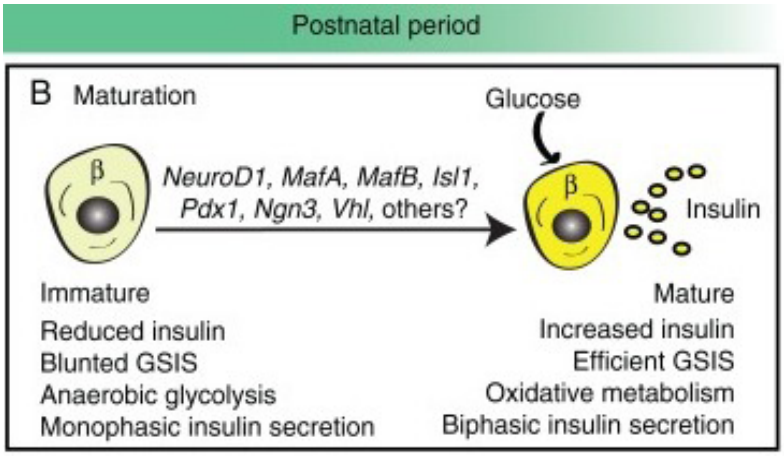

Figure 6. Events in postnatal β cell maturation. Expression of MafA, MafB, Nkx6.1, and Pdx1 contribute to mature β cell function in the postnatal period. Functional maturity is largely characterized by components of tightly regulated and adequate glucose-stimulated insulin secretion. Image from Benitez et al. (2012).[23]

The large Maf factor, MafA, was discovered to bind the *Insulin* gene and promote transcription, yet it also promotes

transcription of *Pdx1*. MafA and its relative, MafB, arise during a developmental period of rapid endocrine cell expansion. In the mouse, both MafA and MafB are expressed in the developing β cell, but MafB is ultimately restricted to α cells in the adult. In human islets, however, MafB remains expressed in many adult β cells. Loss of MafA in rodent models results in reduced insulin, impaired glucose-stimulated insulin secretion, and decreased expression of Pdx1 and Glut2.[21,32-37]

Importantly, *in vivo* and *ex vivo* studies link reductions in these four transcription factors, Pdx1, Nkx6.1, MafA and MafB, to T2DM (Figure 7). MafA and Nkx6.1 protein levels are decreased in the *db/db* diabetic mouse model (Figure 7A), and both mRNA (Figure 7B) and protein of all four of the human transcription factors PDX1, NKX6.1, MAFA and MAFB (Figure 7C-E), are dramatically lower in islets from T2DM patients.[38] Importantly, expression of ISL1, and NEUROD1, other β cell–specific transcription factors, were unaltered in T2DM islets, suggesting that the four factors listed above are specifically sensitive to damage during disease progression. Data from the *db/db* diabetic mouse indicates that Mafa may be affected earlier, with Nkx6.1 and Pdx1 levels remaining normal until a longer duration of exposure to the hyperglycemia and insulin resistance of that model. This concept of temporally-specific responses of different transcription factors to metabolic stress has not yet been well defined in human tissues.

Glucose-Stimulated Insulin Secretion

The insulin-producing β cell is the most abundant islet cell type. The primary purpose of the β cell is to produce and secrete the hormone insulin, and it is the only cell type in the body that does so. In response to an increase in local blood glucose concentrations, glucose enters the β cell via facilitated diffusion, through the glucose transporter (GLUT-1 or GLUT-2). Upon entry,

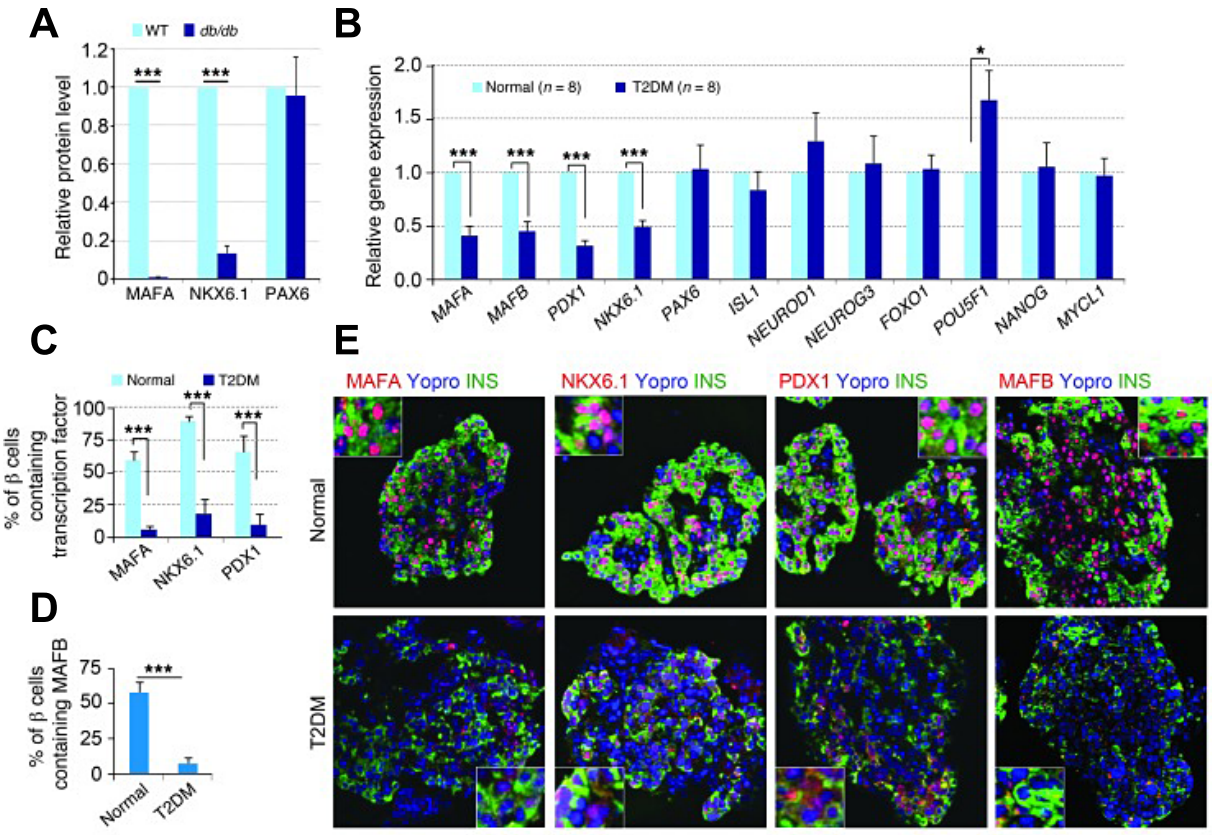

Figure 7. Critical β cell transcription factors are dramatically reduced in islets from T2DM patients. A. MafA and Nkx6.1 mRNA is severely reduced in islets from db/db mice, but the pan-endocrine marker Pax6 is unaffected. B. Gene expression of MAFA, MAFB, PDX1, and NKX6.1 are significantly and specifically reduced in T2DM human islets. C. The percent of β cells with MAFA, NKX6.1, or PDX1 protein is reduced in T2DM islets. D. The percent of β cells with MAFB protein is similarly reduced in T2DM islets. E. Immunohistochemical staining shows loss of transcription factors from β cell nuclei in T2DM islets (lower panels) compared to normal islets (upper panels). Images from Guo et al. (2013).[38]

glucose is promptly phosphorylated to glucose-6-phosphate by glucokinase, without which glucose would be able to diffuse back out of cell. An increase in the intracellular concentration of glucose-6-phosphate increases flux through the glycolytic pathway, which culminates in the mitochondrial electron transport chain. Increased glycolytic flux produces the high-energy molecule adenosine triphosphate (ATP), raising the ratio of ATP to adenosine diphosphate (ADP). In conditions where ATP exceeds ADP in the β cell, ATP outcompetes ADP for binding to the SUR1 component of the Kir6.2 KATP channel, resulting in channel closure and depolarization of the β cell plasma membrane. This depolarization triggers the opening of voltage-gated calcium channels (VDCCs) and the release of calcium from the endoplasmic reticulum. The resulting elevation in intracellular calcium promotes the fusion of pre-formed, insulin-containing granules with the plasma membrane and the consequent release of insulin into the extracellular space (Figure 8).[39,4] A secondary mechanism that promotes insulin secretion is the elevation of intracellular cyclic AMP (cAMP) levels. Elevation of cAMP activates either PKA or EPAC (exchange protein activated by cAMP), both of which increase the efficacy of Ca^{2+} in promoting exocytosis. Hormones and peptides, such as glucagon and GIP (gastric inhibitory peptide) physiologically increase cAMP levels in β cells, as does treatment with any phosphodiesterase

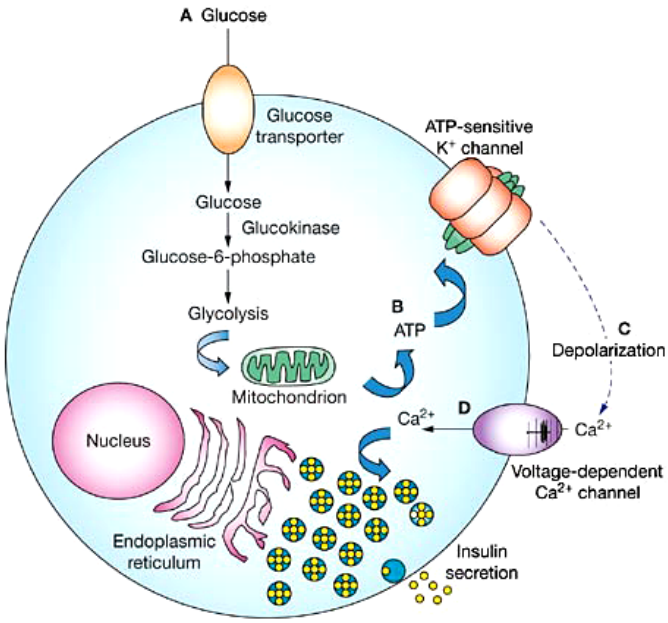

Figure 8. Glucose-stimulated insulin secretion (GSIS). Glucose enters the β cell via GLUT-2-facilitated diffusion and is metabolized by glycolytic pathways, generating ATP. The rise in intracellular ATP concentration promotes closure of the KATP channel, inducing depolarization of the plasma membrane and the subsequent opening of voltage-gated calcium channels. The influx of calcium stimulates fusion of insulin granules with the plasma membrane, and insulin is released from the cell. Image from De León and Stanley (2007).[40]

inhibitor, by reducing the rate of cAMP degradation.[39] Although glucose is the only nutrient that can independently induce insulin secretion, glucose-stimulated insulin secretion is potentiated by lipids and amino acids. Free fatty acids (FFAs) can enter the β cell either through diffusion or by binding a free fatty acid receptor (FFAR), such as GPR40. FFAs can acutely enhance insulin secretion by the general acylation of important functional proteins, direct effects on L-type Ca^{2+} ion channel function, and activation of protein kinase C (PKC).[39] The specific amino acid type dictates the intracellular mechanism of potentiation. Some directly or indirectly depolarize the cell membrane, namely L-arginine and L-alanine, respectively. Others, such as aspartate and glutamate, enter NADPH shuttles in the mitochondria and contribute to the generation of ATP.[39,41,42]

Species Differences in Islet Physiology

Rodent models, the mouse in particular, have been and remain critical for advancing our understanding of islet biology and disease. Nonetheless, caution is required when translating mouse-derived data to human islet physiology. This caution is predicated on specific differences between mouse and human islets, which, as a group, underscore the importance of research on human islets.[43]

Architecture and cell ratios

Multiple species differences have been observed in islet morphology and function. In the mouse, β cells regularly constitute close to 80% of the endocrine cells in each islet, and they are tightly grouped in the interior of the islet structure. The other cell types, especially α cells, are arranged in a “mantle” around the β cell core (Figure 9A). In human islets, however, the spatial arrangement of cell types is highly heterogeneous, with α cells frequently penetrating the islet core (Figure 9B). In addition, the ratio of cell types varies greatly in human islets, with α cells

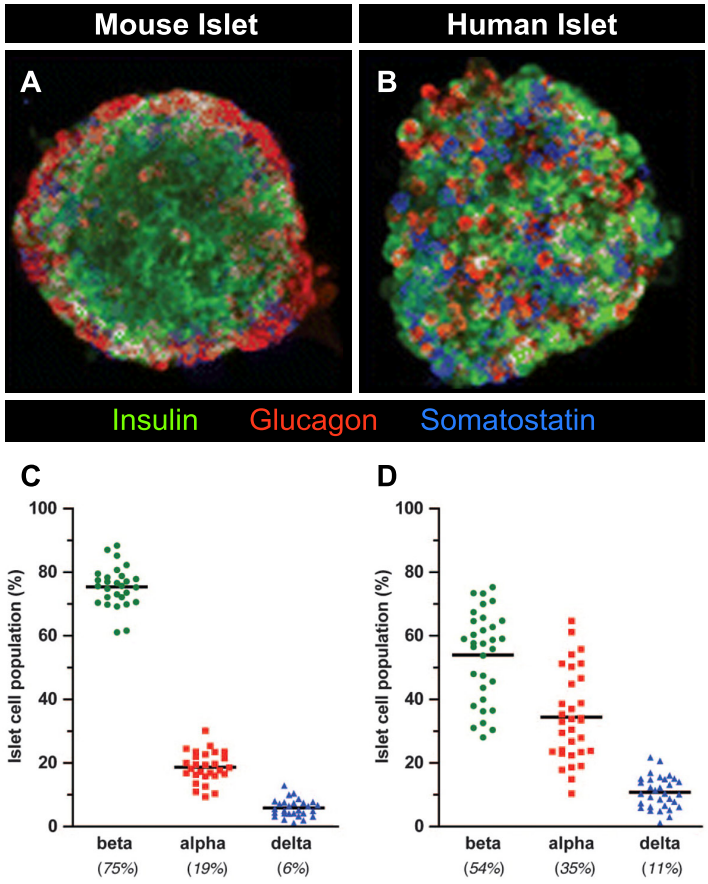

Figure 9. Islet morphology and composition varies between mice and humans. (A) Mouse and (B) human islets labeled for insulin (green), glucagon (red), and somatostatin (blue). Images exemplify the heterogeneous arrangement of cell types in the human islet, compared to the define beta cell "core" and alpha cell "mantle" of the mouse islet. Percent of each cell type in (C) mouse islets, n=28, and (D) human islets, n=32, quantified from optical sections taken at various depths throughout the islet. Human islet composition was significantly different ($p<0.0001$) for all endocrine cell populations examined. Horizontal bar shows the mean value for each cell type. Image adapted from Brissova et al., 2005.[26]

representing a much larger percent of islet cells (Figure 9C). This has implications, for example, for whole islet transcription data, where there is an assumed ratio of cell types in the mouse that is not appropriate for human islets.[44,45]

Gene expression and insulin secretion

The expression of certain critical β cell genes is highly glucose-responsive in mouse islets, but not in human. As published previously,[46] 48-72 hour treatment with high glucose does not increase gene expression of glucose-sensing genes, transcription factors, or insulin itself in human islets, as it does in mouse islets (Figure10 A-D). As is mentioned earlier in this chapter, MAFB expression is maintained in human adult β cells, whereas its expression is restricted to α cells in adult mouse islets. The insulin secretory profiles of mouse and human islets also vary. When directly compared, human islets secrete more basal insulin, but the fold increase in secretion upon stimulation with high glucose is smaller in human than in mouse (Figure 10E-F), and insulin content experiences a smaller fold increase in human islets than mouse, after 24 hour treatment with high glucose.[46]

Proliferative capacity and expansion of β cell mass

The establishment of β cell mass and the general proliferative frequency of β cells also differs between species. In the adult mouse, basal β cell proliferation is approximately 2-5%, but the ability of mouse β cells to proliferate in response to obesity, pregnancy, and other conditions of increased insulin demand has been clearly documented.[47,48] Some studies suggest that mouse β cell mass more than doubles in pregnancy. Most therapeutically intriguing have been studies suggesting that mouse β cell regeneration can resolve diabetes.[49]

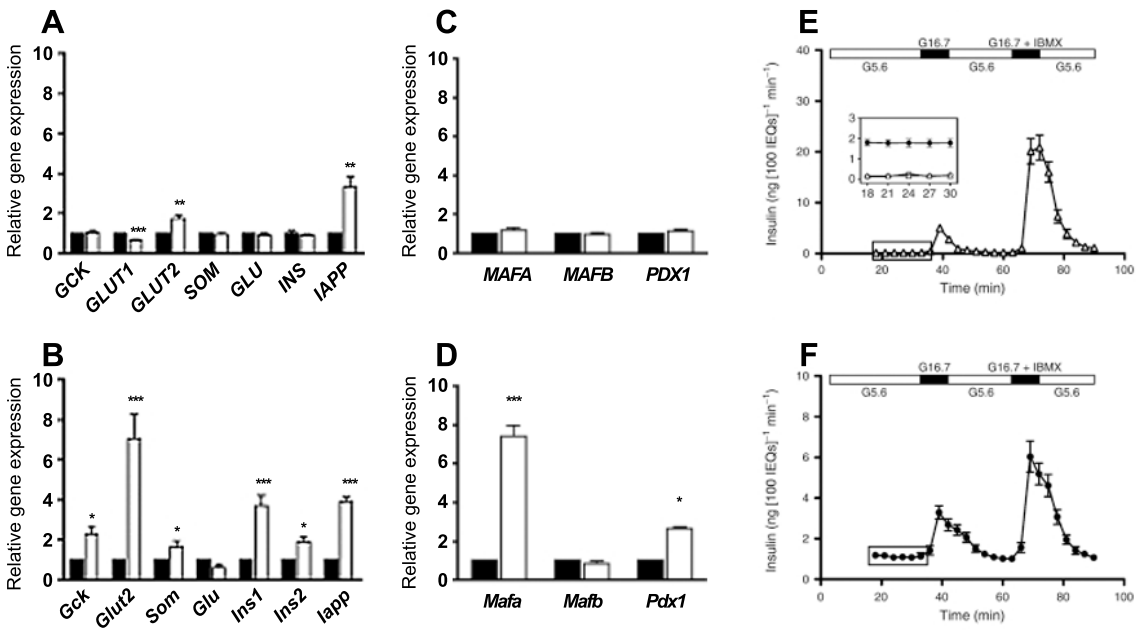

Figure 10. Differences in glucose-responsive gene expression and glucose-stimulated insulin secretion in human and mouse islets. Human (A) and mouse (B) expression of glucose-sensing genes and islet secreted factors after culture in 5 mM (black bars) or 11mM (white bars) glucose. Human (C) and mouse (D) transcription factor expression after culture in 5 mM (black bars) or 11mM (white bars) glucose. Islet perifusion profiles of human (E) and C57Bl/6 mouse (F) isolated islets, showing that human islets secrete more insulin basally (at 5.6 mM glucose) but have a smaller fold increase in secretion upon stimulation with 16.7 mM glucose. Images from Dai et al. (2012).[46]

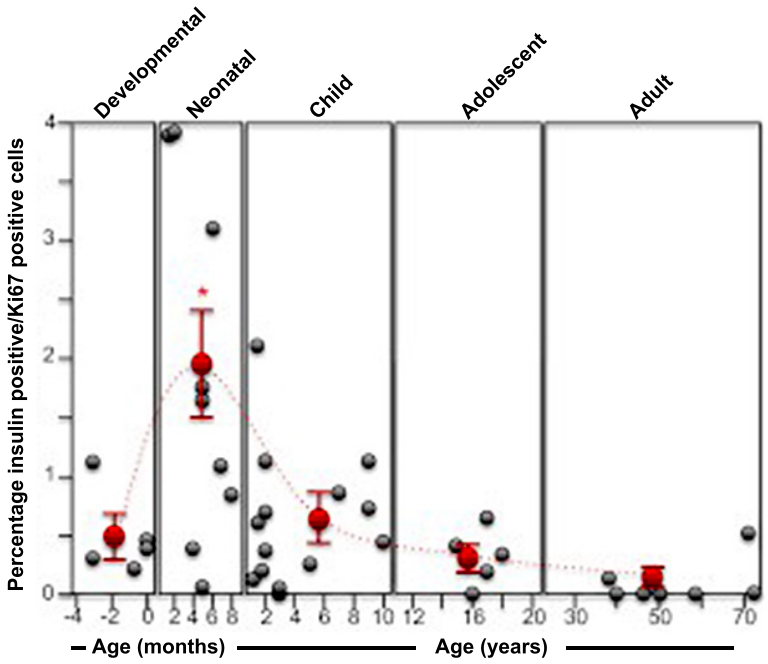

Figure 11. Levels of human β cell proliferation across life periods. Graphical representation of peak human β cell proliferation during the neonatal period, with β cell proliferation dropping to or below 1% during childhood. Gray points are derived from individual donor pancreata, red points are the mean values in each time category, with the dashed curve representing the change trend between the average value in each life period. Image from Gregg et al. (2012).[50]

In human islets, there is a transient burst of β cell proliferation in the postnatal period, but rates drop precipitously and remain very low (0.1-0.5%, by most estimates) during adulthood.[50] Although autopsy studies provide evidence that increased body mass index (BMI) correlates with greater β cell mass,[51] the lack of longitudinal studies precludes the conclusion that this is due to β cell mass expansion in individual patients, and it seems that β cell mass adaptation in human pregnancy is minor, compared to that in mice.[52]

The cyclins and cyclin-dependent kinases (cdks) responsible for both mouse and human β cell progression through the cell cycle have been well, if not completely, defined.[53,54] As a result, there has been great therapeutic interest in defining mouse and human β cell mitogens, with the end goal of increasing or replacing β cell mass and alleviating diabetes.[55] However, due to the relatively modest proliferative response of human β cells to stimuli, it remains unclear whether it will be feasible to address human diabetes with the stimulation of human β cell proliferation.

Insulin

Structure and signaling

Insulin is a 53-amino acid peptide that results from two cleavage events, the first by PC1/3 (proprotein convertase 1/3), converting preproinsulin to proinsulin during translocation of the protein into the ER, and the second by PC2 (prohormone convertase 2), cleaving proinsulin to insulin inside the insulin granules. The result of the PC2 reaction is removal of the "C-peptide," a peptide portion that connects the "A" and "B" segments of the insulin protein (Figure 12). C-peptide is

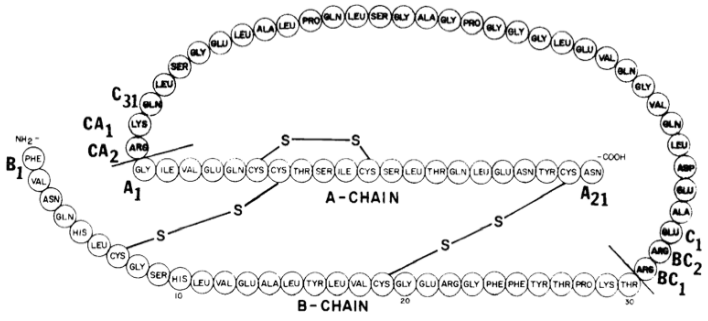

Figure 12. Structure of the insulin prohormone. Amino acid sequence of proinsulin, showing the A-chain, B-chain, and C-peptide, the last of which is removed by PC2-mediated cleavage and is co-secreted with insulin. Image from Kitabchi (1977).[56]

secreted in equimolar amounts with insulin from the secretory granules but is considered to be biologically inert. Importantly, C-peptide has a much longer half-life than insulin in the blood (hours versus minutes). For this reason, C-peptide is a more useful indicator of prior insulin secretion, and the equimolarity of C-peptide to insulin allows direct quantification of previous insulin release.[56]

Insulin signals via its designated receptor, the insulin receptor (IR). The IR is found on the cell surface of almost all mammalian cells, but its role in glucose metabolism is greatest in the brain, liver, skeletal muscle, adipose tissue, α cells, and the β cells themselves. The receptor is a tetrameric, transmembrane receptor tyrosine kinase, with two α and two β subunits. In the absence of ligand, the α subunits conformationally suppress the intrinsic transphosphorylation activity of the β subunits. However, upon binding of insulin to the α subunits, this repression is removed, and the two β subunits transphosphorylate tyrosine residues (Figure 13).[57-60]

Multiple signaling sequences occur downstream of IR phosphotyrosines, and much of insulin-induced signaling is mediated by the phosphorylation of a family of proteins called insulin-receptor substrates (IRS), some of which are tissue-specific.[61] IRS-1, for example, initiates signaling through PI(3)K and Akt, which contributes to GLUT4 translocation in skeletal muscle cells. IRS-1 and IRS-3 mediate MAPK signaling, through Grb2 and SHP2, respectively (Figure 13). Although the IR promotes these signaling programs through tyrosine phosphorylation, the IR β subunits and IRS isoforms also contain serine and threonine residues. Mitigation of insulin receptor signaling appears to depend on dephosphorylation of the IR and IRS proteins, as well as particular S/T phosphorylation events, which play an important role in modulating the balance of insulin's intracellular effects.[57-59]

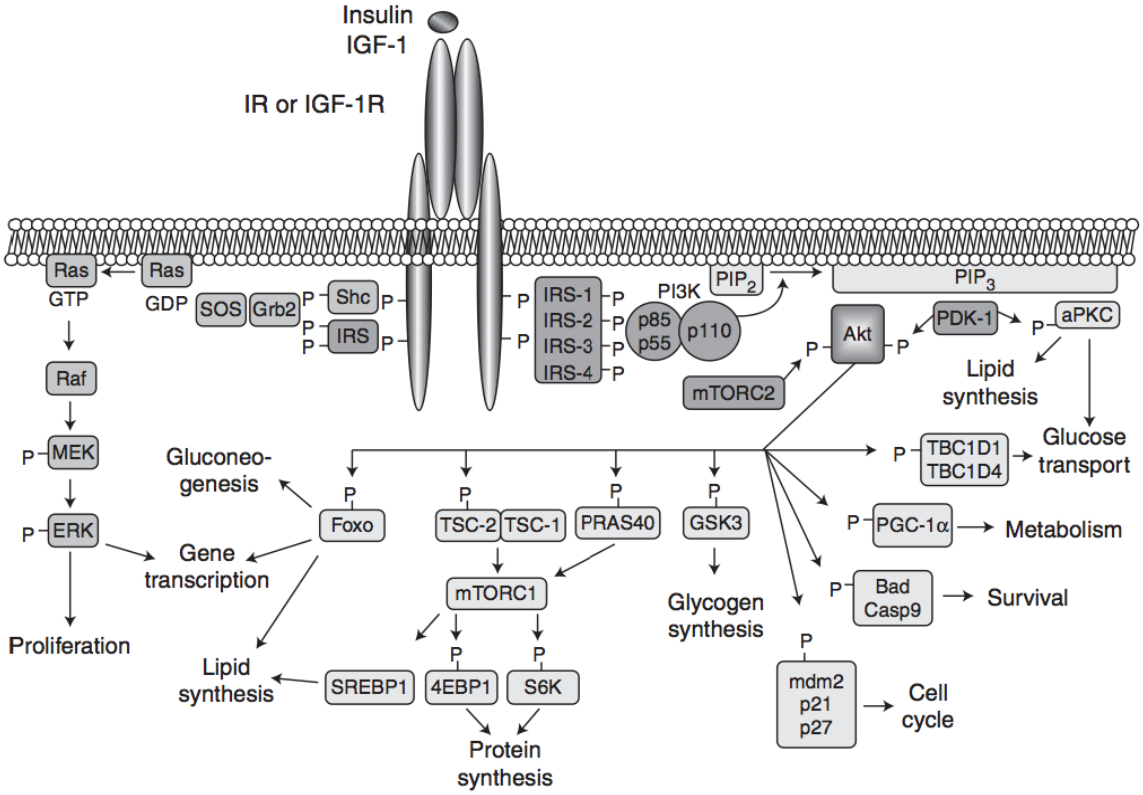

Figure 13. Signaling through the insulin receptor. Depiction of tyrosine phosphorylation on the intracellular portion of the insulin receptor β subunits, which initiates two main insulin-induced signaling pathways. The PI(3) kinase pathway initiates the majority of insulin's metabolic consequences, and the MAP kinase pathway initiates mitogenic and inflammatory consequences. Image from Boucher et al. (2014).[61]

Action in peripheral tissues

Insulin is a potent anabolic hormone with critical, tissue-specific intracellular influences. In skeletal muscle, the primary effect of insulin signaling is to promote cellular uptake of glucose from the bloodstream. As briefly mentioned above, this occurs by translocating the glucose transporter GLUT4 from the cytoplasm to the cell membrane, where it allows facilitated diffusion of glucose. In adipose tissue, insulin promotes lipid synthesis by increasing activity of enzymes such as pyruvate dehydrogenase, fatty acid synthase (FAS), and acetyl-coA carboxylase, and potently suppresses lipolysis through inhibition of hormone-sensitive lipase. In the liver, insulin also has a dual agenda, to promote storage of glucose as glycogen and to suppress gluconeogenesis. The former is directly accomplished partly by activating glycogen synthase (GS). The suppression of gluconeogenesis, however, is more complex, incorporating direct suppression of the gluconeogenic enzyme phosphoenolpyruvate carboxykinase (PEPCK) with indirect effects, such as reduced glycerol and non-esterified fatty acids, due to its effects in adipocytes, and reduced glucagon secretion from islet α cells. Insulin secretion and action is clearly a central component of carbohydrate and lipid metabolism, the dysregulation of which has wide-spread and severe consequences for overall health.[58,59,62]

Diabetes Mellitus

Incidence and Pathological Types

Diabetes mellitus is a group of metabolic diseases that are characterized by an insufficient insulin response to adequately control blood glucose levels, resulting in hyperglycemia and related complications. The diagnosis of diabetes, regardless of type, is defined by a fasting blood glucose value above 7mM (126 mg/dL) or an HbA1C value over 6.5%.[63] HbA1C is a measure of percent glycosylated hemoglobin in the blood, which indicates the average blood

glucose value of a patient over the preceding three-month period. In addition, glucose tolerance tests are often used in diagnosis. Two hours after delivery of a 75g glucose bolus, blood glucose of more than 11.1mM (200 mg/dL) indicates diabetes. Importantly, there are separate definitions for “prediabetes” that indicate abnormal glucose metabolism (5.7% < HbA1C <6.5 and 100 mg/dl < fasting glucose < 126 mg/dL).[64] These values are important warnings for patients who, without potent intervention, are likely to progress to frank diabetes. Importantly, the pathogenesis that leads to the condition defined by these metrics differs fundamentally between the most common forms of diabetes, Type 1 and Type 2.

Type 1 Diabetes

Pathogenesis and Pathophysiology

Type 1 diabetes (T1DM) is generally categorized as an autoimmune disease, in which β cells are targeted by T-cell-mediated immune processes. The majority of new diagnoses occur in childhood or adolescence, particularly between ages 5-7 and around the beginning of puberty. However, presentation can occur in very young children, as well as in young adults, into their 20s and 30s. Type 1 diabetics are frequently diagnosed after presentation with polydipsia, polyuria, and/or polyphagia, all of which indicate the presence of extreme hyperglycemia. The presence of autoantibodies against

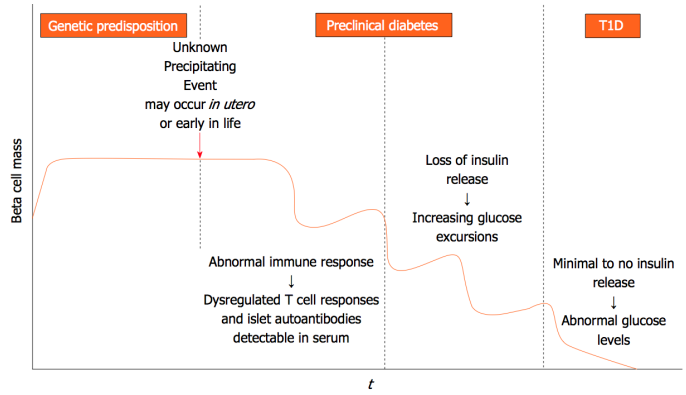

Figure 14. A natural history of T1DM. Depiction of proposed events in the progression of T1DM pathogenesis. A genetic predisposition establishes susceptibility such that, upon the occurrence of some precipitating event, an abnormal immune response is triggered, leading to T-cell-mediated attack of β cells. During the period of preclinical diabetes, there is a gradual and progressive loss of β cell mass and insulin release, leading to increased incidence of glucose excursions. Upon loss of 80-90% of β cell mass, clinical symptoms manifest, as the total insulin release dwindles below the required amount to maintain proper glucose metabolism. Image from Simmons et al. (2015).[66]

β cell proteins can be highly predictive of progression toward T1DM, long before symptom presentation, and at least one autoantibody is present at the time of 90% of diagnoses. In particular, antibodies against IAA (insulin), GAD (glutamic acid decarboxylase), ZnT8A (zinc transporter 8), and IA2A (insulinoma-associated autoantigen 2) indicate current or future immune attack on β cells. These antibodies can precede disease symptoms by months or years, as it is thought that frank diabetes does not occur until approximately 80-90% of β cell mass has been lost (Figure 14). Most T1DM patients have very few, if any, insulin-containing islets, although there is evidence that, even after decades of the disease, some patients still test positive for low levels of C-peptide, indicating ongoing insulin production. T1DM islets are often characterized by varying degrees of insulitis, predominantly composed of CD8+ T cells.[65,66]

Epidemiology

The incidence of T1DM has been increasing in recent decades, to the confusion of clinicians and researchers. As of 2015, the global incidence is increasing 2.3% per year, although the prevalence varies significantly among countries, with Caucasian populations having the highest incidence. Hypotheses abound to explain this increase, but there is no consensus. Considerations include both global and regional changes in hygiene and germ exposure, patterns of viral infection, environmental factors, and evolving genetics.[67]

Therapeutic options

Despite extensive basic and clinical research, delivery of exogenous insulin has remained the primary therapeutic option for Type 1 diabetics since insulin's discovery in 1922. Frequent blood glucose monitoring and calibrated exogenous insulin therapy have allowed many Type 1 diabetics to live with the disease for decades, but only immunomodulatory therapies can address the underlying autoimmune etiology of the disease. Beginning in 2000, clinical transplantation of islets from human donors has been an attractive treatment option for the most

severe and poorly controlled cases of Type 1 diabetes. This procedure can temporarily eliminate the need for exogenous insulin therapy in some patients, but the survival of the islet grafts requires immunosuppressive drugs, and most islet grafts eventually lose efficacy.[68-70]

Maturity onset diabetes of the young

A rare form of diabetes is maturity onset diabetes of the young, or MODY, a set of monogenic, autosomal dominant mutations in islet factors. MODY patients generally present with moderate hyperglycemia in childhood or adolescence, often as a result of routine blood work, but MODY is sometimes mis-diagnosed as other forms of diabetes. Importantly, MODY patients do not produce islet autoantibodies and lack the insulin resistance that is common in T2DM. Instead, a primary defect in insulin secretion is responsible for the hyperglycemia. To date, eleven MODY genes have been identified: HNF-4α (MODY1), glucokinase (MODY2), HNF-1α (MODY3), IPF-1 (MODY4), HNF-1β (MODY5), NEUROD1 (MODY6), KLF11 (MODY7), CEL (MODY8), PAX4 (MODY 9), INS (MODY10), and BLK (MODY11). Interestingly, the specific MODY mutations in these genes are numerous and often vary by family. Treatment of MODY often involves simple dietary changes, although oral medication to increase insulin secretion is sometimes needed.[71,72]

Type 2 Diabetes

Epidemiology

Type 2 diabetes (T2DM) represents more than 90% of diabetes cases worldwide, equaling a total of 285 million individuals (6.4% of the global population) in 2010. T2DM is often associated with obesity and/or increased age, but its incidence in young patients is rising rapidly, in concordance with increased obesity in youth. There is a strong genetic component to T2DM,

estimated to be more than 50%, but weight, diet, exercise, and other lifestyle factors often play a determinant role.[63,64]

Pathogenesis and Pathophysiology

T2DM is associated with resistance to insulin signaling in the liver, skeletal muscle, and adipose tissue, termed peripheral insulin resistance. Although the order of events in the pathology of T2DM remains contested, it is widely proposed that insulin resistance places a level of insulin demand on the islet that β cells eventually cannot sustain, leading to their dysfunction or even death (Figure 15A).[63]

Insulin resistance (IRes) is a condition in which insulin signaling and its intracellular consequences are blunted, requiring a greater amount of insulin to elicit the same intracellular effect. Although insulin resistance can be observed in all insulin-sensitive tissues, insulin resistance in the liver is particularly detrimental to overall glucose metabolism. The inability of insulin resistant individuals to suppress gluconeogenesis and glycogenolysis is the largest peripheral (extra-pancreatic) contributor to the hyperglycemia of T2DM. In skeletal muscle, IRes reduces glucose uptake from the blood and subsequent storage. In adipocytes, IRes limits lipid storage and results in unchecked lipolysis, the consequence of which is increased circulating lipid concentrations. This dyslipidemia carries its own set of deleterious consequences, both by promoting inflammation in peripheral tissues, which further hinders insulin signaling, and by directly acting on the β cell.[59,62,73]

The progression from normal glucose metabolism to insulin resistance to T2DM depends on a shift in the curve relating β cell function to insulin sensitivity (Figure 15B). Those individuals that can move up the curve by increasing β cell function adequately as insulin sensitivity declines can maintain normal glucose tolerance (NGT). As the curve shifts left and the level of β cell

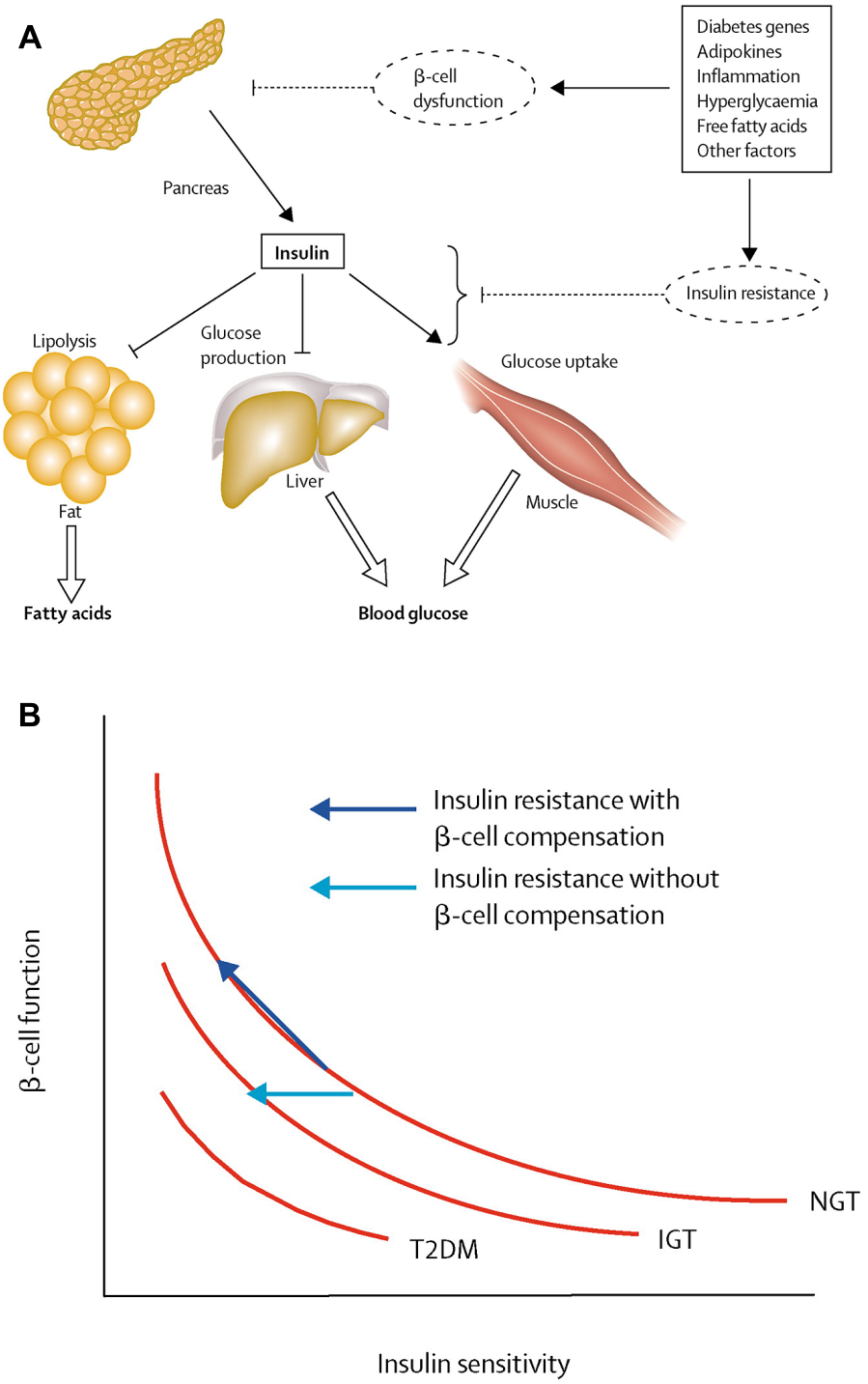

Figure 15. Mechanisms and evidence of T2DM progression. A. Schematic of insulin's action in peripheral tissues and how components of T2DM indirectly (via β cell dysfunction) and/or directly (insulin resistance) alter these effects. B. The relationship between β cell function and insulin sensitivity on curves representing normal glucose tolerance (NGT), impaired glucose tolerance (IGT) and T2DM. Images from Stumvoll et al. (2005).[63]

function at a particular insulin sensitivity level is lower than required, impaired glucose tolerance results. A further shift in the curve depicts the transition to frank T2DM.[63]

The results of insulin resistance increase blood glucose. Sustained hyperglycemia, or even regular hyperglycemic excursions, exerts a plethora of negative consequences. The chronic complications of diabetes are broadly categorized as microvascular or macrovascular. The former includes retinopathy (the most common cause of adult blindness in the United States), neuropathy (either nerve pain or loss of sensation), and nephropathy (necessitating dialysis or renal transplantation for some patients). Macrovascular complications include coronary, cerebral, and peripheral vascular dysfunction. For example, the risk of cardiovascular disease is four-fold greater in T2DM patients. As a whole, these complications place significant financial and quality-of-life burdens on large patient populations.[74,75]

Despite the importance of insulin resistance in most cases of T2DM, recent studies have placed deserved focus on the β cell. There is now strong evidence that patients with T2DM harbor an inherent β cell defect that limits insulin secretion.[73] The hypothesis follows that it is patients with an initial, sub-clinical deficit in insulin secretion that fail to cope with insulin resistance, when it subsequently develops. This idea is supported by the presence of a “healthy obese” population that becomes insulin resistant but never diabetic. Interestingly, genome-wide association studies of T2DM patients return gene associations related to β cell function more often than any other category of gene product.[76-78] Although this component of T2DM pathogenesis is still poorly understood, it highlights the importance of ever better understanding fundamental β cell biology.

Therapeutic options

Although weight loss, exercise, and careful dietary changes are the first line of intervention, many patients progress to requiring the addition of exogenous insulin and/or oral medications to adequately control their hyperglycemia. The main categories of oral medications currently

prescribed include metformin, which reduces hepatic glucose production, sulfonylureas, which directly promote insulin secretion by closing the K_{ATP} channel and inducing cell depolarization, sodium channel blockers that promote excretion of glucose in the urine, PPARγ receptor agonists, which improve insulin sensitivity, and incretin mimetics, which promote satiety, weight loss, and protection of β cells.[63,79]

Transplantation of Human Islets

Clinical transplantation

Despite years of improvements in delivering exogenous insulin therapy to control Type 1 (and now often Type 2) diabetes, many patients still experience dangerous hyperglycemic and/or hypoglycemic excursions. The cumulative effect of hyperglycemic excursions over many years is an increased risk for a panel of diabetic complications. Acute hypoglycemia, conversely, can induce anything from dizziness and nausea to death, particularly if the hypoglycemic event occurs while the patient is asleep. Even well-controlled patients struggle with both ends of this glycemic spectrum, but blood glucose control is unusually difficult to modulate in some patients.

The first human islet transplantation occurred in 1977, but it wasn't until the advent of the Edmonton protocol in 2000,[68] which reported 7 consecutively successful transplantations (insulin independence after 12 months in all patients) with steroid-free immunosuppression, that clinical success and interest in the procedure rose. The attractiveness of islet transplantation lies partly in the potential for temporary insulin independence. Between the years of 2007 and 2010, the average duration of graft function and insulin independence has lengthened, with 44% of patients from the Collaborative Islet Transplant Registry (CITR) remaining insulin independent at 3 years after transplantation.[80]

Despite multiple areas of recent improvement, immunosuppression is a daunting prospect for many patients, and the benefit of transplantation for glycemic control is only deemed superior for patients with great difficulty on exogenous insulin therapy. It is the hope of many clinicians and patients that, with continued advancement in donor registration, donor selection, islet isolation protocols, and immunosuppression regimens, that islet transplantation may become beneficial for more T1DM patients.

Human islets in basic research

As clinical transplantation has increased in popularity, the rise in human islet use for basic research has been dramatic. Although T2DM patients do not currently qualify for clinical transplantation, researchers increasingly rely on human islet studies to understand the pathogenesis of Type 2 diabetes.[81] Given the previously discussed species differences between mouse and human islet physiology, the ability to directly study human islets is critical for translational research. The factors that are carefully considered when selecting donors (cause of death, body mass index, ischemic time, etc.) for clinical transplant are also important for basic research. In particular, the range of insulin secretory profiles among human islet preparations can have huge consequences for research data, as will be described in Chapter IV. As both the number of investigators conducting human islet research and the number of acquired human islet preparations for research continues to increase,[82] these issues are ever more pertinent to the larger field of islet biology.

Transplantation of human islets, most frequently into immunodeficient mouse models, has become a valuable and accepted means of studying human islet biology. The combination of human tissue and the *in vivo* environment is the most clinically-relevant scenario available to most researchers. Unlike in clinical transplantation, where islets are injected into the portal

vein, islets transplanted into mice are often placed under the kidney capsule, where the cells can coalesce, revascularize, and be readily retrieved for ex vivo study.[83,84] The use of a human-specific radioimmunoassay for insulin has allowed investigators to distinguish human insulin from mouse insulin in the blood, which is critical in models where mouse and human islets co-exist. To promote islet graft survival, selection of an immunocompromised or immunodeficient mouse model is essential, and many appropriate choices are now available.[85,86]

Glucotoxicity and Lipotoxicity

Hyperglycemia and hyperlipidemia negatively affect an abundance of tissues, evidenced by the plethora of diabetic complications. Importantly, there is now a widespread understanding that excess glucose and lipid have some direct negative consequences on the β cell itself. These consequences were termed “glucotoxic” or “lipotoxic,” depending on the responsible nutrient. Many *in vitro* studies have probed the underlying mechanisms of these glucotoxic and lipotoxic effects in cell lines and isolated islets, and *in vivo* mouse models have advanced some of these findings.

Experimental evidence for glucotoxicity and lipotoxicity

One main category of “toxicity” is dysfunction or reduced function of β cells. In that vein, studies of β cell lines cultured in high glucose show reductions in insulin gene transcription, insulin content, glucose-stimulated insulin secretion, and exocytotic events.[87-90] Similar results have been shown in studies of isolated islets.[87] A number of *in vitro* studies have examined combinations of high glucose and high lipid, showing evidence of reductions in stimulated insulin secretion, glucose uptake into β cells, mitochondrial activity, calcium release, intracellular insulin content, and docking of insulin granules from rat and mouse islets.[91,92] It has even been suggested that the negative effects of high lipid on β cells are dependent on the co-existence

of high glucose,[93-95] thus generating the idea of “glucolipotoxicity”. However, this is contested by studies of lipid perfusion in normal rats and of human islets cultured with FFAs only, in which glucose-responsiveness, glucose metabolism, insulin gene expression and glucose-stimulated insulin secretion were all suppressed.[96-102] Despite the pathological importance of β cell dysfunction, the ultimate form of “toxicity” is β cell apoptosis. High glucose has been shown to promote β cell apoptosis in cultured human islets,[103-105] and cadaveric studies of T2DM patients echo this conclusion.[106,107]

Important considerations of all the above studies include the difficulty of selecting relevant glucose and lipid concentrations that reflect concentrations in the interstitial space *in vivo*, as well as selecting appropriate lipid types. For example, saturated fatty acids seem to be detrimental, but unsaturated species can be protective for β cells.[108,109] Exposure time also appears to be central to the nature and degree of the β cell effect, with the time required for seeing β cell damage inevitably differing based on the chosen nutrient concentrations. *In vivo* rodent models like the ZDF rat, which do not require this sort of decision-making, are limited by the inability to separate the influences of glucose and lipid.

Proposed mechanisms of glucotoxicity and lipotoxicity

Oxidative stress

An unavoidable consequence of glycolytic flux in the β cell is the generation of reactive oxygen species (ROS), as these highly volatile molecular species are a byproduct of the metabolism of oxygen in the mitochondrial electron transport chain (Figure 16).[110] ROS such as superoxide, hydrogen peroxide, and hydroxyl radicals are important signaling molecules in the β cell, needed for proper glucose-stimulated insulin secretion.[111,112] However, above certain concentrations, they can have deleterious effects by altering the structure and

function of proteins, lipid, and DNA.[113]

Physiological responses to elevated ROS include expression of antioxidant enzymes that neutralize the hyperreactivity of these molecules.[113] However, β cells express abnormally low levels of antioxidant enzymes compared to other tissues, particularly in the cases of superoxide dismutase, catalase, and glutathione peroxidase (Figure 17).[114-116] Thus, as glycolytic flux increases in the β cell, which is an inherent consequence of hyperglycemia, ROS production rises (Figure 18),[117] but the antioxidant response is thought to be inadequate. The resulting state of chronically elevated ROS levels is termed “oxidative stress.” Importantly, lipids can also contribute to ROS generation,[118,119] making oxidative stress an attractive candidate for both glucotoxic and lipotoxic consequences in the β cell.[118,119]

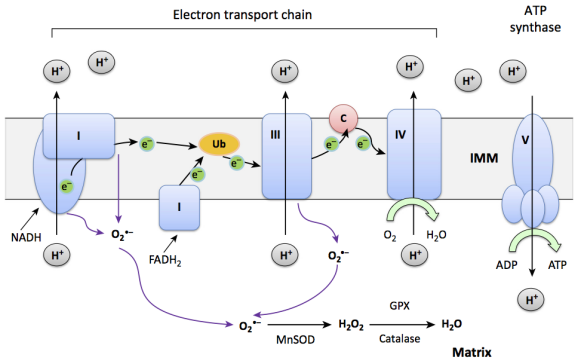

Figure 16. Reactive oxygen species generation and neutralization in the mitochondria. Schematic depicting the exchange of electrons in the mitochondrial membrane, along the electron transport chain of proteins. Superoxide ($O_2^{\bullet-}$) is produced at Complex I and Complex III and, in the presence of superoxide dismutase (SOD) is transformed into hydrogen peroxide (H_2O_2). Catalase or glutathione peroxidase (GPX) can then further neutralize H_2O_2 to water. Image from Yu et al. (2014).[110]

Oxidative stress has been faulted for many events in the pathogenesis and progression of β cell dysfunction and apoptosis,[120] but the effects on transcription factor function have been of particular interest. Studies have shown that MafA,[38,121] Pdx1,[38,122] and Nkx6.1[38] levels and/or function are reduced in the presence of high ROS, with broad implications for the general relationship between ROS and general β cell transcription. Additionally, there is evidence that amelioration of oxidative stress by antioxidant supplementation can reverse components of β cell dysfunction (*in vitro* studies) and diabetes (*in vivo* studies).[123,124]

Endoplasmic reticulum stress

Under normal physiological conditions, proteins are folded, modified, and packaged in the endoplasmic reticulum (ER), with the assistance of chaperones and modifying enzymes. When, in the course of normal cell function, an inevitable subset of proteins progress in unfolded, misfolded, or improperly modified forms, mechanisms exist to remove and degrade them (Figure 19).[125,126] If improperly processed proteins substantially accumulate, the unfolded protein response (UPR) is initiated, to increase expression of critical processing proteins, such that the backlog of unfolded proteins, or ER stress, can be resolved. Importantly, initiation of the UPR also halts the processing of any new protein. The presence of unfolded proteins is detected by direct and indirect signaling through a trio of ER transmembrane proteins, PERK, ATF-6, and IRE1α, which initiate transcriptional changes needed to address the glut of unfolded proteins.[127,128] If the UPR is chronically unable to relieve the ER stress, apoptotic mechanisms are triggered.[126,129]

A. Tissue	Cu/Zn SOD (% of liver)	Mn SOD (% of liver)
Liver	100 ± 7	100 ± 17
Kidney	99 ± 7	125 ±19
Brain	77 ± 8	67 ± 16
Lung	80 ±12	66 ± 17
Skeletal muscle	59 ± 7	95 ± 14
Heart muscle	70± 10	142 ± 9
Pituitary gland	79 ± 19	47 ± 11
Adrenal gland	175 ± 16	239 ± 25
Pancreatic islet	38 ± 9	30 ± 5

B. Tissue	Catalase (% of liver)	Glutathione Peroxidase (% of liver)
Liver	100 ± 10	100 ± 5
Kidney	78 ± 8	91 ± 9
Brain	36 ± 10	39 ± 8
Lung	50 ±10	58 ± 9
Skeletal muscle	41 ± 12	40 ± 10
Heart muscle	72± 11	39 ± 7
Pituitary gland	23 ± 2	66 ± 11
Adrenal gland	45 ± 7	77 ± 12
Pancreatic islet	n.d.	15 ± 6

Figure 17. β cells have extremely low levels of antioxidant enzymes. Tissue content of (A) superoxide dismutase (SOD), (B) catalase, and (B) glutathione peroxidase in a variety of tissue types, showing that in all cases, pancreatic islets have the lowest protein levels of any tissue presented. Data presented as percent of protein level detected in liver. Tables adapted from Lenzen et al. (1996).[115]

Secretory cells, such as β cells, that have constantly high levels of protein folding and processing, are particularly susceptible to ER stress. In conditions that further increase the demand for insulin production, such as insulin resistance and/or hyperglycemia, ER stress is additionally likely. ER stress has been proposed as a mechanism of β cell dysfunction and

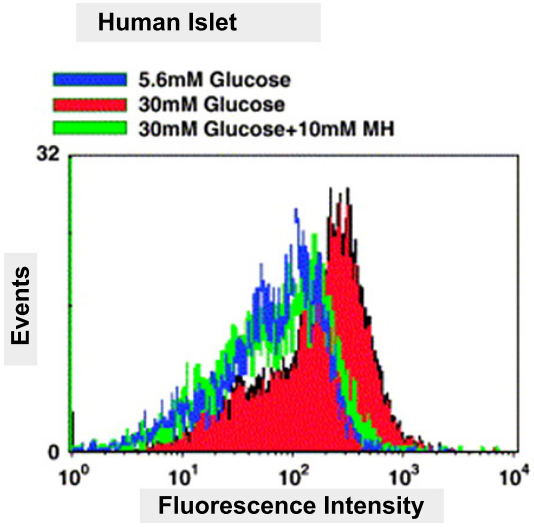

Figure 18. Glucose increases peroxide levels in isolated human islets. Flow-cytometric analysis using fluorescein-labeled dye to detect peroxide after 72 hour-incubation with 5.6mM glucose, 30mM glucose, or 30mM glucose with the hexokinase inhibitor mannoheptulose (MH), which prevents glucose metabolism. 30mM glucose increased peroxide levels, interpreted from the right-shift in the red peak, but prevention of glucose metabolism by MH ablated this effect (represented by the overlap of the green and blue peaks). Image from Robertson and Harmon (2006).[117]

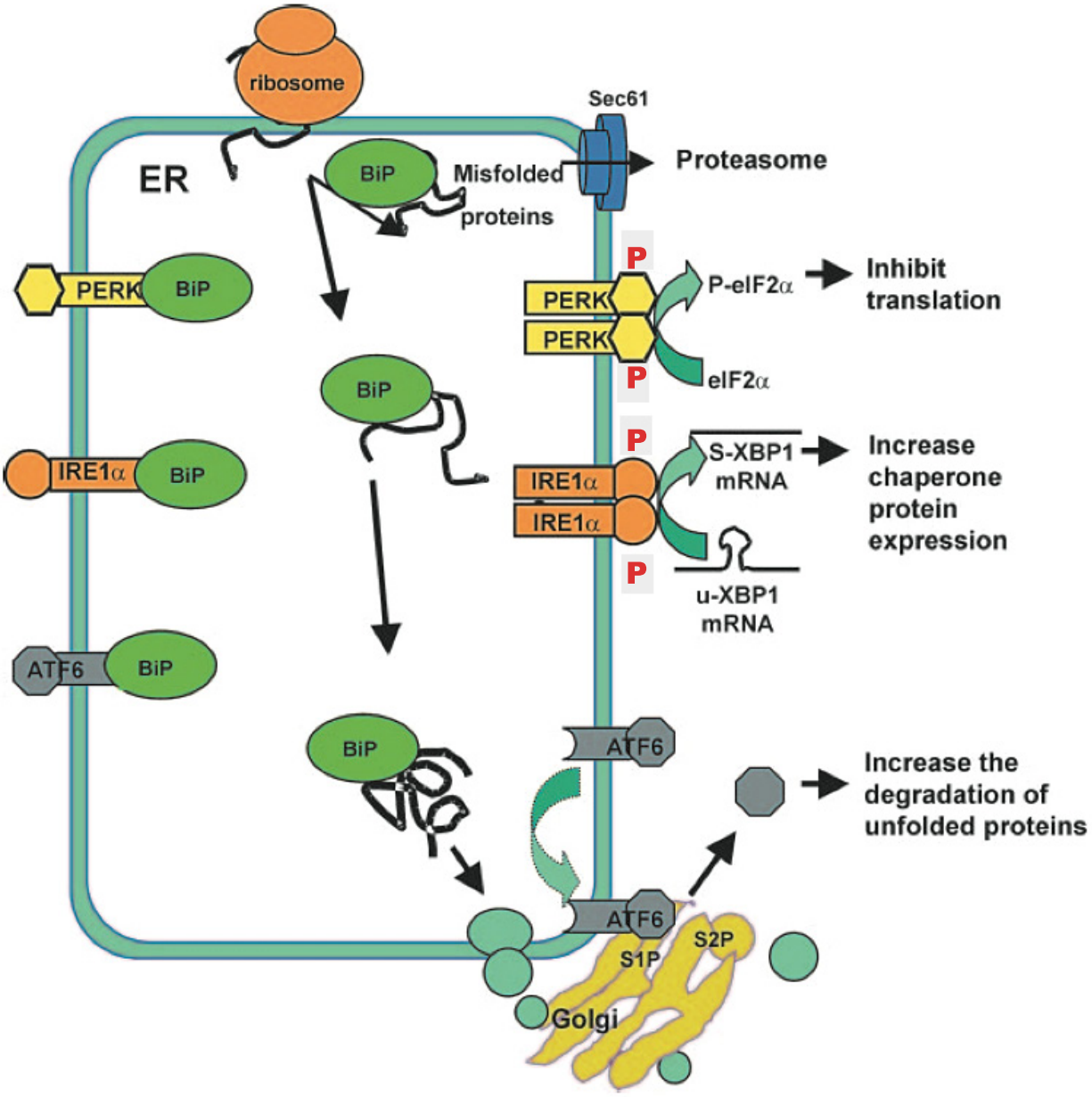

Figure 19. The unfolded protein response resolves ER stress. Depiction of the chaperone BiP mediating protein folding in the endoplasmic reticulum. Normal levels of misfolded proteins are delivered for proteasomal degradation. In cases of misfolded protein build-up, PERK signaling inhibits translation of new proteins, IRE1α signaling increases expression of chaperone proteins, and ATF6 signaling increases unfolded protein degradation. As a group, PERK, IRE1α, and ATF6 collaborate to ameliorate ER stress. Image from Haataja et al. (2008).[125]

apoptosis in diabetes,[128-131] although there remains disagreement as to whether ER stress is a major or minor contributor in the disease process.

Amyloid

Included among the contents of the insulin granule are the monomers of islet amyloid polypeptide (IAPP), a peptide implicated in the progressive loss of β cell function in T2DM.[125,132,133] IAPP is processed to its mature form in the Golgi and in the insulin granule, where it exists in a ratio of approximately 1:100 with insulin.[134,135] IAPP appears to have important roles in normal physiology, including contributions to gastric emptying, satiety signaling, and suppression of glucagon secretion.[134] However, human IAPP is capable of aggregating into both extracellular (Figure 20A) and intracellular (Figure 20 B-C) fibrils and larger deposits.[136,137] Importantly, mouse IAPP is not amyloidogenic and lacks the amino acid sequence identities that have been correlated with fibril formation in the human form.[138,139] The islets of T2DM patients have marked islet amyloid deposition,[133,135] and amyloid has been proposed to induce β cell dysfunction by multiple mechanisms, including induction of mitochondrial dysfunction, ER stress, oxidative stress, and autophagy dysregulation (Figure 20D).[136,140] *In vitro* studies have shown that amyloid formation can induce islet cell apoptosis,[106,107,141,142] potentially by disrupting the cell membrane.[143,144] In the context of islet transplantation, amyloid deposition correlates with graft failure,[145] underscoring the detrimental effect of amyloid deposition for β cell function. However, the mechanism(s) connecting amyloid and β cell dysfunction remain inadequately defined.

Aims of Dissertation

The aim of this work is to address the direct consequences on human islets *in vivo* of two characteristic components of Type 2 diabetes pathology, namely hyperglycemia and hyperlipidemia. Our understanding of gluco- and/or lipotoxicity in human islets is limited, in

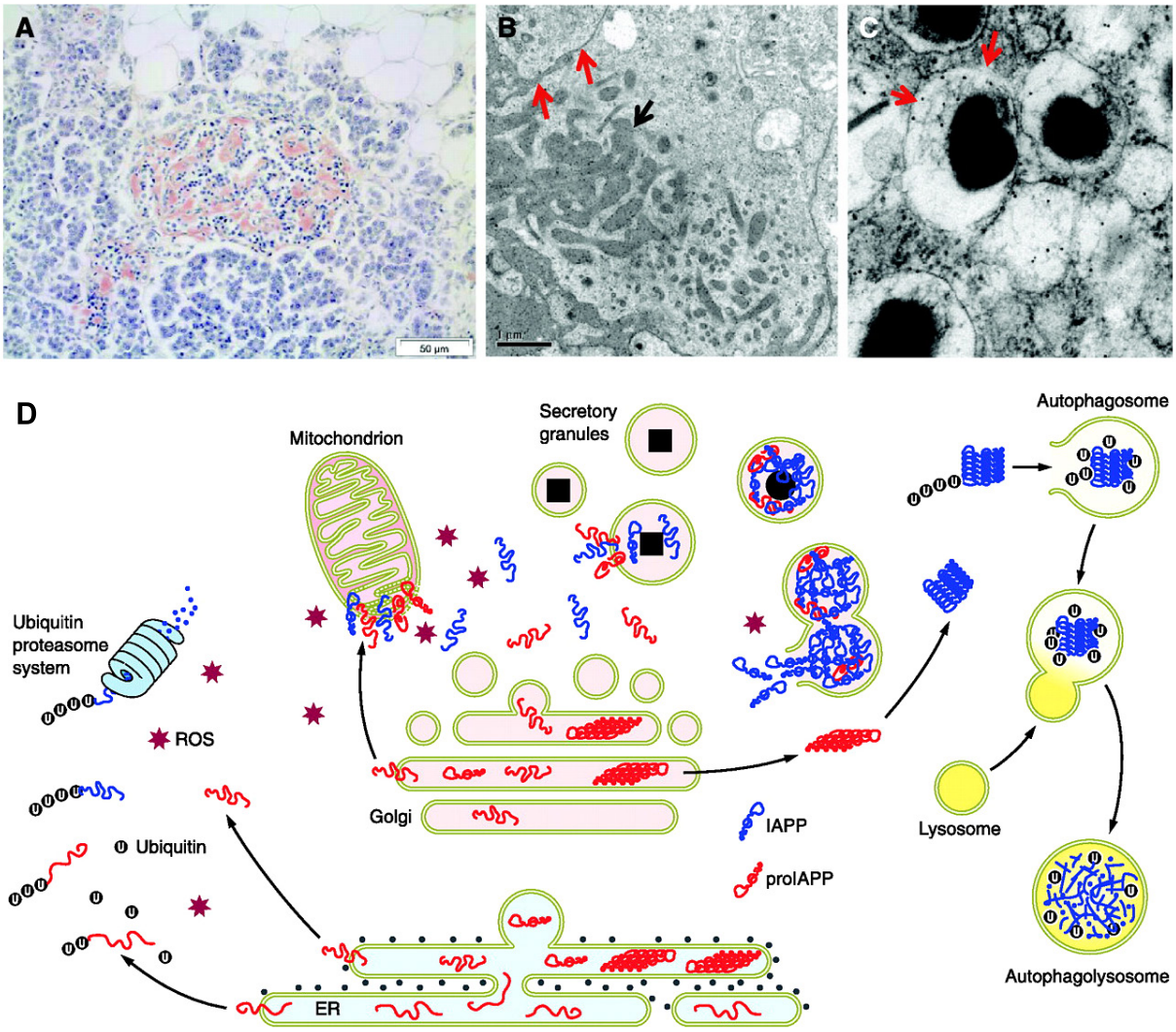

Figure 20. Evidence and proposed toxicity of islet amyloid. A. Congo red staining showing extracellular amyloid deposition in an human islet. B. Electron micrograph of human β cell showing intracellular amyloid fibrils (black arrow). C. Electron micrograph showing insulin granules of human IAPP transgenic mouse fed high-fat diet. ProIAPP-specific antibodies showing fibrils within insulin granules (red arrows). D. Schematic of proposed mechanisms of amyloid toxicity in β cells, depicting inappropriate formation of amyloid oligomers in the ER and Golgi, abnormal IAPP/oligomer presence in the cytosol, interference with mitochondrial membrane integrity, secretory granule fusion and/or rupture, and requirement of autophagy for oligomer degradation, rather than proteasomal breakdown. Images from Westermark et al. (2011).[139]

large part due to the difficulty of performing mechanistic studies in human islets *in vivo*. In Chapter III, we present work using three models in which human islets are exposed *in vivo* to hyperglycemia, insulin resistance, or both, with which we not only defined and probed the effects on human islets but also compared the response of human and mouse islets to identical metabolic conditions. Additional benefits of these studies include the ability to transplant human islets under normoglycemic conditions and only subsequently induce hyperglycemia. This sequence of events improves general graft survival and function and reduces confounding factors that impact studies of islet transplantation into hyperglycemic mice. In addition, this model exposes human islets to hyperglycemia without insulin resistance, a separation that is uncommon in mouse models. Conversely, the high-fat diet model used in these studies induces only mild hyperglycemia. Together, these two models allow us to address the boundaries of glucotoxicity versus lipotoxicity and determine what mechanisms may be distinct to, or more dominant in, one type of nutrient excess or the other.

An inherent complicating factor of all human islet studies is the variation in donor attributes, pancreas processing center, isolation protocol, and *in vitro* function among human islet preparations. Perifusion insulin secretion profiles vary to an unknown degree among islet preparations distributed for research. This has fundamental consequences for how human islet data is grouped and interpreted, as well as for decisions about which islet preparations to use for transplantation studies. To further our understanding of the relationships between donor/isolation attributes and islet function, we performed a comprehensive and systematic, post-hoc analysis of 183 human islet preparations used in our laboratory. This work is presented in Chapter IV.

The islet field maintains interest in growth factors that may promote increased β cell proliferation and enhanced function. In Chapter V, work is presented from early in my graduate studies that

aimed to define the role of epidermal growth factor receptor signaling in islet physiology. The extremely mild consequences of EGFR removal in β cells were unexpected.

The experimental methods used in these studies are detailed in Chapter II. A summary of findings, a discussion of their significance, and a description of future directions are presented in Chapter VI.

CHAPTER II

MATERIALS AND METHODS

Some methods in this chapter have been published in Kayton et al., 2015,[146] and others have been submitted for publication.

Mouse Models

All animal studies were approved by the Vanderbilt Institutional Animal Care and Use Committee. All animals were monitored by the Vanderbilt University Division of Animal Care, kept on a 12-hr light / 12-hr dark cycle, and allowed unrestricted access to food and water, expect where noted. Immunodeficient animals were housed in a certified pathogen-free barrier facility. All studies with human islets used de-identified samples and thus were not deemed human studies.

NSG-ob/ob

Adult male and female B6.Cg-+/*Lep*^{ob} mice (#000632, The Jackson Laboratory, Bar Harbor, ME) were mated with NOD.Cg-*Prkdc* ^{scid}*Il2rg*^{tm1Wjl}Sz (NSG) mice[147] (#005557, The Jackson Laboratory), and the *Lep*^{ob} mutation (abbreviated as *ob)* was subsequently backcrossed for 10 generations to the NSG strain to create the NSG-*ob* strain. The colony was maintained by intercrossing NSG +/*ob* heterozygotes. These crosses produced NSG-*ob/ob* mice as well as NSG +*/ob* and +/+ wild type (wt) controls. NSG-*ob/ob* and NSG-wt controls were studied at 3, 6, and 11 weeks of age.

NSG-Glut4$^{-/-}$

(B6;129 Sv)-*Glut4*$^{+/-}$ mice were mated with NSG mice, and the *Glut4* mutation was subsequently backcrossed for 10 generations to the NSG strain to create the NSG-*Glut4* strain. The colony was maintained by intercrossing NSG +/*Glut4* heterozygotes. These crosses produced NSG-*Glut4*$^{-/-}$ mice as well as NSG-*Glut4*$^{+/-}$ and *Glut4*$^{+/+}$ wild type (wt) controls.

NSG-HFD

To create diet-induced insulin resistance on the immunodeficient background, we fed NSG mice with regular or high-fat diet (HFD). Two high-fat diets were used: 45% or 60% of calories from fat (Research Diets, New Brunswick, NJ). The 45% HFD (D12451) contained 45% from fat, 35% of calories from carbohydrate, and 20% from protein. The 60% HFD (D12492) contained 60% of calories from fat, 20% from carbohydrate, 20% from protein. The 60% HFD was used in subsequent studies and was compared to a regular chow diet (Lab Diet, St. Louis, MO, #5001), which contained 13.5% of calories from fat, 58% from carbohydrate, and 28.5% from protein.

NSG-DTR

NSG-Tg(Ins2-HBEGF)6832)Ugfm/Sz mice, referred to as NSG-RIP-DTR mice, were developed by backcrossing the RIP-DTR transgene from a B6;CBA-RIP-DTR stock that was kindly provided by Pedro Herrera. The original B6;CBA Tg(Ins2-HBEGF)6832)Ugfm/Sz mice were made by injecting the RIP-DTR construct into B6;CBA eggs. The transgene was backcrossed using a marker assisted speed congenic method to the NOD.*Cg-Prkdc*^{scid}*Il2rg*^{tm1Wjl}*/SzJ* (abbreviated as NOD-*scid IL2r*γ^{null} or NSG) strain background. These NSG-RIP-DTR mice express the human diphtheria toxin receptor (DTR) driven by a rat insulin promoter (RIP). The RIP-DTR transgene was then fixed to homozygosity and maintained as a homozygous line. Transgenic mice, with two autosomal copies of the RIP-DTR transgene,[148] in which diphtheria

toxin receptor expression is driven by the rat insulin promoter, were backcrossed onto the NSG background[147] for more than 10 generations, resulting in the NSG-DTR mouse.

InsCreEGFR$^{fl/fl}$

EGFR$^{fl/fl}$ mice[149] on a mixed background were kindly provided by William Russell and Larry Scheving, at Vanderbilt University Medical Center. This line was backcrossed more than 10 generations onto the C57Bl/6 background. The C57Bl/6 EGFR$^{fl/fl}$ mouse was then crossed with the Tg(Ins2-Cre)1^{Herr},[150] here called the "InsCre" mouse, also on the C57Bl/6 background, yielding InsCre^{pos}EGFR$^{fl/+}$ animals, which were then crossed with the EGFR$^{fl/fl}$ mouse to yield a population of InsCre^{pos}EGFR$^{fl/fl}$ pups.

Islet isolation

Mouse islet isolations were performed by Anastastia Coldren of the Vanderbilt Islet Procurement and Analysis Core, part of the Vanderbilt Diabetes Research and Training Center. After dissection to expose the pancreas, the bile duct was ligated by suturing. Collagenase P (3mL of 0.6 mg/mL solution in Hank's balanced salt solution (HBSS), Gibco) was injected into the bile duct, resulting in infusion into and inflation of the pancreas. The pancreas was then removed and further digested in the same Collagenase P/HBSS solution by a wrist action shaker in a 37^{o}C water bath, then shaken manually at room temperature. Addition of cold HBSS with 10% fetal bovine serum (FBS) inactivated the collagenase. The digested tissue was washed three times in HBSS/10%FBS solution, with 2-minute 4^{o}C centrifugation at 1000 RPM and disposing of supernatant in between each wash. Islets were then plated in Petri dishes in the same solution and placed on ice until hand-picking in sterile, RNase-free conditions, to achieve near 100% islet purity (absence of exocrine tissue).

Human islet acquisition

Human islets were received by overnight shipment from centers supported by the National Institutes of Health (NIH), the Integrated Islet Distribution Program (IIDP, iidp.coh.org), Juvenile Diabetes Research Foundation (JDRF), or the Islet Cell Resource Centers (icr.coh.org), during the years 2002–2013. Islet preparations originated from the centers listed in a following section (Isolation centers). Islets were shipped overnight to Vanderbilt and plated into 15 ml of CMRL1066 medium at a density of 12,000 –15,000 IEQ per 10-cm nontreated tissue culture dish (Corning, Corning, NY; cat. no. 430591). From 2002 to 2007, 100 islets were perifused, and in each case an islet equivalent (IEQ) value was calculated, based on islet diameter. Since 2006, 60 islets of 180 um diameter (104 IEQs) have been used. Data from all years were normalized to 100 IEQ. Islets were handled and perifused as described below. Importantly, all human islet preparations were hand-picked in our laboratory prior to perifusion, enhancing the purity of human islets beyond the purity reported by the isolation center. Some perifusion profiles analyzed in Chapter IV were part of previously published datasets.[16,45,46,84]

Islet perifusion

Experimental protocol

Assessment of human or mouse islet function was performed by perifusion on the day of islet arrival (human), or the day after isolation (mouse) as previously described[46,146] and adapted from Wang et al., 1997.[151] The media base for all secretagogues was prepared fresh on the day of each perifusion. A batch of 1mL media was prepared by combining 1 bottle of Dulbecco's modified Eagle's medium powder (Sigma, #D5030), 3.2g $NaHCO_3$ (Sigma, #S6014), 0.58g L-glutamine (Sigma, #G8540), 0.11g sodium pyruvate (Sigma, #P2256), 1.11g HEPES (Sigma, #H7523), 1.0g RIA-grade BSA (Sigma, #A7888), 3mL of 0.5% phenol red (Sigma, #P0290), and

1L of deionized water. After dissolving into solution on a stir plate, the media was filter-sterilized (Millipore, #SCGPU05RE) and de-gassed for 30 minutes, in a 37°C water bath. 60 size-matched islets of 180-um diameter were perifused with 5.6mM glucose, 16.7mM glucose, and 16.7mM glucose with 100 μM 3-isobutyl-1-methyl-xanthine (IBMX) (Sigma, St. Louis, MO, #I5879-1G). Islets were loaded into Omnifit chromatography columns (Sigma, St. Louis, MO) with filtering frits (25um filtration size) and submerged in a 37°C water bath. The different media described were run to the columns by peristaltic pumps (Model CP 78001-00, Ismatech, Glattbrugg, Switzerland), through capillary tubing. Media fractions were collected every 3 minutes, at a rate of 1mL/min, by robotic fraction collectors (#2110, Bio-Rad). The insulin content of each fraction was measured by radioimmunoassay, and insulin content values were normalized to 100 IEQs.[146]

Islet transplantation

NSG-HFD, NSG-DTR, and NSG-S961 models

NSG or NSG-DTR male mice, between 12 and 20 weeks of age, were used for transplantation. For the NSG-HFD model: each mouse received 1500 IEQ human islets, 140 islets isolated from NSG mice, or 200 islets from C57BL/6J mice, transplanted under the kidney capsule. After two weeks of engraftment, the mice were placed on a regular diet (RD) or a high fat diet (HFD) for 12 weeks. For the NSG-DTR model: each recipient mouse received 2000 or 4000 human islet IEQs. For the S961 model: each recipient mouse received 4000 human islet IEQs. All data with human islets in Chapter III, from all models, were normalized to 2000 transplanted IEQs. Mouse islets for transplant were isolated from 13-15 week-old NSG or C57BL/6J mice (Jackson Laboratory, Bar Harbor, ME).

General transplantation protocol

Human and mouse islets were transplanted after overnight culture in 5mM glucose. Islets were loaded into tubing connecting to a 1mL syringe via a gel loading tip. Recipient mice were anesthetized with a mixture of 90 mg/kg ketamine (#45-290, Zoetis, Inc., Kalamazoo, MI) and 10 mg/kg of xylazine (#139-236, Lloyd Laboratories, Shenandoah, IA). The left side of the back was shaved and sterilized to prepare the surgical site. Once the mouse was fully anesthetized, a cut was made through the skin and muscle, and the kidney was exposed. A channel was created in the renal capsule using a 23-gauge butterfly needle, in preparation for insertion of the tubing. Islets were injected into the space underneath the capsule. Surgical glue was used to seal the puncture hole in the capsule. The muscle and skin were then closed using Vicryl 18” sutures (#5-0, Ethicon, Somerville, NJ), and the skin was stapled with 9mm Reflex9 stainless steel wound clips (CellPoint Scientific, Inc., Gaithersburg, MD). The mice recovered from anesthesia while wrapped in gauze, on a heating pad. Staples were removed 10-14 days after transplantation.

Nephrectomy

To remove the graft-containing kidney via survival surgery, the initial transplantation steps were followed until exposure of the kidney. The left renal artery and vein were ligated with 5.0 black braided silk suture (#SUT-15-1, Roboz Surgical, Rockville, MD). The kidney was then removed by severing the tissue between the ligation suture and kidney, using a scalpel. The incision site was then closed, according to general transplantation steps. Animals were sacrificed within 48 hours after nephrectomy.

Human Islet Assessment

Individual isolation centers have performed static culture of isolated human islets and now regularly report these data to the IIDP (some of these data are presented in Fig. 43H, thanks to the assistance of Barbara Olack). The IIDP-published protocol for this static culture (QA-005 Potency Test: Glucose Stimulated Insulin Release Assay) can be found at https://iidp.coh.org/investigator_sops.aspx. Static culture assays performed in our laboratory (Fig. 43I) measured insulin secretion from 60 size-matched islet into RPMI medium over 1 h at 37°C. Previously published data points (open squares) reflect the stimulation index of secretion at 11 mM glucose divided by secretion at 5 mM glucose. New data points (closed squares) reflect the stimulation index of secretion at 16.7 mM glucose divided by secretion at 5.6 mM glucose.

Isolation centers

Islets in the studies found in Chapter IV were procured from the following isolation centers (in alphabetical order): Emory University (Atlanta, GA), National Institutes of Health (Bethesda, MD), Northwestern University (Chicago, IL), Scharp Lacy Research Institute (Irvine, CA), Southern California Islet Consortium (City of Hope, Duarte, CA), University of Alabama (Birmingham, AL), University of Colorado (Denver, CO), University of Illinois (Chicago, IL), University of Massachusetts (Worcester, MA), University of Miami (Miami, FL), University of Minnesota (Minneapolis, MN), University of Pennsylvania (Philadelphia, PA), University of Pittsburgh (Pittsburgh, PA), University of Wisconsin (Madison, WI), and Washington University (St. Louis, MO). The ordering of this list has no relation to Centers 1–15, as labeled in Chapter IV.

Definition of donor and islet attributes

"Donor attributes," characteristics of the human pancreas donor reported by the Organ Procurement Organization (OPO) to the islet isolation center, and "Islet attributes," characteristics of isolated islet preparations that the IIDP/ICR reports to investigators, are listed in Table 5. Protocols for viability and purity quantification are available on the IIDP website at http://iidp.coh.org/investigator_sops.aspx.

Definition of perifusion attributes

"*In vitro* responsiveness" was defined by Baseline (the insulin concentration of the last fraction collected before introduction of 16.7 mM glucose), $Peak1_{Max}$ (highest point of the Peak in response to 16.7 mM glucose), $Peak2_{Max}$ (highest point of the Peak in response to 16.7 mM glucose + IBMX), Fold 1 ($Peak1_{Max}$/Baseline), Fold 2 ($Peak2_{Max}$/Baseline), and Peak Difference ($Peak2_{Max}$-$Peak1_{Max}$). A Peak is defined as having a collected fraction with an insulin concentration more than 1.5 times that of the Baseline value.

Insulin content of pancreas and islet grafts

Harvested pancreata were rinsed with 1X PBS, blotted to remove excess liquid, weighed, immersed in 2 mL of acid alcohol (1 mL of 10N HCL brought up in 110 mL 95% ethanol), and placed on ice. Mechanical homogenization was achieved with the Polytron PT 10/35 homogenizer (Brinkmann Instruments, Riverview, FL). During homogenization, 3 mL additional acid ethanol was added to each sample. Tubes rotated for 48 hours at 4^{o}C to complete insulin extraction. Supernatant from 30-min. centrifugation at 2500 rpm was stored at -80^{o}C until further use. Mouse and human islet grafts were excised from under the renal capsule after removal of the kidney from anesthetized mice. Kidney tissue was surgically removed to the greatest extent possible, and grafts were placed into 200uL acid ethanol. Grafts were manually homogenized

using polypropylene pestles until samples were visually homogenous. Samples rotated for 48 hours at 4°C to complete insulin extraction. Tissue human insulin or total insulin (mouse and human) was measured using species-specific radioimmunoassays from Millipore (Billerica, MA, catalogue #RI-14K or #RI-13K, respectively), either in the laboratory or by the Vanderbilt University Hormone Assay and Analytical Services Core. Serum mouse insulin was calculated as the difference between total (mouse/rodent, cross-reactive with human) and human-specific insulin measurements.

Genotyping

The REDExtract-N-Amp™ Tissue PCR Kit (XNAT-100RXN, Sigma, St. Louis, MO) was used to extract DNA from mouse tail snips and to prepare PCR samples, and all aspects of the kit were used according to manufacturer's instructions. DNA samples were stored at 4°C or used immediately for PCR. Primers for InsCre and EGFR were obtained from Integrated DNA Technologies (Coralville, IA). Original primer stocks were reconstituted from powder in DNase-free water to 100 uM and were then diluted to working stocks of 20 uM in RNAse-free water (#46-000-CI, Corning cellgro, Manassas, VA) and stored at -20°C. The DNA was amplified by PCR, and the products were resolved on 1.5% agarose gels with (#A20090Research Products International Corp., Mt. Prospect, IL) with 100 ng/mL ethidium bromide (#161-0433, Bio-Rad, Hercules, CA) in 1X TBE buffer and compared to a 100 base-pair ladder. Primer sequences and thermocycler programs are listed in Table 1.

Glucose Tolerance Tests and Blood Glucose Measurements

Intraperitoneal glucose tolerance tests were performed after a 6-hour fast in cages with ALPHA-dri™ bedding, to prevent ingestion of corncob bedding particles. 10% glucose solution was made by dissolving D-(+)-Glucose (G7528, Sigma, St. Louis, NJ) in 1X phosphate buffered

Table 1. PCR primers and conditions for genotyping		
Mouse Model	**Genotyping Primers**	**PCR Conditions**
NSG-*ob/ob*	5' TGT CCA AGA TGG ACC AGA CTC - 3' (forward) 5' ACT GGT CTG AGG CAG GGA GCA 3' (reverse)	1. 94°C….3′ 2. 94°C….30″ 3. 62°C….1′ 4. 72°C….45″ Repeat 35 cycles 72°C….2′ 10°C….hold
NSG-*Glut4*$^{-/-}$	5' - TCT TGA TGA CCG TGG CTC TG - 3' (forward) 5' - GAA TGG GCT GAC CGC TTC CTC GTG - 3' (reverse)	95°C….15′ 94°C….30″ 67°C….30″ 72°C….1′ Repeat 34 cycles 72°C….8′ 4°C….hold
Ins-Cre	5' - TAA GGC TAA GTA GAG GTG T - 3' (forward) 5' - TCC ATG GTG ATA CAA GGG AC - 3' (reverse)	94°C….3′ 94°C….30″ 55°C….30″ 72°C….1′ Repeat 39 cycles 72°C….10′ 4°C….hold
RIP-Cre	5' - TGC CAC GAC CAA GTG ACA GC - 3' (forward) 5' CCA GGT TAC GGA TAT AGT TCA TG - 3' (reverse)	93°C….3′ 93°C….20″ 60°C….20″ 72°C….45″ Repeat 30 cycles 72°C….5′ 4°C….hold
EGFR$^{fl/fl}$	5' - CTT TGG AGA ACC TGC AGA TC - 3' (forward) 5' - CTG CTA CTG GCT CAA GTT TC - 3' (reverse)	94°C….5′ 94°C….30″ 60°C….1′ 72°C….1′ Repeat 35 cycles 72°C….7′ 4°C….hold

saline (PBS**)** (#14190-144, Gibco), and sterilized by syringe filter (Thermo Scientific/Nalgene 0.22um PES 25-mm filter). Solution was allowed to equilibrate for 5 hours prior to use. Animals were weighed at the end of the fasting period and received 2g/kg glucose. Blood glucose values were measured from nicks in the tail vein at the zero-minute and fifteen-minute timepoints, using an Accucheck Aviva glucometer and compatible strips (Roche, Indianapolis, IN). Intraperitoneal injections were performed with a 27-gauge needle and 1mL insulin syringe (Becton Dickinson & Co., #305109 and #329654). Blood glucose was subsequently measured at 15, 30, 60, 90, and 120 minutes after glucose injection.

Insulin tolerance tests

Mice were fasted for 4 hours and weighed, then fasting blood glucose was measured. Mice were then injected i.p. with 0.5units/kg of Novolin R, diluted in 1X PBS from 100U/mL stock solution (NDC 0169-1833, Novo Nordisk, Plainsboro, NJ). Blood glucose was subsequently measured at 15, 30, 60, 90, and 120 minutes (or until the blood glucose level returned to fasting levels) after injection. All other materials and methods are as described above, for glucose tolerance tests.

Glucose-arginine stimulation

In vivo insulin secretion by human or mouse islets was assessed by glucose-arginine stimulation. Following a 6-h fast, each animal, regardless of weight, received a 500 uL intraperitoneal injection of solution containing 62.5 mg dextrose (#G7528) and 62.5 mg L-arginine (#A6969-25G, Sigma, St. Louis, MO). Blood samples were drawn from the retroorbital space both before and 15 minutes after the injection, using heparinized blood collection tubes (#02-668-10, Fisher Scientific, Pittsburgh, PA), and immediately placed on ice. Plasma was separated as supernatant after 10-minute centrifugation at 13,000 rpm of total

blood samples, and plasma was stored at -80°C until further use. All *in vivo* insulin secretion data used in the retrospective analyses of human islet preparations (Chapter IV) reflect human islets that were transplanted into normoglycemic mice on regular chow diet, and data were normalized to the number of islet equivalents transplanted.

Serum lipid quantification

Serum triglyceride and cholesterol levels were measured from 10uL of plasma, collected retro-orbitally, using commercially available kits (#R85457 and #R80035, Raichem, Cliniqa, San Marcos, CA), according to manufacturer's instructions.

Percent fat and lean mass

Mouse body composition was measured using a Bruker Minispec Analyzer (Bruker Optics, TX) in the Vanderbilt Mouse Metabolic Phenotyping Center.

Compound preparation and delivery

Diphtheria toxin

Diphtheria toxin (DT) (Product #150, List Biological Laboratories, Inc., Campbell, CA) was administered in a single, 300uL i.p. injection of 0.5, 1.0, 2.5, 5.0, 10, or 25 ng total DT. Control NSG-DTR mice (PBS) were treated with an equal volume of 1X PBS (Sigma, St. Louis, MO). All animals in a cohort (with human islets from the same human donor) were injected with DT or PBS on the same day. Stock solutions reconstituted with water were stored at -20°C, according to manufacturer's recommendations, and stock solution aliquots were diluted for each use.

S961

S961 reagent[152,153] was provided by Dr. Lauge Schäffer, Novo Nordisk, Denmark. S961 is a 43-amino acid peptide antagonist that induces many consequences of insulin resistance in rodents, including hyperglycemia, hyperinsulinemia, decreased hepatic glycogen storage, and decreased adipocyte triglyceride storage.[152,153] S961 or 1X PBS was loaded into either Alzet 2001 (200 uL at 10nM) or Alzet 1002 (100 uL at 20nM) osmotic pumps (Alzet, Cupertino, CA). Pumps were implanted subcutaneously, 2 weeks after human islet engraftment. Animals were sacrificed and tissues were harvested at either 7 or 14 days after pump implantation.

Recombinant EGF

Recombinant murine EGF (PeproTech, Rocky Hill, NJ, #315-09) was reconstituted from lyophilized powder in MilliQ water, to a concentration of 1.0ug/uL. Using the molecular weight of EGF, 50nM concentrations were calculated and used in media for static islet culture experiments. Reconstituted EGF was stored at 4^{o}C for up to one week, or at -20^{o}C for longer periods.

Islet static culture with EGF

Aliquots of 30 size-matched islets were cultured for two hours in serum-free perifusion media, rather than in RPMI-1640, to avoid potential pre-experimental exposure to EGF from serum. Within 6-well, non-treated tissue culture plates, islets were transferred to wells containing one of the following conditions: (i) 5.6 mM glucose, (ii) 5.6 mM glucose + 50 nM EGF, (iii) 16.7 mM glucose, or (iv) 16.7 mM glucose + 50 nM EGF. Each condition was performed in triplicate. Islets were cultured in experimental media for 1 hour at 37^{o}C, after which islets were collected from media and a 1mL sample from each experimental well was collected for insulin RIA. Insulin values were normalized to 100 IEQ.

Tissue Collection, Fixation, and Preparation

Upon dissection from anesthetized animals, pancreata or graft containing kidneys were fixed in 4% paraformaldehyde (Electron Microscopy Sciences, #15710) in 0.1M PBS (a solution of 2.0g KCl, 2.04g monobasic KH_2PO_4, 8.0g NaCl, and 12.07g dibasic Na_2HPO_4, in purified water). After 90 minutes of fixation on ice, with mild agitation on a rocker, samples were washed with pure 0.1M PBS 4 times over the course of 2 hours. Tissues then equilibrated overnight in a 30% (w/w) sucrose solution at 4°C. Equilibrated tissues were then prepared for cryosectioning. Samples were embedded in Tissue-Tek Optimal Cutting Temperature (OCT) reagent, housed in Tissue-Tek cryomolds (VWR, Radnor, PA, #25608-930 and #25608-916). Pancreata were oriented with the long dimension of the organ running top-to-bottom in the mold. Graft-bearing kidneys were cut across the width of the organ (a cross-section) at the edge of the islet graft, and both halves of the kidney were placed, cut surface facing down, into the mold. Embedded tissues were completely frozen through on dry ice before storage at -80°C. Cryosections of 5-8um were cut on a cryostat and placed on Superfrost Gold Plus slides (Fisher Scientific, #15-188-48). All slides were stored at -80°C.

Immunohistochemistry

Immunohistochemical studies were performed as described.[45,154-156] Primary antibodies used are listed in Table 2, and secondary antibodies are listed in Table 3. Frozen slides thawed and dried at room temperature, then tissue sections were circled with a Super PAP Pen HT hydrophobic marker (#195505, Research Products International). In most cases, tissues were post-fixed for 10 minutes in 1% paraformaldehyde before three 5-minute washes in 1X PBS. Tissue was permeabilized by treatment with 0.2% Triton X-100 for ten minutes, then washed three times more in 1X PBS. Tissue was blocked with 5% normal donkey serum for 90 minutes in a humidified chamber, to minimize non-specific binding of secondary antibodies that were

raised in donkey. Primary antibodies were then applied at the concentrations listed in Table 2. All antibodies (primary and secondary) were diluted in 0.1% Triton X-100 with 1% BSA. Sections incubated in primary antibodies overnight, at 4°C. Before addition of secondary antibodies, sections then underwent three 10-minute washes in 0.1% Triton X-100, to remove unbound primary antibodies. Sections incubated in secondary antibodies at room temperature for one hour before three 15-minute washes in 0.1% Triton X-100, followed by three 5-minute washes in pure 1X PBS. Slides were mounted with SlowFade Gold antifade reagent with DAPI (#S36938, Invitrogen, Waltham, MA), sealed with fingernail polish, and allowed to dry completely before imaging.

Imaging

Images for morphometric analyses were acquired using an Olympus BX-41 fluorescence microscope connected to a MicroFire camera (Olympus America). Confocal imaging was performed in collaboration with the Vanderbilt University Cell Imaging Shared Resource, with a Zeiss LSM 510 META laser confocal microscope (Carl Zeiss Microimaging).

Electron microscopy

Ultrastructure of β cells and vasculature were studied by transmission electron microscopy.[156,157] Mouse pancreas and grafts were perfused intracardially with fixative (a solution of 2% paraformaldehyde, 2.5% glutaraldehyde in 0.1M sodium cacodylate, and 1% $CaCl_2$), with the assistance of Masakazu Shiota. Pancreata and graft-containing kidneys were removed after perfusion and fixed in 2.5% gluteraldehyde in 0.1M cacodylate buffer for 1 hour, then stored at 4°C overnight. The next day, samples were washed 3 times in 0.1M cacodylate buffer, incubated for 1 hour in 1% osmium tetroxide, and washed again with the 0.1M cacodylate buffer. Samples then went through a graded ethanol dehydration protocol (30%, 50%, 70%, 80%, and 95%

Table 2. Primary antibodies for immunohistochemistry and immunocytochemistry				
Antigen	**Species**	**Dilution**	**Source**	**Catalog #**
Insulin	Guinea pig	1:500	Dako	A0564
Glucagon	Rabbit	1:100	Cell Signaling	2760s
Glucagon	Mouse	1:500	abcam	ab10988
MafA	Rabbit	1:25000	Dr. Roland Stein (Vanderbilt University)	BL1225
Pdx1	Goat	1:10000	Dr. Christopher V.E. Wright (Vanderbilt University)	N/A
Somatostatin	Sheep	1:500	American Research Products	13-2366
Caveolin-1	Rabbit	1:2000	Abcam	ab2910
mouse PECAM	Rat	1:100	BD Pharmingen	550389
Ki67	Rabbit	1:500	Abcam	ab15580
Nkx6.1	Rabbit		Beta Cell Biology Consortium	N/A
Insulin	Guinea Pig	1:200	Linco	4030-01F
human CD31	Mouse	1:500	BD Pharmingen	555444

Table 3. Secondary antibodies for immunohistochemistry and immunocytochemistry					
Host Species	**Primary Ab Species**	**Fluorophore**	**Dilution**	**Source**	**Catalog #**
Donkey	Rabbit	Cy2	1:200	Jackson Immunoresearch	711-225-152
Donkey		Alexa488	1:200	Jackson Immunoresearch	711-545-152
Donkey		Cy3	1:500	Jackson Immunoresearch	711-165-152
Donkey		Cy5	1:200	Jackson Immunoresearch	711-175-152
Donkey	Goat	Cy3	1:500	Jackson Immunoresearch	705-165-147
Donkey	Rat	Cy2	1:200	Jackson Immunoresearch	712-225-153
Donkey	Sheep	Cy2	1:200	Jackson Immunoresearch	703-225-155
Donkey		Cy5	1:500	Jackson Immunoresearch	713-175-147
Donkey	Guinea Pig	Cy2	1:200	Jackson Immunoresearch	706-225-148
Donkey		Alexa488	1:200	Jackson Immunoresearch	706-545-148
Donkey		Cy3	1:500	Jackson Immunoresearch	706-165-148
Donkey		Cy5	1:200	Jackson Immunoresearch	706-175-148
Donkey		Alexa647	1:200	Jackson Immunoresearch	706-605-148
Donkey	Mouse	Alexa488	1:200	Jackson Immunoresearch	715-545-150
Donkey		Alexa 594	1:200	Jackson Immunoresearch	715-585-150

ethanol, then three washes in 100% ethanol). Dehydrated samples were then incubated in 100% ethanol and propylene oxide, then in two washes of pure propylene oxide. Samples underwent a series of incubations in increasing epoxy resin concentrations, culminating in tissue embedding in pure resin and polymerization at 60^{o}C for 48 hours. Embedded tissue sections of 500nm thickness were stained with 1% toluidine blue and imaged on a light microscope, to detect the location of islets. Thin sections (60-80nm) were cut, collected on copper mesh grids, and stained with 2% uranyl acetate and lead citrate. Samples were then imaged on the Philips/ FEI Tecnai T12 microscope at various magnifications, with the assistance of Janice Williams.

Morphometric analysis

Quantification of Ki-67^{+} cells, TUNEL^{+} cells, intracellular lipid droplets, and area analyses of amyloid and β cells were all performed using MetaMorph 7.7 software (Molecular Devices, Sunnyvale, CA). In all cases, at least 3 sections per animal were analyzed. For cell counting, at least 1000 β cells per animal were counted.

Detection of apoptosis, superoxide, and amyloid

Apoptosis was assessed by immunofluorescent TUNEL stain using the TUNEL Apoptosis Detection Kit (#17-141, Millipore, Billerica, MA) according to the manufacturer's instruction. Dihydroethidium (DHE) (#D7008, Sigma, St. Louis, MO) was used to measure O_2^- in cryosections. Sections were washed 3 times by PBS followed by DHE staining for 30 minutes, followed by staining for hormones. Fluorescence intensity of islet grafts was quantified using ImageJ software and was normalized to regular diet group [158]. To assess amyloid deposits, frozen tissue sections were incubated with 0.5% concentration Thioflavin S (#T-1892, Sigma, St. Louis, MO) in PBS for 30 minutes, prior to further staining.

Quantitative RT-PCR

Total RNA from human grafts or mouse islets was isolated using an Ambion RNAqueous kit (#AM1912, Ambion, Austin, TX), as previously described.[46] Contaminating trace DNA was eliminated using the Ambion TURBO DNA-free kit (#AM1907). In preparation for RNA isolation, islets or grafts were washed three times in 1X PBS, with all solution removed after the third wash, and stored at -80°C. The quality of extracted RNA was analyzed by the Vanderbilt Genome Sciences Resource. An RNA Integrity Number (RIN) greater than 7 was required for quantitative RT-PCR. cDNA was generated from RNA using the High-Capacity cDNA Archive Kit with RNase inhibitor (#4368814 and #N8080119, Applied Biosystems, Waltham, MA). Quantitative RT-PCR was performed using the TaqMan primer-probe and reagents from Applied Biosystems (Foster city, CA) as described,[46] using the primers listed in Table 4. Quantitative PCR was performed on the iQ5 Multicolor Real-Time PCR Detection System (Bio-Rad). *ACTB*, *TBP*, and *TFRC* were used as endogenous control genes. Relative changes in mRNA expression were calculated by the comparative ΔCt method using Applied Biosystems' Step One Plus software. Quantitative RT-PCR analysis followed the MIQE guidelines.[159]

siRNA-mediated knockdown in EndoC-βH1 cells

Knockdown of NKX6.1 and MAFB was accomplished 3 days prior to GSIS using the Dharmafect #1 reagent following manufacturer's protocol. Briefly, ON-TARGETplus Smartpool siRNA against human NKX6.1 (#L-020083-00), human MAFB (#L-009018-00; GE Dharmacon) and scrambled non-targeting siRNA (#D001810; GE Dharmacon) were introduced into $2x10^6$ EndoC-βH1 cells[160] in antibiotic-free media. Following an overnight incubation, the cells were grown in normal growth media for an additional 36h, and then overnight in low glucose medium (1.1mM Glucose, 2% bovine serum albumin, 50μM 2-mercaptoethanol, 10mM nicotinamide, 5.5μg/mL transferrin, 6.7ng/ml selenite and penicillin-streptomycin at 100units/mL). Cells were incubated

Table 4. Primers for quantitative real-time PCR			
Primer	**Assay ID (human)**	**Primer**	**Assay ID (mouse)**
INS	Hs02741908_m1	*Ins2*	Mm00731595_gh
GCG	Hs01031536_m1	*Gcg*	Mm01269055_m1
IAPP	Hs00169095_m1	*Iapp*	Mm00439403_m1
GCK	Hs01564555_m1	*Gck*	Mm00439129_m1
SLC2A1	Hs00892681_m1	*not measured in mouse*	N/A
SLC2A2	Hs01096904_m1	*Slc2a2*	Mm00446229_m1
GLP1R	Hs00157705_m1	*Glp1r*	Mm00445292_m1
BID	Hs00609632_m1	*Bid*	Mm00626981_m1
BAD	Hs00188930_m1	*Bad*	Mm00432042_m1
DDIT3	Hs00358796_g1	*Ddit3*	Mm00492097_m1
SOD1	Hs00533490_m1	*not measured in mouse*	N/A
SOD2	Hs00167309_m1	*not measured in mouse*	N/A
CAT	Hs00156308_m1	*not measured in mouse*	N/A
GPX1	Hs00829989_gH	*not measured in mouse*	N/A
UCP2	Hs01075225_m1	*not measured in mouse*	N/A
NFE2L2	Hs00975961_g1	*not measured in mouse*	N/A
HSPA5	Hs00607129_gH	*Hsp5a*	Mm00517690_g1
HSP90b1	Hs00427665_g1	*Hsp90b1*	Mm00441926_m1
PDIA4	Hs01115905_m1	*Pdia4*	Mm00437958_m1
NKX6.1	Hs00232355_m1	*Nkx6.1*	Mm00454961_m1
MAFA	Hs01651425_s1	*Mafa*	Mm00845206_s1
MAFB	Hs00534343_s1	*Mafb*	Mm00627481_s1
PDX1	Hs00236830_m1	*Pdx1*	Mm00435565_m1
PAX6	Hs00240871_m1	*Pax6*	Mm00443081_m1
FOXO1	Hs01054576_m1	*Foxo1*	Mm00490672_m1
EGFR	Hs01076078_m1	*Egfr*	Mm00433023_m1
ERBB2	Hs01001580_m1	*ErbB2*	Mm00658541_m1
ERBB3	Hs00176538_m1	*ErbB3*	Mm01159987_m1
ERBB4	Hs00955525_m1	*ErbB4*	Mm01256813_m1
ACTB	Hs99999903_m1	*Actb*	Mm00607939_s1
TBP	Hs99999910_m1	*Tbp*	Mm00446971_m1
TFRC	Hs99999911_m1	*Tfrc*	Mm00441941_m1

for 1h in DMEM base medium supplemented with 5.5mM glucose or 15.5mM glucose. Secreted insulin was analyzed from culture medium and was normalized to the insulin content following cell lysis (cell lysis buffer: 1M Tris, Triton x-100, glycerol, 5M NaCl, 0.2M EGTA, protease inhibitor tablet). Insulin levels were analyzed by the Vanderbilt Hormone Assay Core.

Statistical analysis

General statistics

Statistics were performed in GraphPad Prism 6 (GraphPad Software, Inc., La Jolla, CA). Results are shown as mean ± SEM. The student *t* test (for two groups) or one-way ANOVA (analysis of variance, for three or more groups) were used for statistical analysis, and a *P* value <0.05 was considered significant.

Statistical analyses of data from human islet preparations

This describes the statistical analyses used in Chapter IV. The criterion of isolation centers with seven or more islet preparations for further analysis was established by examining the distribution of islet preparations per center. We chose the cut-off point of seven as it provided the best balance between observations per center and number of different centers examined. To study the full spectrum of individual attributes at each site required a control for any potential effect of the center and a sufficient number of islet preps from each center. For univariate analyses, we used a Wilcoxon rank sum test to assess differences between the distributions of islet attributes for each donor attribute. This nonparametric test makes no assumptions about the normality of the islet attribute. We compared our univariate results to an analysis of variance (ANOVA) of log-transformed islet attributes and found no meaningful differences; thus, for all further adjusted analyses, we continued with the log-transformed ANOVA approach,

which provides easier interpretation and the ability to adjust for covariates. We also examined the impact of variable missingness on all islet attributes, treating missingness as a categorical variable; this revealed no relationships be- tween missingness and islet attributes. All categorical variables (Center, Race, Sex, Cause of Death, Estimated Culture Time, and Year) were treated as factors. Continuous variables (Cold Ischemia Time, age, BMI, Viability, and Purity) were modeled as a continuous variable in linear regression and were also binned into quantiles and treated as a categorical variable in an ANOVA. For univariate analyses, statistical significance (calculation of a *P* value) was assessed by a Student's *t*-test of the regression coefficient. For adjusted analyses, significance was assessed by a one-degree-of-freedom likelihood ratio test comparing a full model (with covariate and variable of interest) to a reduced model (with the covariate only). Polytomous regression was conducted to examine pairwise differences between categorical outcomes. Individual perifusion data points (24 per islet preparation, fractions 7–30) were modeled using a nonlinear mixed-effects model with an eight-knot spline function. Eight knots were chosen to optimally capture the characteristic features of the islet response curve while preserving degrees of freedom. This analysis hierarchically fits an islet response curve separately within each categorical group of the analysis, allowing qualitatively different curve fits within each group. The spline analyses were performed assessing the effects of categorical variables, allowing different insulin secretion response curves to be fitted within different categories of the variable. Continuous variables were not modeled in this way, because selecting cut-off values to generate categorical "bins" would not be biologically informed and would significantly reduce statistical power. Statistical significance for these analyses was assessed by a likelihood ratio test comparing a full model (with one random effect for the variable of interest and one for the individual) to a reduced model (with a random effect for individual alone). All statistical analyses were conducted using R 3.0.1, packages (nlme,

lmeSplines), and functions (lm, glm, aov, and lme). The procedures used for this modeling are available upon request. Linear regression analyses were performed using Prism v. 6.0d.

CHAPTER III

IN VIVO METABOLIC STRESS IMPAIRS ISLET TRANSCRIPTION FACTOR EXPRESSION AND INSULIN SECRETION IN HUMAN ISLETS

The text and data in this chapter are part of a submitted manuscript. Some figures from that paper, included in this chapter, represent data collected by Chunhua Dai.

Introduction

Patients with Type 2 Diabetes (T2DM) have impaired insulin secretion in response to glucose,[96,161,162] and this β cell dysfunction is progressive, often requiring exogenous insulin therapy. Physiological levels of glucose and lipid stimulate insulin secretion. In excess, however, these nutrients are thought to directly impair insulin secretion and other aspects of β cell function and survival, a phenomenon often referred to as “glucotoxicity”, “lipotoxicity”, and “glucolipotoxicity,” indicating the pathological consequences of excess glucose and/or lipid.[120,163-165] Glucotoxicity and lipotoxicity are widely regarded as important contributors to the progressive decline of β cell function in T2D.

Using rodent cell lines,[89,93,166,167] cultured rodent and human islets,[92,168] and *in vivo* rodent models,[99,169] investigators have suggested that excess glucose and/or lipid reduce insulin gene transcription,[166] insulin content, glucose-stimulated insulin secretion,[102,170,171] and exocytotic events.[89,90,92] Use of somatostatin, to “rest” β cells by halting insulin secretion, does not reverse or prevent these effects, suggesting that these toxicities are not simply due to insulin depletion.[172] Increased islet amyloid deposition, which is associated with β cell dysfunction and apoptosis in T2D patients,[140,173] is also a proposed consequence of excess glucose and/or lipid.[174,175] Both *in vitro* and *in vivo* studies in rodent models have implicated excess glucose and/or lipid in promoting β cell apoptosis.[103,176] Based on *in vitro* studies, the lipid contribution

to apoptosis depends on the lipid species, with saturated fatty acids promoting apoptosis,[177] potentially through ceramide formation,[178,179] altered lipid partitioning,[180,181] or oxidative stress.[118-120]

Expression and function of transcription factors critical to β cell development and function, particularly MafA, Nkx6.1, and Pdx1, were also reduced by high glucose and/or lipid in cultured islets or *in vivo* rodent T2D models.[38] In fact, transgenic mis-expression of MafA is able to partially rescue many of islet β cell deficiencies in db/db mice, a model of T2D.[182] Moreover, MAFA, NKX6.1, and PDX1 were also selectively lost in T2D,[38] as was the MAFB transcription factor, which is co-produced with MAFA in human, but not mouse, islet β cells. Due to the relative sensitivity of these transcription factors to T2D stressors and their established to role in regulating mouse islet cell function, it was proposed that staging of T2D β cell dysfunction/death reflects the early loss of MAFA and/or MAFB with overt changes reflecting the subsequent changes in NKX6.1 and/or PDX1.

Mechanistic and molecular studies of human islets *in vivo* are difficult to perform. However, alternative approaches involving studies of excess glucose and/or lipid in islet cell lines and islets in culture, whether mouse or human, do not mimic islets *in vivo*, as cultured islets lack vascularization and innervation, and islet culture itself leads to changes in islet function and gene expression. Furthermore, such *in vitro* studies are challenged by selection of individual lipid species, lipid concentrations, and/or glucose concentrations. Most rodent models of T2D, such as the ZDF rat or *db/db* mouse, do not allow experiments that differentiate the effects of hyperglycemia from those of hyperlipidemia. Importantly, human islets differ from mouse islets in fundamental ways, such as islet architecture,[44,45] relative expression of some islet-enriched transcription factors, regulation of transcription factor expression,[46] and proliferative capacity.[54,183,184]

As a result of these experimental limitations and species differences, the mechanisms of how excess glucose and/or lipid specifically impair human islet function *in vivo* are incompletely understood. To address this, we generated or used three models of metabolic stress, in which human islets, engrafted into immunodeficient mice, are exposed to hyperglycemia (glucotoxicity) and/or excess lipid and consequent insulin resistance (lipotoxicity). Using these models, we examined insulin secretion, oxidative stress, transcription factor expression, the unfolded protein response, proliferation, apoptosis, and amyloid deposition in human islets *in vivo*, as well as the species-related differences between human and mouse islet physiology under metabolic stress.

Results

To examine the consequences of excess glucose and/or excess lipid on human islets *in vivo*, we developed and characterized animal models involving transplanted human islets exposed to chronic hyperglycemia (NSG-DTR model), chronic excess lipid and consequent insulin resistance (NSG-HFD), or acute hyperglycemia and acute insulin resistance (NSG-S961) (Figures 21B and 21J). Each model capitalizes on the profound immunodeficiency of the NSG mouse,[85,86,185,186] to facilitate human islet engraftment. In every case, we performed pre-experimental assessment of human islet function, to ensure islet quality (Figure 21A). Importantly, these models also allowed comparison of the *in vivo* response of human and mouse islets to these metabolic stresses. The advent of the NSG mouse, which lacks B cells, T cells, NK cells, and mature dendritic cells, has made possible the generation of “humanized” mice in many research contexts, including mice containing human immune systems. [147,187] It has significantly improved the ability to study transplanted human islets by dramatically reducing the amount of immune infiltration in islet grafts.

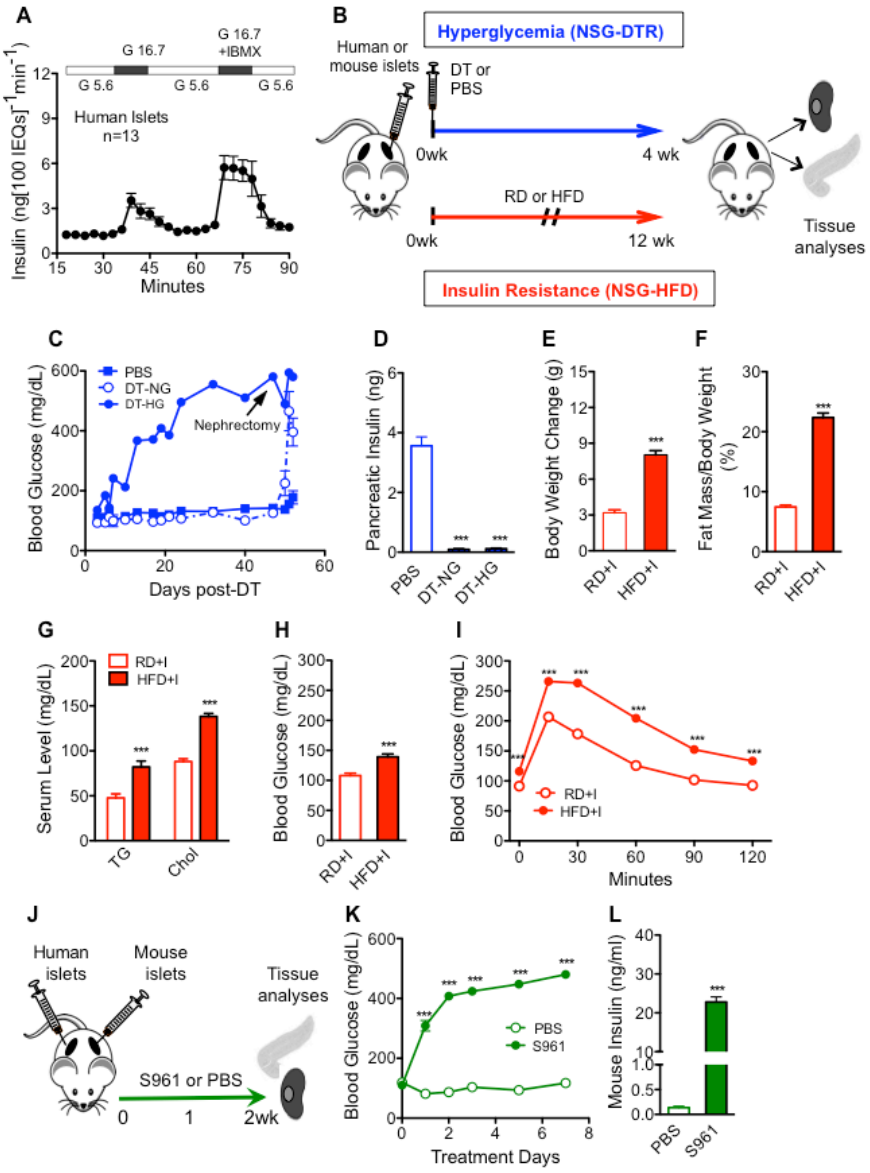

Figure 21. Models of chronic metabolic stress. (A) Isolated human islet preparations (n=13) perifused, prior to transplantation, with media containing 5.6 mM or 16.7 mM glucose (G 5.6 and G16.7), then 16.7 mM glucose with the phosphodiesterase inhibitor IBMX (51). (B) Experimental design. After islet engraftment period, NSG-DTR mice were injected with 5ng diphtheria toxin (DT) or saline and monitored for 4 weeks; NSG mice were placed on HFD or RD for 12 weeks. For all subsequent figures, blue colors are used for the NSG-DTR model, red colors for the NSG-HFD model, and green colors for the NSG- S961 model. Pastel and patterned color bars are used for human islet data, white and solid color bars are used for mouse islet data. (C) Random blood glucoses of NSG-DTR groups after DT injection (n=6/ group). Nephrectomy indicates survival surgery to remove graft-containing kidney. (D) Pancreatic insulin content in NSG-DTR mice, 4 weeks after DT injection (n=4-6/group) (E) Mouse body weight change after 12 weeks diet (RD, n=29; HFD n=30). *** p<0.001 (F) Fat mass (NSG-RD, n=29; NSG-HFD, n=30 (G) Serum triglyceride and cholesterol levels after 11 weeks on diet (NSG-RD, n=8; NSG-HFD, n=9). (H) Random blood glucose after 8 weeks diet (RD, n=20; HFD, n=21) (I) Glucose tolerance test (GTT) after 8 weeks on diet (NSG-RD, n=31; NSG-HFD, n=33). *** p<0.001. (J) Experimental timeline of S961 model. Two weeks after islet transplantation, S961 is delivered by implantation of osmotic pump. Analyses were performed at 1 or 2 weeks after pump implantation. (K) Random blood glucose measurements of S961 and PBS-treated mice from 0-7 days after pump implantation. *** p<0.001. (L) Random (non-fasting) mouse insulin values. *** p<0.001. PBS, n=8; S961, n=12.

Chronic hyperglycemia model (NSG-DTR)

To directly examine the effect of chronic hyperglycemia on human islets *in vivo*, we developed a model in which one could specifically ablate the native, mouse pancreatic β cells without harming transplanted human islets, which engrafted under normoglycemic conditions. To ablate mouse β cells, we used the RIP-DTR mouse, in which human diphtheria toxin receptor (DTR) expression is controlled by the rat insulin promoter,[148] generating DTR-expressing mouse β cells. The RIP-DTR mouse was crossed onto the NSG background, to produce the NSG-DTR mouse, a severely immunodeficient mouse with excellent xenograft tolerance, in which diphtheria toxin (DT) injection can now ablate mouse β cells (Figure 22A and F). We examined the response of NSG-DTR mice to a range of DT doses. A single injection of 5ng DT rapidly generated extreme and persisting hyperglycemia (Figure 22B) and dramatically reduced both mouse pancreatic insulin content (Figure 22C and Figure 21D) and islet size (Figure 22E and F). The 5ng DT dose did not alter transplanted human islet function, insulin content, or islet survival (Figure 22D, G, and H).

To generate and compare mice that become hyperglycemic after DT injection with mice that remain normoglycemic after DT injection, we analyzed how these conditions were affected by different IEQs of transplanted human islets. We determined that 4000 IEQ maintained normoglycemia (NG) in the majority of NSG-DTR+I mice (NSG-DTR mice with transplanted human islets) after DT-induced mouse β cell ablation, but that most mice with only 2000 IEQ quickly became hyperglycemic (HG) and remained so. To reflect the glycemic level to which human islets were exposed, we grouped mice and their data based on their observed glycemic status, rather than by the number of islets transplanted. Thus, we use the terms DT-HG (hyperglycemia after DT), DT-NG (normoglycemia after DT), and PBS (animals given PBS instead of DT) to describe the human islet transplanted groups.

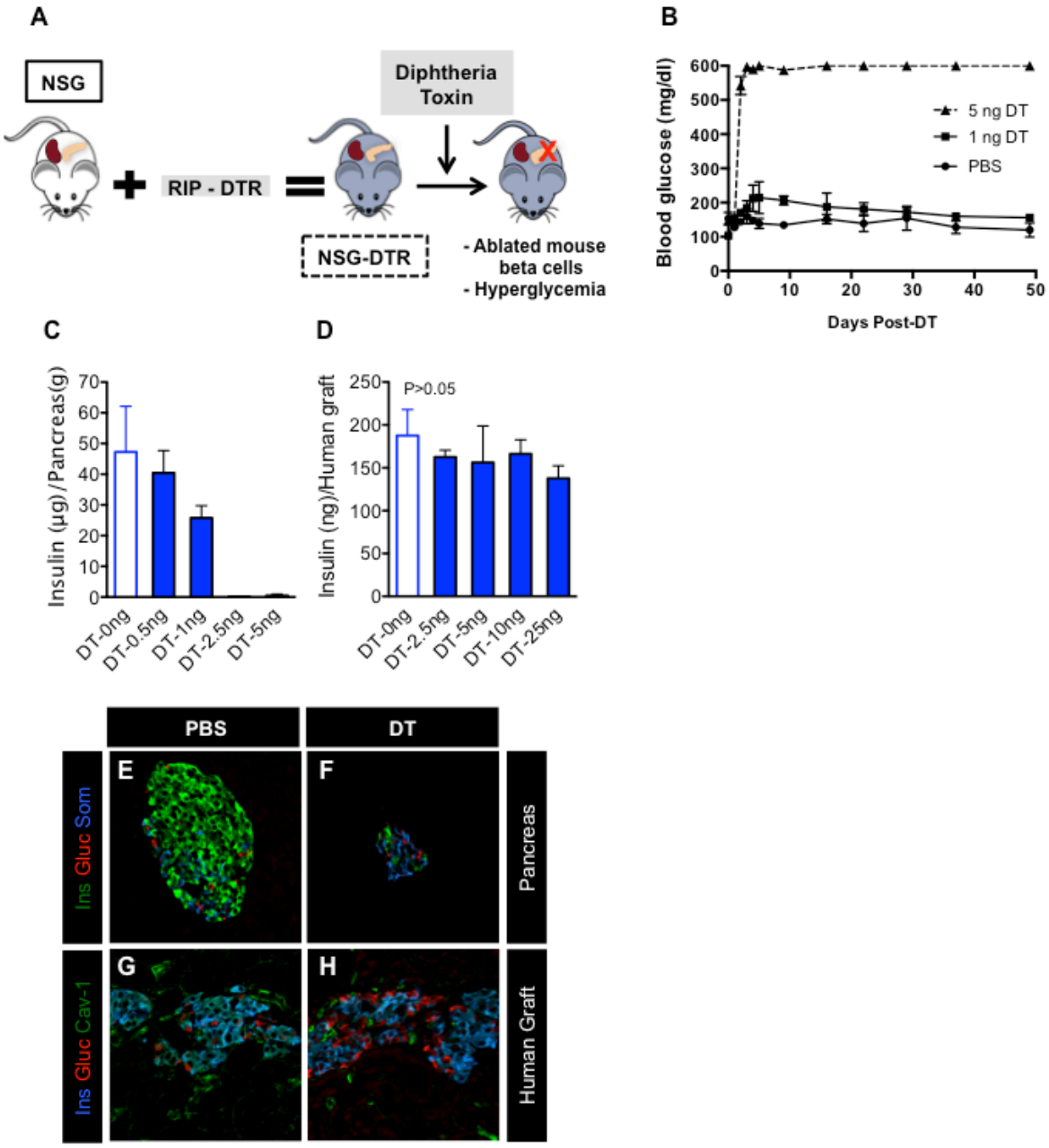

Figure 22. Establishment of chronic hyperglycemia model (NSG-DTR). (A) Breeding of NSG mouse with RIP- DTR transgenic mouse yields NSG- DTR mouse. Injection of diphtheria toxin ablates mouse β cells and results in hyperglycemia. (B) Blood glucose values of NSG-DTR mice in response to a single injection of 5ng DT, 1ng DT, or PBS. (C) Pancreatic insulin content of NSG-DTR mice (no human islets) injected with different DT doses (n= 3). (D) Human graft insulin content after injection with different DT doses (n=3). Representative images of NSG-DTR pancreata or human grafts after treatment with PBS (E, G) or DT (F, H). (E-F) Green = insulin, red = glucagon, blue = somatostatin. (G, H) Blue = insulin, red = glucagon, green = caveolin-1.

Chronic insulin resistance model (NSG-HFD)

A high-fat diet (HFD) was used to introduce excess dietary fat and to induce insulin resistance on the NSG background. Some mice exhibited high sensitivity to the diet (HFD-HS), and others exhibited low sensitivity (HFD-LS), as defined by the change in body weight and fat mass, glucose tolerance, and serum insulin (Figures 23 and 24). On HFD, body weight (Figure 23A), percent fat and lean mass (Figure 23C and E), glucose tolerance (Figure 24A and C), and fasting serum insulin (Figures 24E and 24G) were affected. Only HFD-HS mice were subsequently used to test the effects of excess lipid and insulin resistance on human islets *in vivo*. We also generated and characterized two widely-used genetic models of insulin resistance on the NSG background: the GLUT4$^{-/-}$ model (NSG-*Glut4*) and the *ob* model (NSG-*ob/ob*). The phenotypes of GLUT4$^{-/-}$ and *ob/ob* mice on the NSG background (Figures 25, 26, and 27) differed from the C57BL/6 background, and these models were not subsequently studied. These unexpected differences exemplify how genetic background can impact the metabolic phenotype.

NSG mice with transplanted human islets were placed on HFD or RD (HFD+I and RD+I mice) for 12 weeks (Figure 21B), and this allowed a comparison of transplanted human islets and endogenous pancreatic mouse islets under the same metabolic condition. One week before sacrifice (11 weeks on HFD), HFD+I mice had almost 3-fold greater weight gain (Figure 21E and Figure 28A), twice the percent fat mass (Figure 21F) and reduced lean mass (Figure 28B) compared to RD+I controls. In addition, HFD+I mice had higher serum triglyceride and cholesterol (Figure 21G), mild hyperglycemia (Figure 21H), and glucose intolerance (Figure 21I). HFD+I mice had dramatic hepatic lipid deposition (Figure 28C), and mouse islet size and β cell mass were increased (Figure 28D and E), recapitulating prior studies on the effect of HFD on mouse islets.[120,164,165]

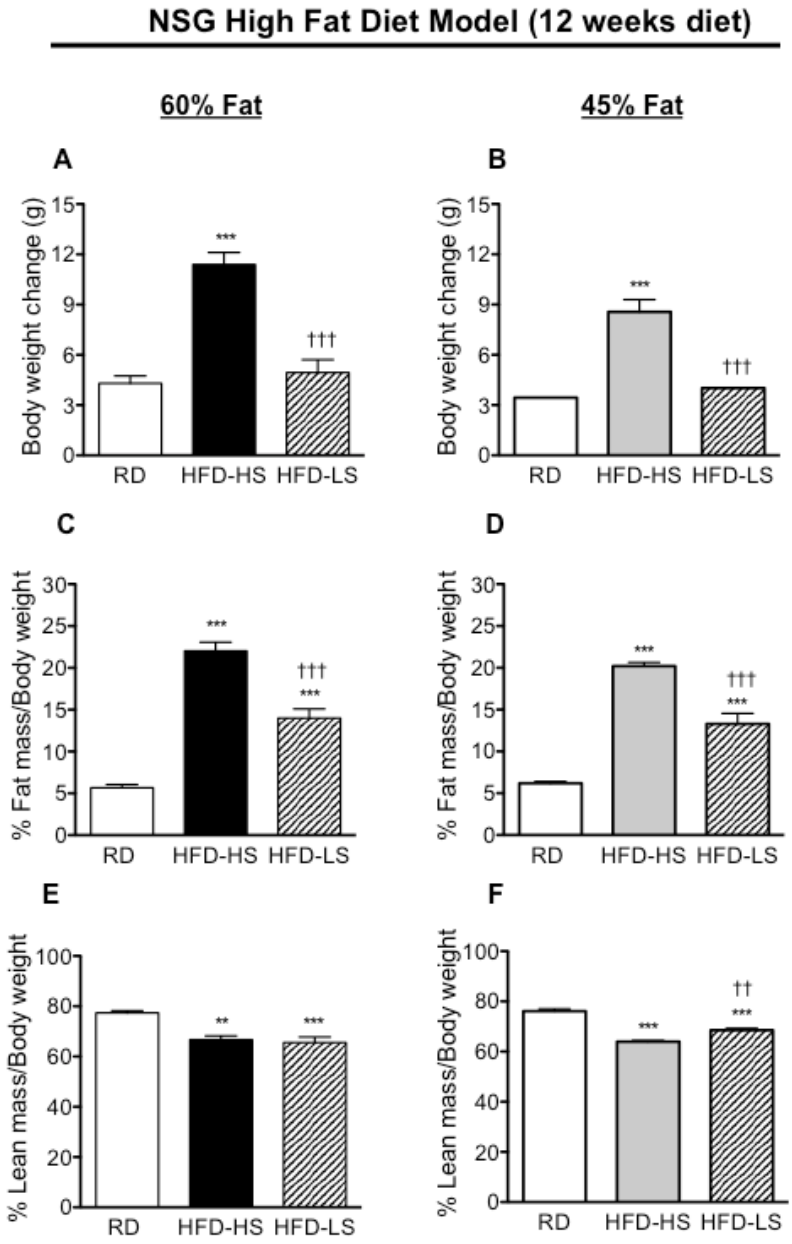

Figure 23. Feeding with either 60% or 45% of high fat diet (HFD) for 12 weeks induces obesity in NSG mice. (A, B) Mouse body weight change is higher on HFD (A. RD, n=8; 60% HFD-HS, n=14, 60% HFD-LS, n=6; B. RD, n=10, 45% HFD-HS, n=10; 45% HFD- LS, n=5). (C-F) Fat mass and lean mass (C, E. RD, n=10; 60% HFD-HS, n=13, 60% HFD- LS, n=5; D, F. RD, n=10, 45% HFD-HS, n=10; 45% HFD-LS, n=5). ** p<0.01, *** p<0.001, HFD vs RD; †† P<0.01, ††† P<0.001, HFD-HS vs HFD-LS.

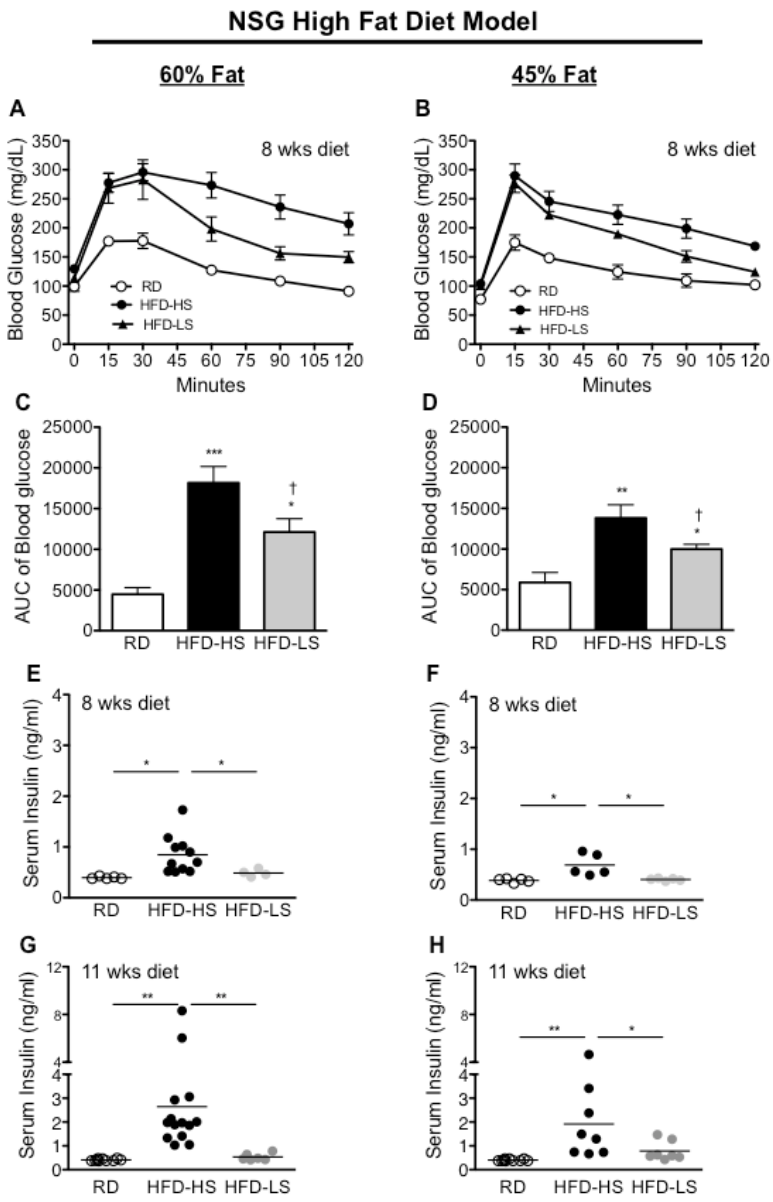

Figure 24. HFD induces insulin resistance in NSG mice. (A, B) Eight weeks of 60% or 45% HFD impaired GTT in the NSG mice. However, the mice with 60% HFD had more severely impaired glucose clearance. (RD, n=10; 60% HFD-HS, n=15; 60% HFD-LS, n=5; 45% HFD- HS, n=10; 45% HFD=LS, n=10) (C, D) Blood glucose area under curve of GTT ** p<0.01, *** p<0.001, HFD vs RD; † P<0.05, HFD-HS vs HFD-LS. (E-H) Mouse serum insulin increases in response to 8 weeks (E, F) and 11 weeks (G, H) 60% (E, G) or 45% (F, H) fat diet. * p<0.05, ** p<0.01. No significant difference showed between RD-LS and HFD-LS.

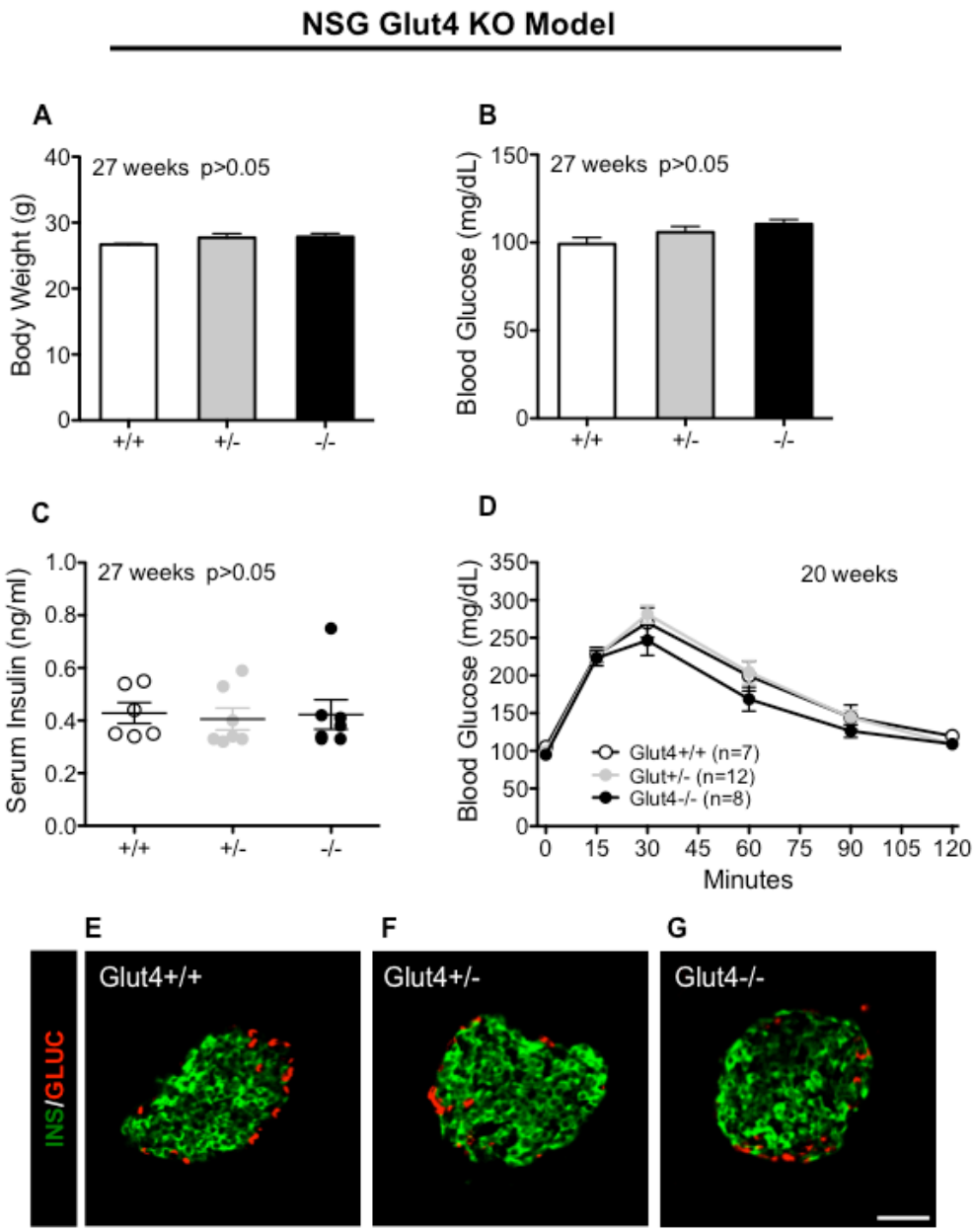

Figure 25. No phenotype in NSG mice with Glut4 deficiency. NSG-Glut4-/- mice. (A) Body weight, (B) blood glucose (6 hour fast), (C) serum insulin (6 hour fast) in wild type (+/ +), heterozygotes (+/-), and homozygotes (-/-) at 27 weeks old. n=6-7/genotype/age. p>0.05 (D) GTT at 20 weeks. P>0.05 at all time points. (E-G) Islet images of three genotypes labeled with insulin (INS, green), glucagon (GLUC, red). Scale bar = 100 μm and applies to E and F.

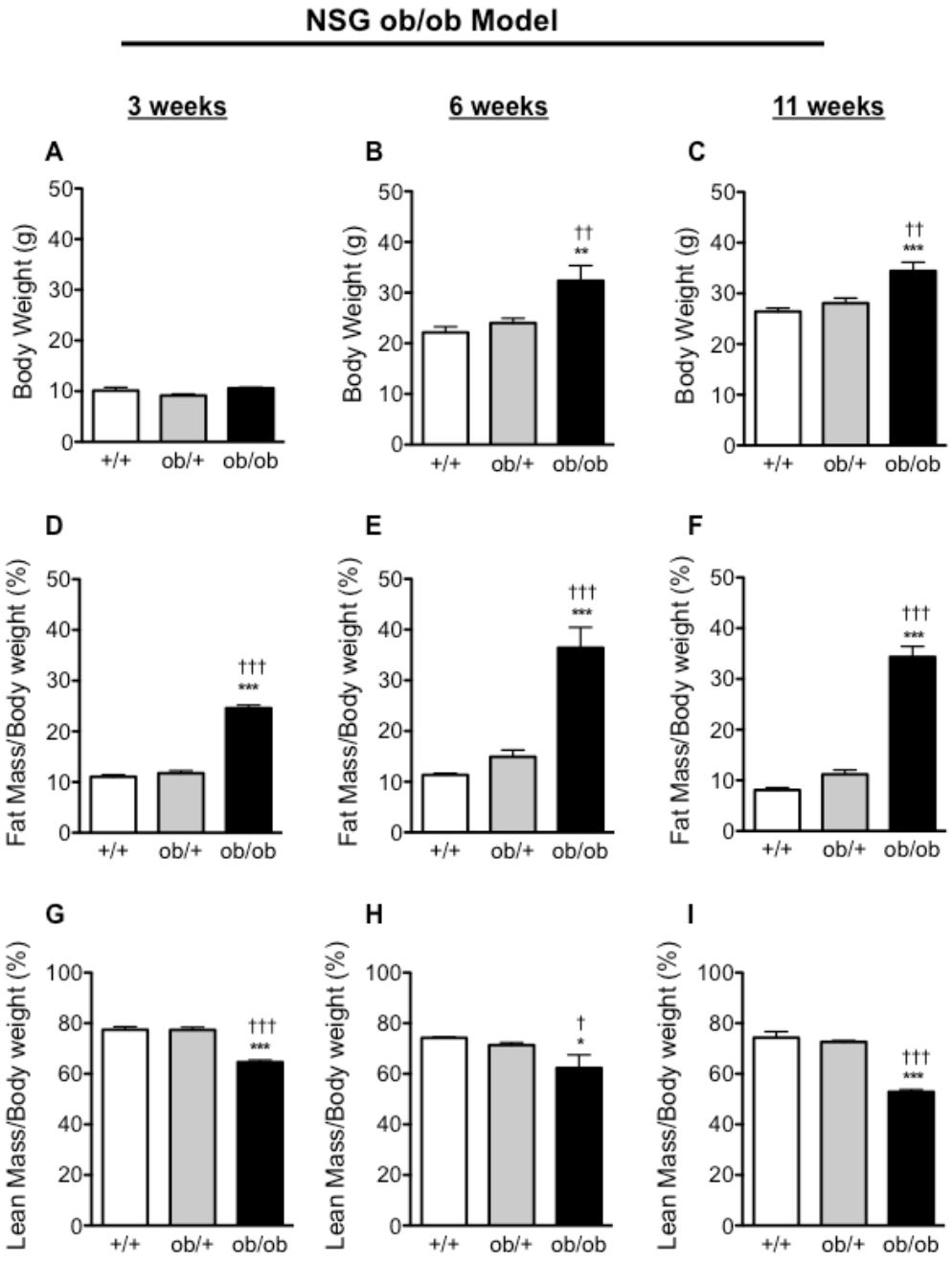

Figure 26. Leptin deficiency causes obesity in NSG mice. (A-C) Body weight of wild type (+/+), heterozygotes (ob/+), and homozygotes (ob/ob) at 3, 6, and 11 weeks old. (D-F) Fat mass and (G-I) lean mass in three genotyping groups at age of 3, 6, and 11 weeks. (3 weeks: n=6, +/+; n=8 (+/ob); n=4, ob/ob; 6 weeks: n=5, +/+; n=12, +/ob; n=5, ob/ob; 11 weeks: n=15, +/+; n=13, +/ob; n=17, ob/ob). * p<0.05, ** p<0.01, *** p<0.001, ob/+ and ob/ob vs +/+; † p<0.05, †† P<0.01, ††† p<0.001, ob/+ vs ob/ob.

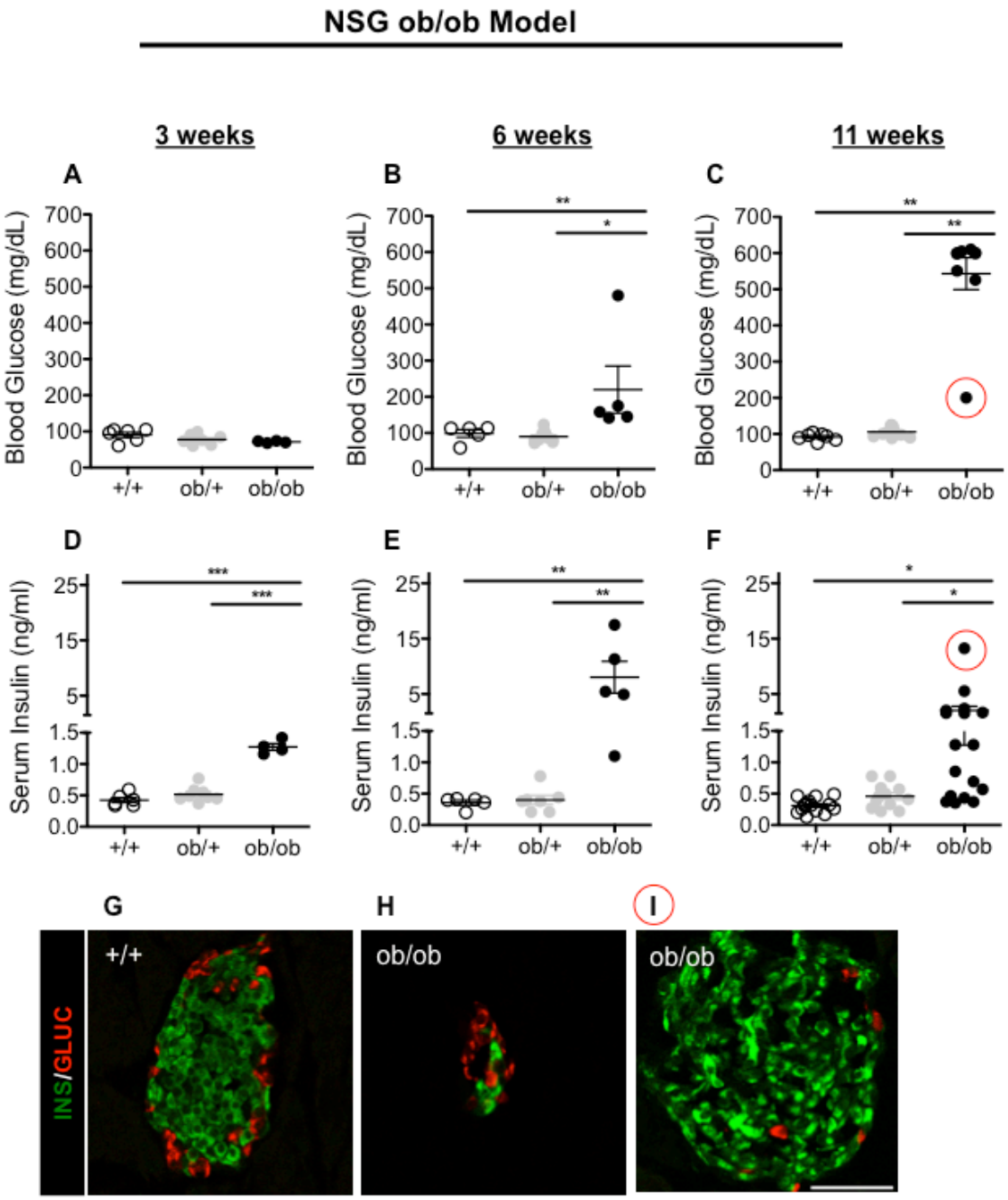

Figure 27. Diabetes occurs earlier in NSG-*ob/ob* mice. Blood glucose after fasted for 6 hours. All mice developed to diabetes (glucose > 500mg/dL, except one mouse – 200 mg/ dL). (D-F) Serum insulin (fasted) significantly increased at 3 weeks old and was dramatically elevated at 6 weeks. However, at 11 weeks the insulin level declined. (G-I) Images of +/+ and ob/ob islets labeled with insulin (INS, green), glucagon (GLUC, red). In most mice at 11 weeks, islet size and the number of β cells decreases in ob/ob mice while alpha cell number increases (H). Red circles represent the data and islet image (I) from same ob/ob mouse that has higher insulin, lower glucose, and larger islets

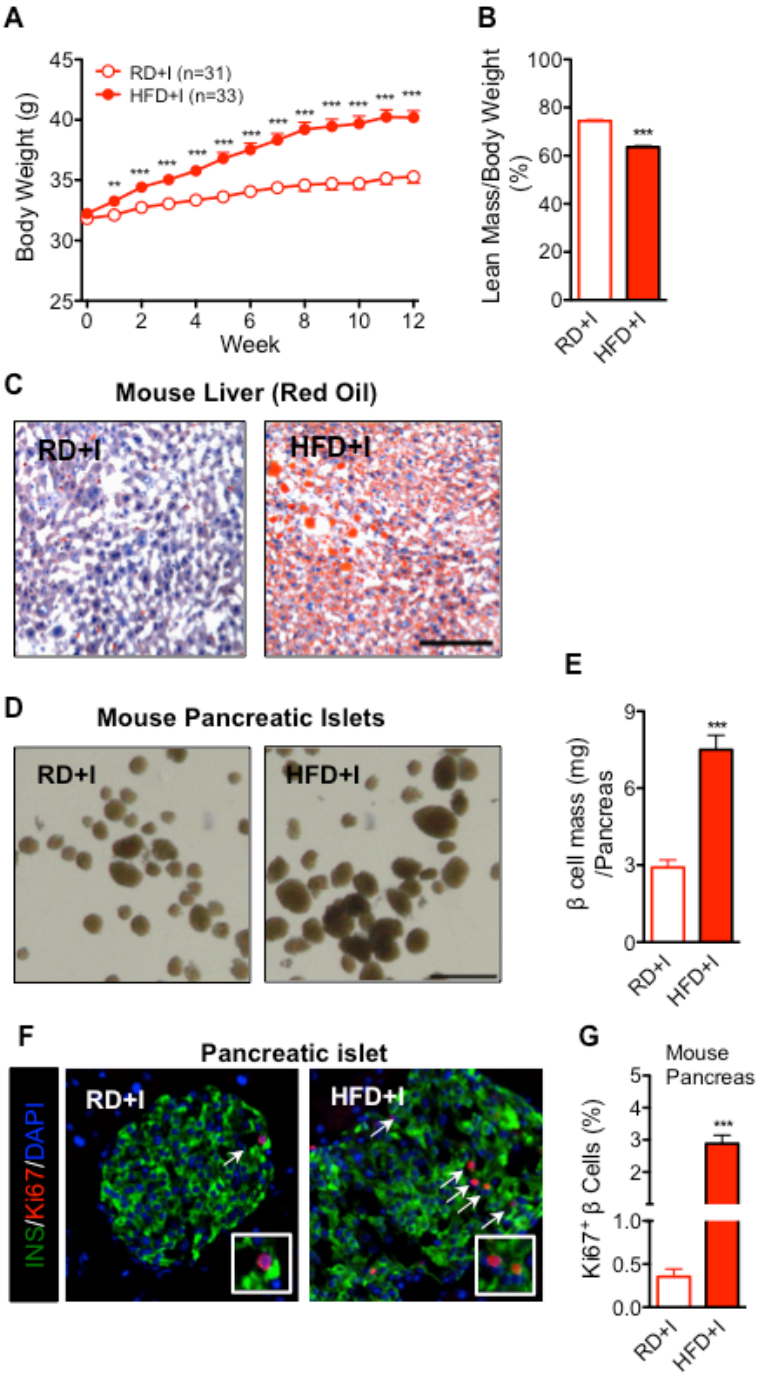

Figure 28. Human islet function assessment and larger mouse islet size in response to HFD. (A) Body weight in NSG mice with transplanted human islets from day 1 to 12 weeks on RD and HFD. *** p<0.001 (B) Lean mass in RD+I and HFD+I. *** p<0.001 (C) Dramatically increased lipid deposit in mouse liver after fed with high fat diet for 12 weeks (Oil Red O stain, lipid is red). Scale bar = 50 “m and also applies to RD+I. (D) Size of mouse islets in response to 12 weeks of HFD. Islets are from one mouse/each diet. Scale bar = 500 “m and also applies to RD+I. (E) β cell mass of mouse pancreas (n=4/diet group). *** p<0.001. (F) Representative mouse pancreatic islet images. White arrows point to proliferating Ki67-positive β cells. (G) Quantification of Ki67-positive ! cells in mouse pancreas (n=9/each diet). The number of β cells counted in each group was 7,000 to 16,000. *** p<0.001.

We examined graft vessel morphology in human and mouse islet grafts in the NSG-HFD model (Figure 29F versus 29H*)*, to ensure that islet graft function is not altered by abnormal vasculature on HFD*.* Given that islet grafts revascularize with both donor and recipient endothelial cells, sometimes forming chimeric vessels,[83] we stained with PECAM, to detect mouse endothelial cells, and with CD31, which identifies human endothelial cells. We found similar vessel morphology (size and density) in both diet groups, with both human and mouse endothelial cells contributing to vessel formation (Figure 29A and B). By electron microscopy, we observed normal fenestration of human vessels on these diets (Figure 29E and F). We found similar results in mouse islet grafts, with similar density, distribution, and size of vessels in these diet groups (Figure 29C, D, G, and H). Taken together, these data indicate that diet does not change the vasculature of transplanted human or mouse islet grafts.

Acute hyperglycemia and insulin resistance model (NSG-S961)

To examine the effect of a shorter duration of metabolic stress on human islets, we treated mice with the insulin receptor antagonist S961 (Figure 21J), a 43-amino acid peptide antagonist known to induce many consequences of insulin resistance in rodents, including hyperglycemia, hyperinsulinemia, decreased hepatic glycogen storage, and decreased adipocyte triglyceride storage.[152,153] In our studies, S961-treated mice became hyperglycemic 24 hours after injection (Figure 21K) and remained so at two weeks (Figure 28A). The insulin resistance of these mice is illustrated by extreme hyperinsulinemia of both human (Figure 28B) and mouse insulin (Figure 21L).

Metabolic stresses impair stimulated human insulin secretion in vivo

DT-HG mice, HFD+I mice, and S961-treated mice all showed hyperglycemia (Figures 30A, E, and J, respectively) and fasting human hyperinsulinemia (Figures 30B, F, and K, respectively).

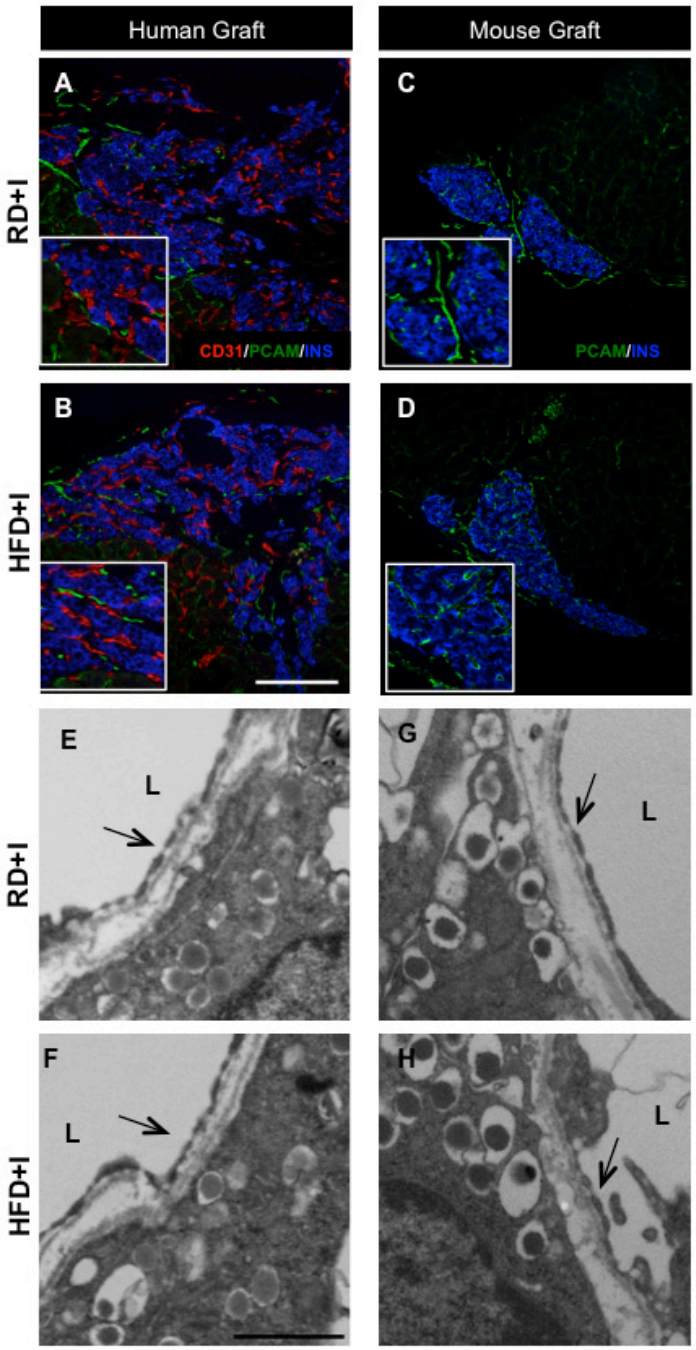

Figure 29. Graft vasculature does not change in mice on high fat diet. Representative images of human (A, B) and mouse grafts (C, D) labeled for insulin (blue), mouse vessels (green), and human vessels (red). Scale bar = 200 μm and applies to A-C. Representative EM images of fenestration in human (E, F) and mouse grafts (G, H). Arrows point to fenestration. L = lumen. Scale bar = 1 μm and applies to E-G.

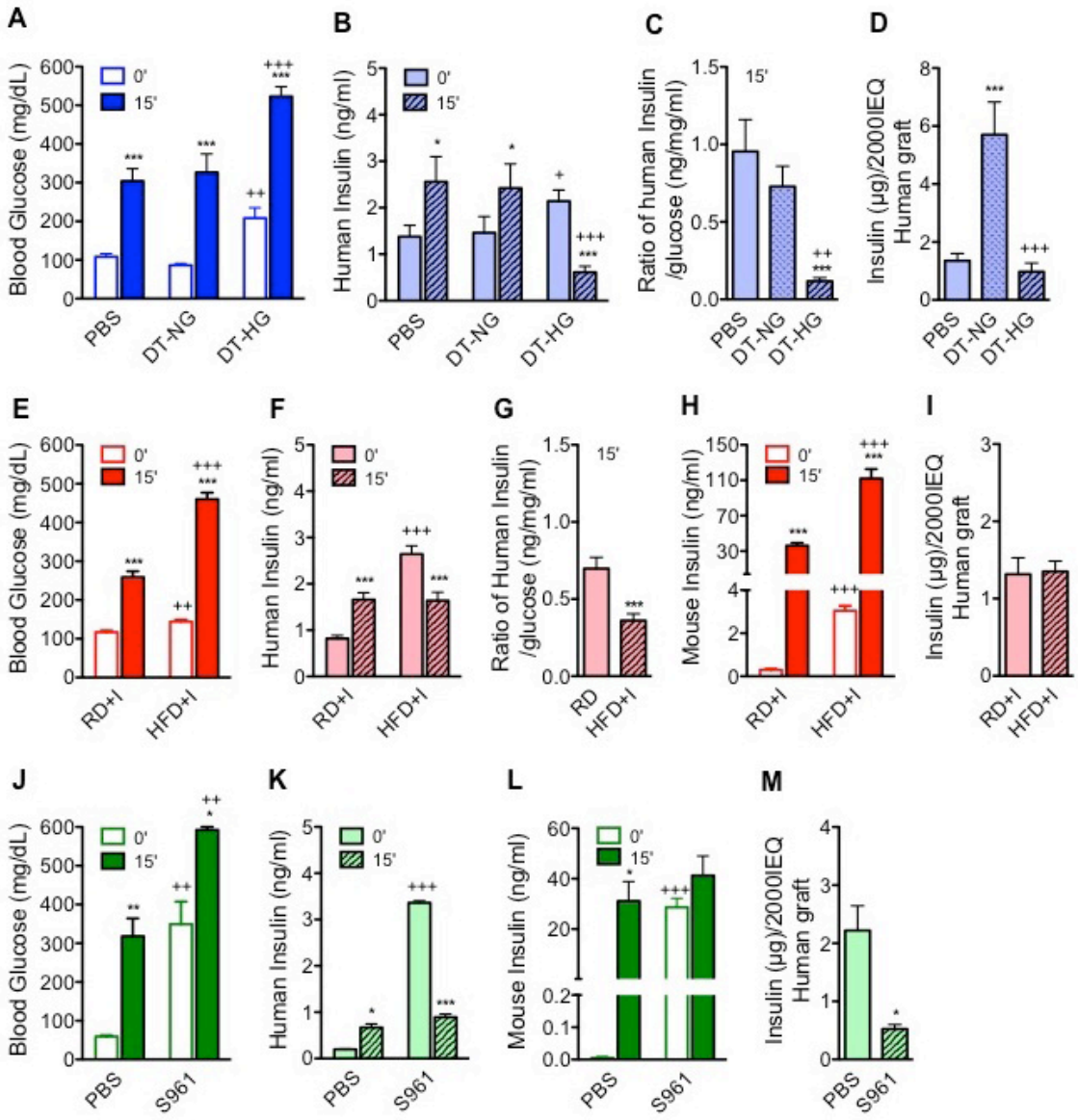

Figure 30. Metabolic stress impairs stimulated insulin secretion from transplanted human β cells. (A) Blood glucose of DTR groups after 6-hour fast (0') and 15 minutes after injection of glucose (2g/kg) plus arginine(2g/kg).***p<0.001, 0'vs15'withineachgroup; †† p<0.01,DT-HG0'vsPBS0'; ††† p<0.001, DT-HG 15' vs PBS 15'. (PBS, n=15; DT-NG, n=13; DT-HG, n=17) (B) Human insulin secretion from glucose-arginine stimulation assay. * p<0.05, *** p<0.001, 0' vs 15' within each group;, † p<0.05, DT-HG 0' vs PBS 0'; ††† p<0.001, DT-HG 15' vs PBS 15' (PBS, n=15; DT-NG, n=13; DT-HG, n=17). (D) Human graft insulin content. *** p<0.001, DT-NG vs PBS, ††† p<0.001, DT-HG vs DT-NG (n=5-6/group). (E-H) Glucose-arginine stimulation of HFD model after 11 weeks on diet. (E) Blood glucose values *** p<0.001, 0' vs 15' within the each diet group; †† p<0.01, 0' vs 0' between two diet groups; ††† p<0.001, 15' vs 15' between two diet groups. (NSG-RD, n=27; HFD; n=34). (F) Human and (H) mouse serum insulin levels. *** p<0.001, 0' vs 15' within the each diet group; ††† p<0.001, 0' vs 0' or 15' vs 15' between two diet groups (NSG-RD, n=27; NSG-HFD; n=34). (I) Human graft insulin content. P=0.880 (NSG-RD, n=12; NSG-HFD; n=14) J-L) Glucose-arginine stimulation of S961 model, 10 days after injection. (J) Blood glucose values, (K) Human insulin secretion, (L) Mouse insulin secretion. * p<0.05, ** p<0.01, *** p<0.001, 0' vs 15' within the each treatment; †† p<0.01, ††† p<0.001, 0' vs 0' or 15' vs 15' between two treatments (n=5/treatment). (M) Human graft insulin content. * p<0.05 (n=5/treatment).

Stimulated human insulin secretion dramatically decreased in these experimental groups (Figures 30B, F, and K). In contrast to the effect on human insulin, stimulated mouse insulin levels were dramatically elevated in HFD+I mice (Figure 30H) and unchanged in S961-treated mice (Figure 30L). The response of mouse insulin was not measured in DT-HG mice, due to their DT-mediated ablation of mouse β cells. This demonstrates a fundamental functional difference between mouse and human islets under identical metabolic conditions.

The ratio of stimulated human insulin to blood glucose, a measure of β cell responsiveness to hyperglycemia, was dramatically reduced in both DT-HG mice and HFD+I mice (Figures 30C, G, and J). Insulin content of the human islet graft was unchanged in DT-HG and HFD+I mice (Figure 30D and 30I), but it was markedly reduced in S961-treated mice (Figure 30M). In contrast, content was increased 3-fold in DT-NG grafts (Figure 30D). Together, these results indicate that the conditions of chronic hyperglycemia, chronic insulin resistance, and acute hyperglycemia with insulin resistance all induce functional impairment of human islets *in vivo* by impairing stimulated human insulin secretion, but that mouse insulin secretion is not similarly affected.

Human β cells do not proliferate in response to hyperglycemia or insulin resistance

Insulin resistance promotes compensatory expansion of rodent β cell mass due to proliferation,[183,184,188-190] and glucose has been reported to be a β cell mitogen in both rodent and human.[191-193] As expected, native mouse, pancreatic islets in HFD+I mice (Figure 28G) and NSG-S961 mice (Figure 31C-D) showed dramatic increases in β cell proliferation. HFD+I mice also had larger islets and increased pancreatic β cell mass (28D and E). Human β cell proliferation was much lower than that of mouse β cells, and in contrast to mouse β cells, it was unchanged by the condition of metabolic stress in each model (Figure 32A-B, D-E, and H-I).

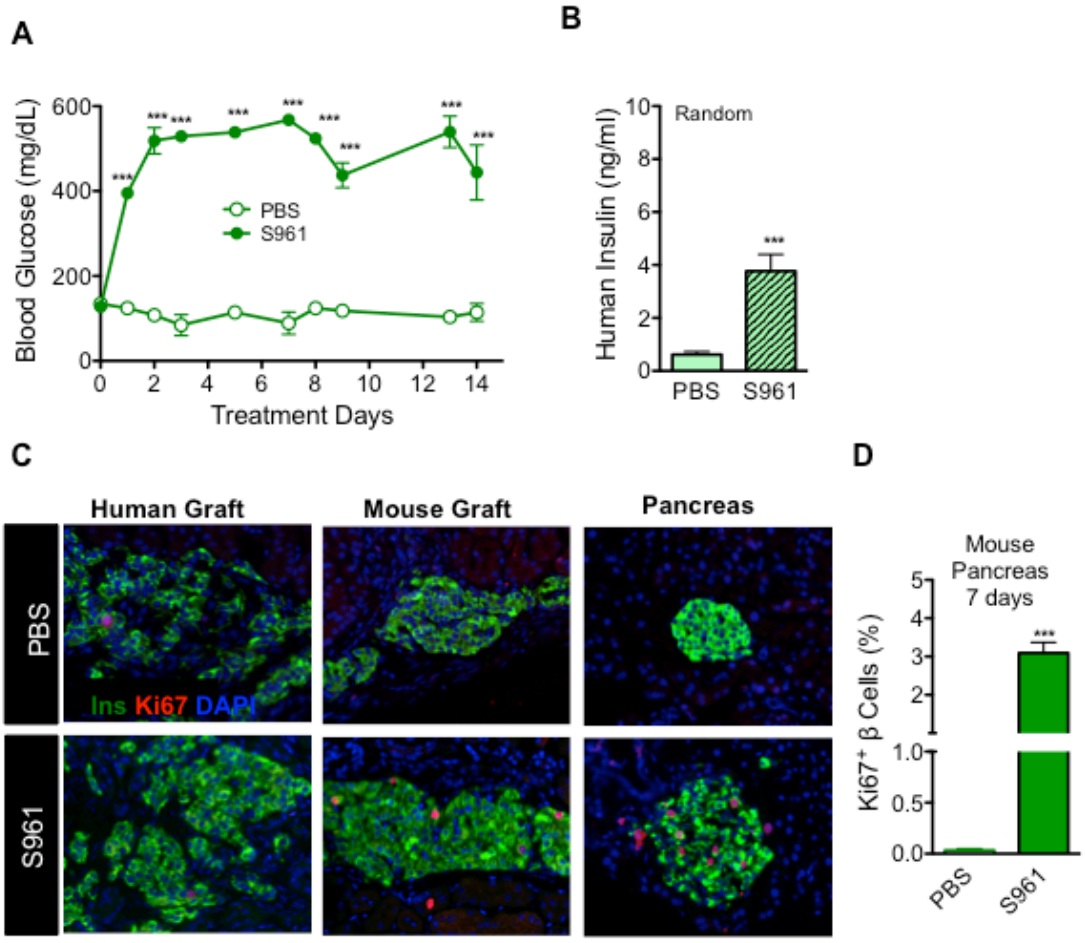

Figure 31. S961 model of acute hyperglycemia and insulin resistance. (A) Random blood glucose measurements of S961 and PBS-treated mice. *** p<0.001, n=4/treatment. (B) Random (non-fasting) human insulin values. *** p<0.001, PBS, n=8; S961, n=12). (C) Representative images showing relative levels of β cell proliferation in human graft, mouse graft, and pancreas of S961- or PBS-treated mice. Green = insulin, red = Ki67, blue = DAPI. (D) Quantification of β cell proliferation in mouse pancreata 7 days after S961 injection. *** p<0.001, n=5/treatment.

To address the possibility that the difference between human and mouse β cell proliferation in response to metabolic stress was related to the kidney capsule transplantation site, we transplanted NSG mice with mouse islets prior to HFD or S961-treatment. Mouse graft β cell proliferation increased more than 6-fold in HFD-fed mice (Figure 32C, F and G) and increased nearly 20-fold in NSG-S961 mice (Figure 32J), similar to other studies using S961.[194,195] These results demonstrate that acute and chronic hyperglycemia and/or insulin resistance potently stimulate mouse, but not human, β cell proliferation *in vivo.* Importantly, this difference was shown to be species-specific and not an effect of the transplantation site.

Neither chronic hyperglycemia nor insulin resistance causes human β cell apoptosis

Multiple *in vitro* studies have suggested that chronic metabolic stresses promote β cell apoptosis and associated decreases in human islets survival.[103,176] To address whether human β cell loss contributed to impaired stimulated insulin secretion, we measured expression of the key apoptosis genes *BID, BAD*, and *DDIT3* (CHOP) in DT-HG and HFD+I human grafts. Two markers of apoptosis were decreased in DT-HG grafts (Figure 32K) and all three were unchanged in HFD+I grafts (Figure 32L). The lack of increased CHOP expression in both models indicates that human β cells under chronic hyperglycemia or chronic insulin resistance were not undergoing stress-induced apoptosis. Indeed, we observed only rare apoptotic β cells in both mouse and human grafts in the HFD model (Figure 33A-F) and in human grafts in the DTR model (Figure 33G), at rates similar to control grafts. Thus, excess glucose or lipid does not lead to apoptosis in human or mouse islets *in vivo*, indicating that β cell death is not impacted in DT-HG and HFD+I exposed islets.

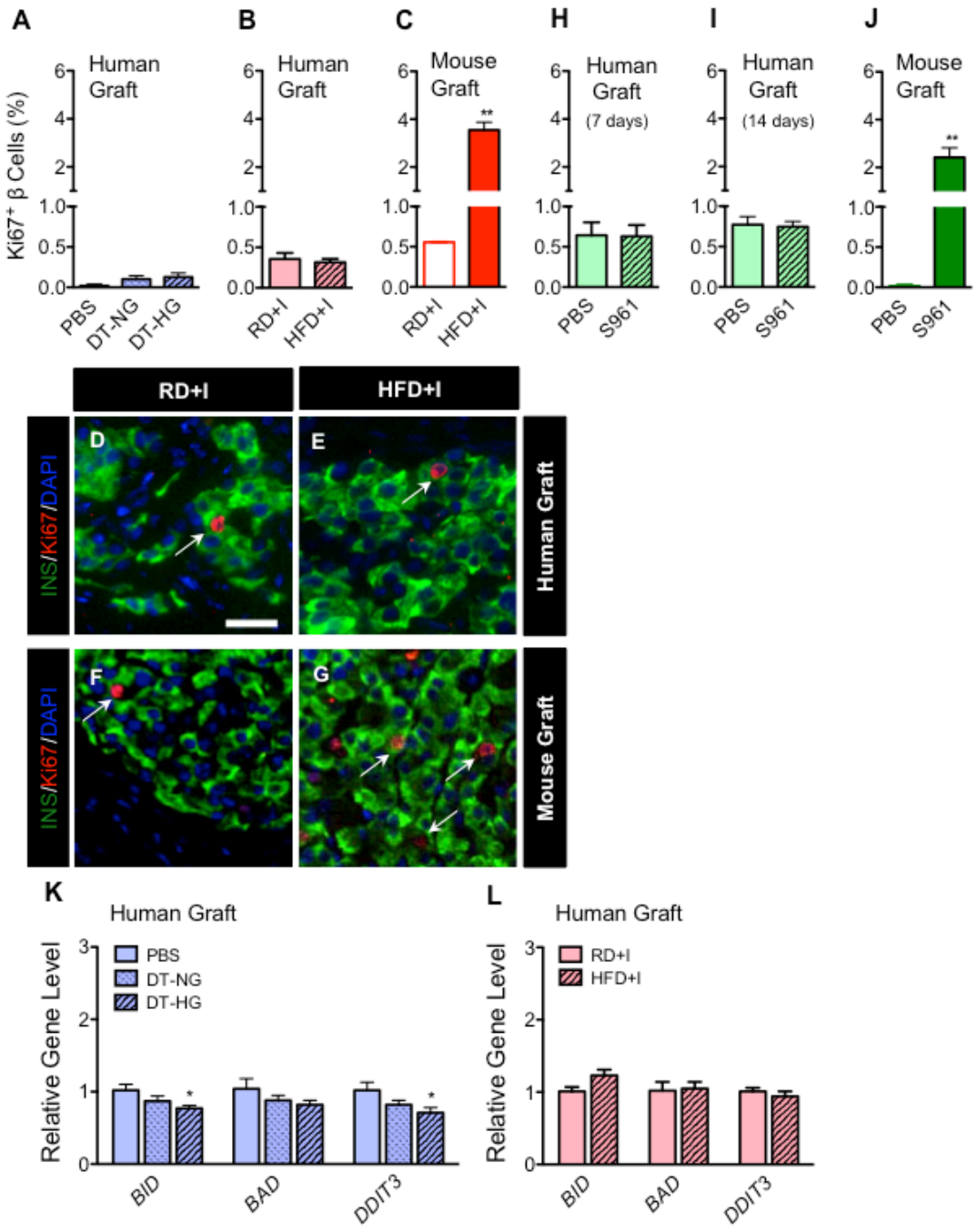

Figure 32. Human β cells do not proliferate in response to hyperglycemia or insulin resistance. Quantification of β cell proliferation in (A) NSG-DTR human grafts, (PBS, n=9; DT-NG, n=5; DT-HG, n=12) (B) NSG-HFD human grafts (n=11/diet, p=0.633), and (C) HFD mouse grafts (n=3/diet) ** p<0.01. The number of β cells counted in each group was 7,000 to 16,000. (D-G) Islet images from human graft (D, E) and mouse graft (F, G) labeled with insulin (green), Ki67 (red), and DAPI (blue). Arrows point to proliferating Ki67-positive β cells. β cell proliferation in S961-treated (H) human grafts (left kidney, n=5/treatment, p=0.644) and (J) contralateral mouse graft (right kidney, n=5/treatment, ** p<0.01) after 7 days. (I) Human grafts after 14 days (n=5/treatment, p=0.8239). (K, L) Expression of apoptosis-related genes BID, BAD, and DDIT3 (CHOP) in human grafts (K) from NSG-DTR model (PBS n=5, DT-NG, n=5; DT-HG, n=10; * p<0.05, DT-HG vs PBS) and (L) from NSG-HFD model (n=5/ diet; p>0.05).

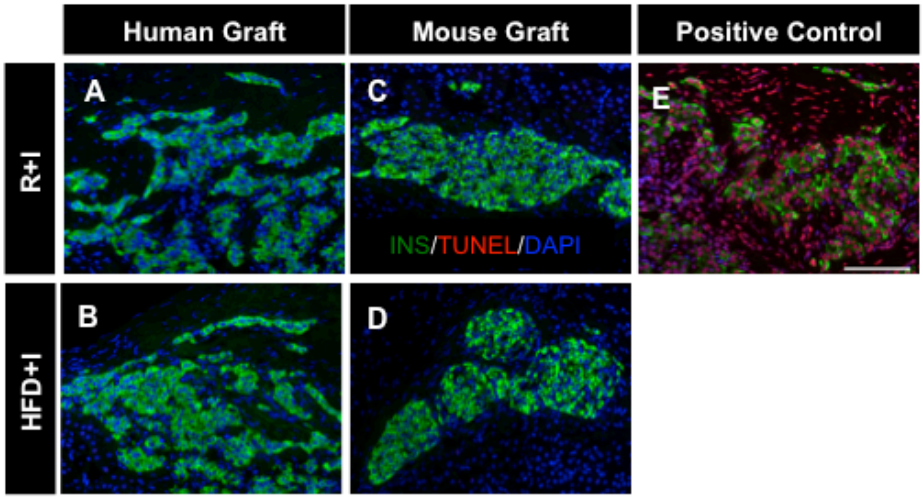

F

NSG-HFD		Total β Cells	TUNEL⁺ β Cells
Human Grafts	RD	10860	0
	HFD	11135	1
Mouse Grafts	RD	1455	0
	HFD	1444	0

G

NSG-DTR		Total β Cells	TUNEL⁺ β Cells
Human Grafts	PBS	4943	1
	DT-NG	2931	1
	DT-HG	3767	1

Figure 33. Chronic hyperglycemia and insulin resistance do not increase β cell apoptosis. Representative images showing lack of TUNEL-positive β cells in NSG+HFD (A, B) human grafts and (C, D) mouse grafts, compared to a positive control. Scale bar = 100 μm and applies to A-D. (E) Tabulated quantification of TUNEL+ β cells in NSG+HFD (F) and NSG-DTR (G) models.

Chronic hyperglycemia or chronic insulin resistance decrease antioxidant enzyme expression and increase superoxide levels in human islet grafts

Oxidative stress from increased levels of reactive oxygen species (ROS) is widely hypothesized as a cause of β cell dysfunction.[120,196] These islet cells are thought to be more sensitive to ROS due to their unusually low levels of antioxidant enzymes compared to other tissues.[114,116,197] We used these models to assess how oxidative stress responder gene products are impacted by chronic *in vivo* hyperglycemia or insulin resistance. In a panel of oxidative stress-related genes, only the transcription factor nuclear factor, erythroid-derived 2-like 2 (*NFE2L2*) was reduced in DT-HG islet grafts (Figure 34A). However, the antioxidant enzymes superoxide dismutase (*SOD1* and *SOD2*) and glutathione peroxidase (*GPX1*), as well as *NFE2L2,* were decreased in HFD+I grafts (Figure 34B). Superoxide levels, as measured by dihydroethidium (DHE) staining, were higher in HFD+I grafts, but they were not changed in DT-HG grafts (Figure 34C-E). HFD+I mouse grafts showed no difference in superoxide levels (Figure 34F), indicating that the higher prevailing level of reactive oxygen species induced by HFD is specific to human islets. These data demonstrate that changes in human islet antioxidant enzyme expression and subsequent increases in ROS are part of the response to chronic insulin resistance and may be a component of the lipotoxic functional consequences of these human grafts. Interestingly, the effect of hyperglycemia and insulin resistance on oxidative stress was different. The insulin resistance of the NSG-HFD model had a greater effect on both antioxidant enzyme expression and ROS levels, suggesting that oxidative stress may be more important as a lipotoxic mechanism than a glucotoxic mechanism.

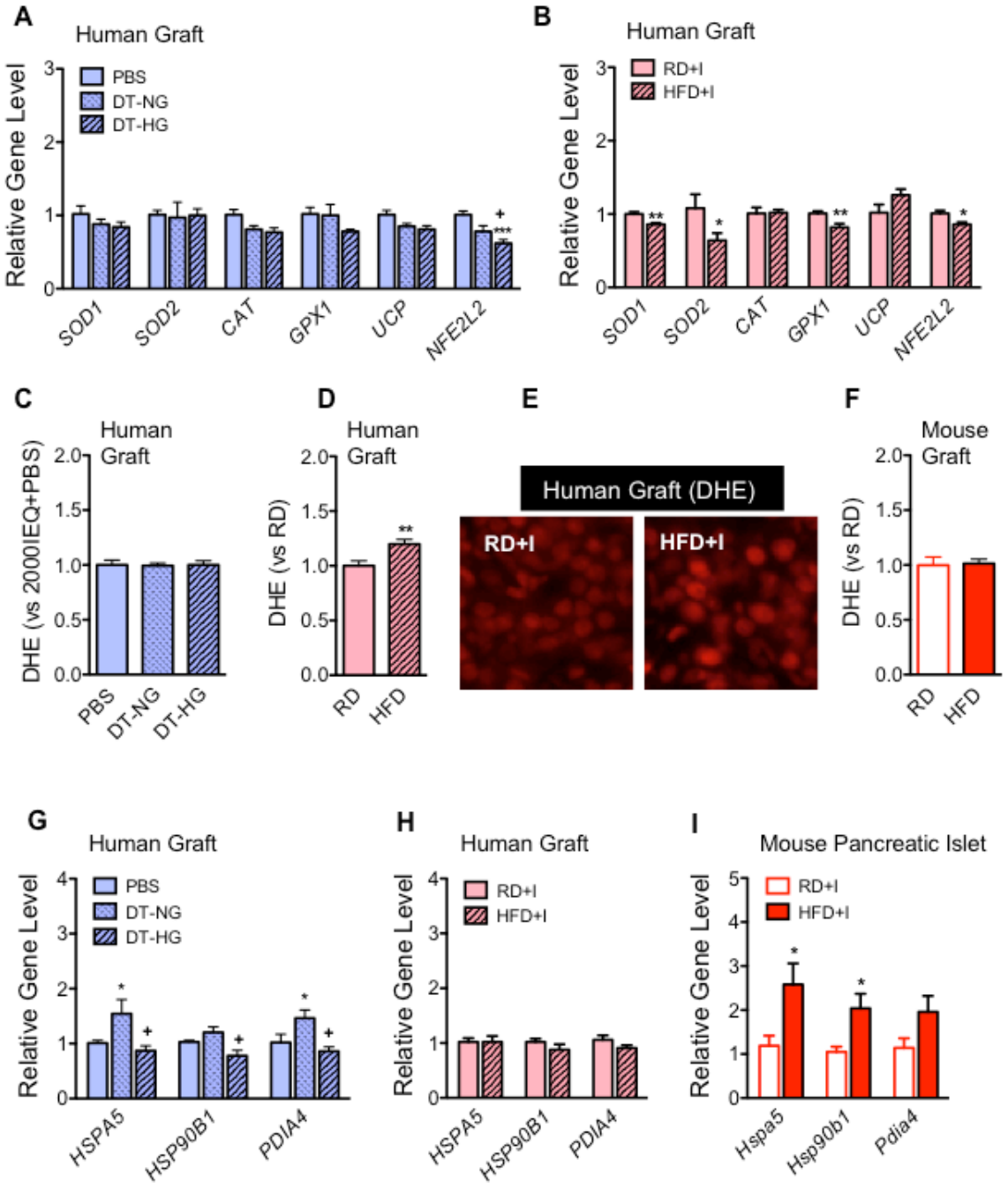

Figure 34. Antioxidant enzymes, ROS, and unfolded protein response. (A-B) Relative expression of antioxidant enzymes (SOD1, SOD2, CAT, GPX1, UCP2) and oxidative stress responding transcription factor (NFE2L2) gene in transplanted human islets from (A) NSG-DTR (PBS n=5, DT-NG, n=5; DT-HG, n=10; *** DT-HG vs PBS, † DT-HG vs DTR-NG) and (B) NSG- HFD (n=5/diet; * p<0.05, ** p<0.01) models. Quantification of superoxide production, measured by dihydroethidium staining, in (C) NSG-DTR human grafts (n=8-10/group), (D) NSG-HFD human grafts (n=10/diet, **p<0.01), and (F) HFD mouse grafts (n=15/diet). (E) Images of DHE staining in NSG-HFD/RD human grafts. Unfolded protein response (UPR) genes are induced in mouse islets and in DT-NG human grafts, but not in DT-HG or HFD+I human grafts. (G-I) mRNA levels of UPR marker genes in (G) NSG-DTR human grafts (PBS n=5, DTR-NG, n=5; DTR-HG, n=10). (H) NSG-HFD human grafts (n=5/diet), and (I) mouse islets (n=5/diet). * p<0.05.

Unfolded protein response is not up-regulated in response to chronic hyperglycemia or chronic insulin resistance

The efficacy of the unfolded protein response (UPR) influences the ability of islets to meet increased insulin demand under metabolic stressors such as chronic hyperglycemia or insulin resistance.[130,198-200] To examine the UPR in human islets exposed to chronic hyperglycemia or insulin resistance, we measured the gene expression of two chaperones central to the UPR, *HSPA5* (GPR78, BIP) and *HSP90B1* (GRP94), as well as protein disulfide isomerase, *PDIA4* (ERP72). *HSPA5* and *PDIA4* were increased in DT-NG grafts (Figure 34G), which successfully maintained normoglycemia, but were unchanged in both DT-HG and HFD+I grafts (Figure 34H), which had impaired insulin secretion. In contrast, pancreatic mouse islets of HFD+I mice, which had robust stimulated insulin secretion, had increased expression of all 3 UPR genes in response to HFD (Figure 34I).

These models demonstrate that islets with preserved stimulated insulin secretion relative to controls, namely DT-NG human grafts and HFD+I mouse islets, up-regulate components of the UPR, but islets with impaired stimulated secretion, namely DT-HG human grafts and HFD+I human grafts, do not. This suggests that inability to stimulate the UPR may be a glucotoxic and lipotoxic consequence. Alternatively, a lack of UPR induction could be a natural downstream response to either reduced or unchanged insulin transcription and/or translation, in which case this lack of UPR induction would reflect an appropriate homeostatic mechanism, rather than dysfunction. Importantly, mouse and human islets responded similarly, suggesting that the UPR may be an aspect of islet function conserved between the species.

Chronic insulin resistance, but not chronic hyperglycemia, increases amyloid deposition in human islet grafts

Peri-islet amyloid deposition is a proposed mechanism of human β cell dysfunction and death in T2D.[133,135,141,145] Specifically, it has been proposed that hyperglycemia and HFD promote amyloid formation by increasing cellular stress.[174,175,201] To test whether this occurs in human islets exposed to chronic hyperglycemia or insulin resistance *in vivo*, we measured graft expression of islet amyloid polypeptide (IAPP). Both IAPP expression and amyloid formation were observed in HFD+I grafts (Figure 35A). HFD+I grafts also had larger amyloid deposits than animals fed RD (Figure 35B and C). In contrast, there was no change in IAPP expression, amyloid presence, or deposit size in the DT-HG grafts (Figures 36A-C). Due to the inherent inability of mouse IAPP to form amyloid,[202] mouse grafts were not examined for amyloid. These data suggest that chronic excess lipid and insulin resistance, but not hyperglycemia, are the primary driver of amyloid deposition in human islets. However, this increased islet amyloid deposition did not cause human β cell apoptosis (Figure 33G).

Human β cells exposed to chronic insulin resistance accumulate a greater number of intracellular lipid droplets

Studies have suggested that excess nutrients promote lipid droplet formation within islets[168] and that these lipid droplets impact β cell function.[203] Using electron microscopy to examine intracellular lipid accumulation, we observed that human β cells (Figures 35D, E and J), but not mouse β cells (Figures 35F-I and K-L), extensively accumulated lipid droplets on RD, and this was increased in response to HFD (Figure 35J). Human pancreatic β cells also had lipid droplets (data not shown), suggesting that droplet presence is not a result of transplantation. These data indicate that intracellular lipid accumulation is a feature of human, but not mouse, β cells, and that HFD increases human β cell intracellular lipid accumulation.

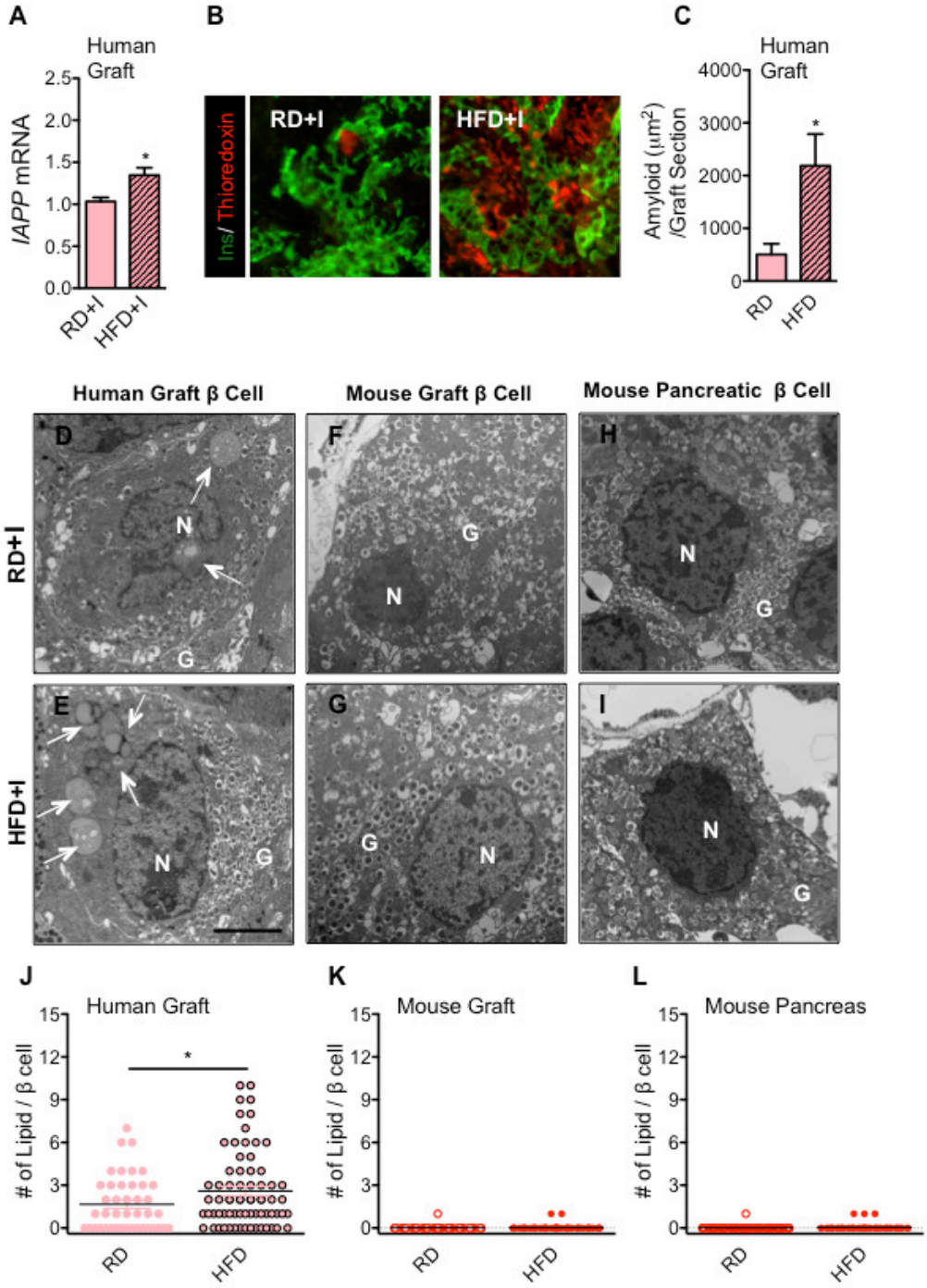

Figure 35. Amyloid deposition in human grafts is increased in NSG-HFD mice. (A) Relative mRNA level of IAPP in human grafts (n=5/diet). * p<0.05. (B) Representative images of amyloid in human grafts labeled with insulin (green), thioredoxin (red). (C) Measurement of thioredoxin area of human grafts. (n=10 grafts/diet). Human, but not mouse, β cells accumulate intra-cellular lipid droplets. EM images of β cells from human graft (D, E), mouse graft (F, G), and mouse pancreas (H, I), Arrows point to lipid droplet(s). N=nuclear, G=granule. Scare bar = 3 μm and applied to A-E. (J-L) The number of lipid droplets per β cell in human grafts (β cell n=45-70), mouse grafts (n=50-71), and mouse pancreatic β cells (n=56-74). * p<0.05.

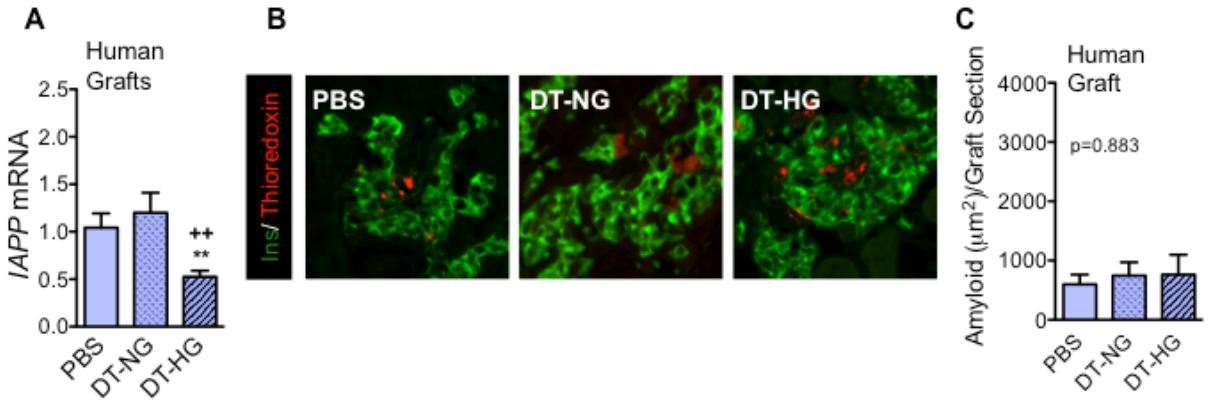

Figure 36. Islet amyloid is not increased by chronic hyperglycemia. (A) mRNA levels of islet amyloid polypeptide (IAPP) in human grafts from DTR mice (n=3). ** p<0.01 vs PBS group, †† p<0.01 vs DT-NG group. (B) Representative images of thioredoxin (red) staining in human islet grafts from each group (green = insulin). (C) Quantification of amyloid area per graft section (n=3).

Chronic insulin resistance and chronic hyperglycemia reduce NKX6.1 and/or MAFB in human β cells

Given the increased ROS in HFD+I human islet grafts, we postulated those β cell-enriched transcription factors sensitive to this stressor would be compromised under these circumstances, specifically MAFA, MAFB, NKX6.1 and/or PDX1, first described in mouse models of diabetes and in type 2 diabetic islets.[38,121] Expression of *MAFB*, which is expressed in both human islet α and β cells,[204] was reduced in both DT-HG human grafts (Figure 37A) and in HFD+I human grafts (Figure 37B), as well as in mouse pancreatic islets in HFD+I mice (Figure 37D). This reduction of *MafB* in mouse islets is most likely due to a decreased ratio of α to β cells, resulting from increased pancreatic β cell proliferation (Figures 28F and G), as *MafB* is not expressed in adult mouse islet β cells. Gene expression and protein levels of *NKX6.1*, a transcription factor critical to β cell identity and function,[29-31] was also decreased in HFD+I human grafts (Figure 37B-C, Figure 38E) but was unchanged in mouse grafts and mouse pancreatic islets in the same mice (Figure 37C-D and Figure 38D). This may indicate that human NKX6.1 in human β cells is more sensitive to HFD-induced insulin resistance than is mouse Nkx6.1 in mouse β cells. Gene expression of *MAFA, PDX1,* and the pan-endocrine marker *PAX6* was unchanged in DT-HG and HFD+I grafts (Figure 37B), but mouse pancreatic islets in HFD+I mice had a dramatic increase in *MafA* expression (Figure 37D). The different responses of MafA and Nkx6.1 between human and mouse islets under metabolic stress may be critically important, given the numerous β cell gene targets of *MafA* and *Nkx6.1*.[30,33,37]

Two of these targets, *INS* and *GCK,* were not changed in HFD+I human islets (Figure 38B), but Ins and Gck were increased in mouse islets from the same mice (Figure 38C). *INS* expression was dramatically reduced in DT-HG grafts, compared to both PBS and DT-NG groups, but *GCK* expression was not changed (Figure 38A). These data suggest that glucotoxic

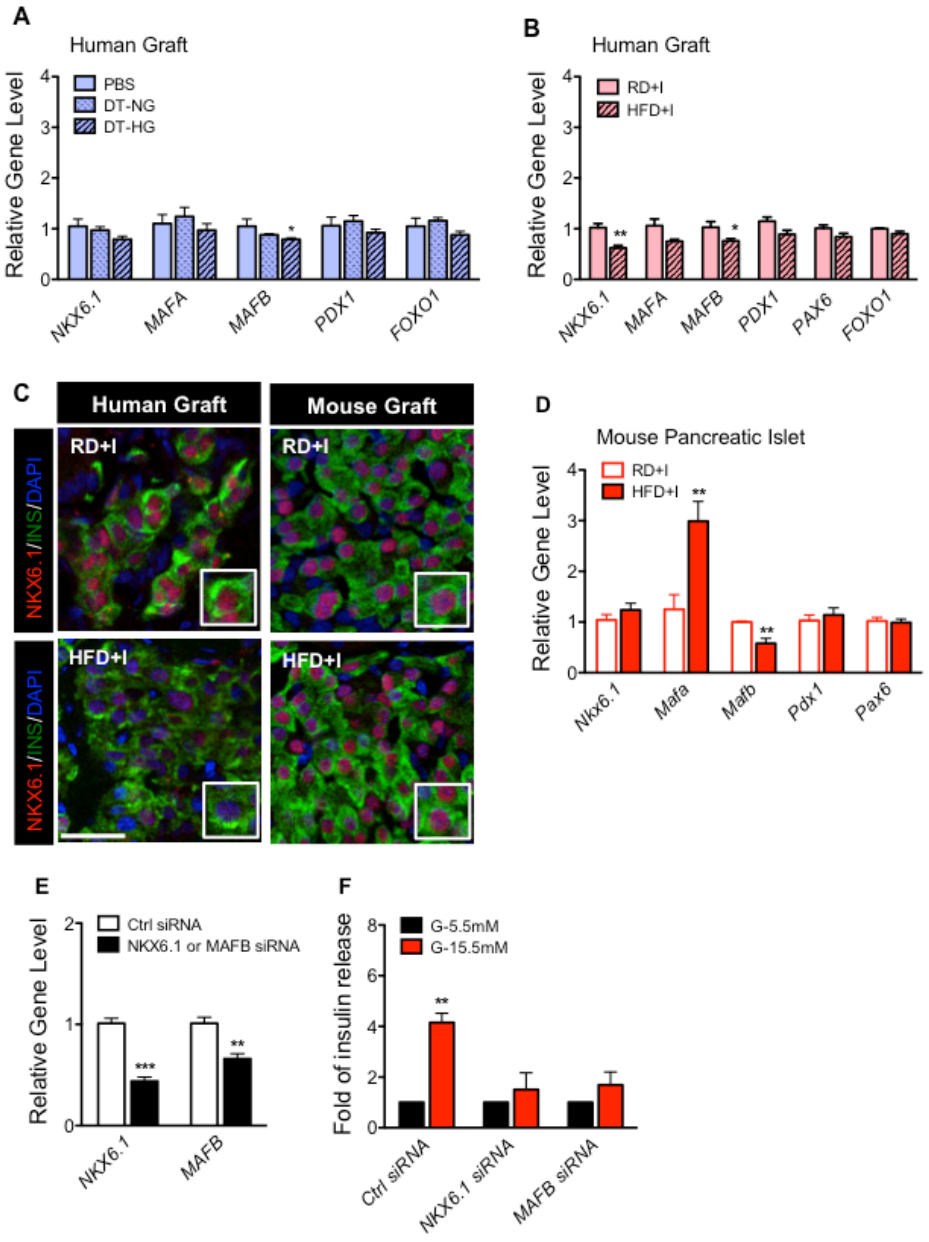

Figure 37. MafB and Nkx6.1 transcription factors are reduced in human islets in DTR and HFD models, respectively. (A, B) mRNA levels of transcription factors in human grafts. * p<0.05, ** p<0.01, DT-HG vs PBS, or NSG-HFD vs NSG-RD (PBS n=5, DTR-NG, n=5; DTR-HG, n=10). (C) Representative images of NKX6.1 protein in HFD+I and RD+I human grafts (left panels) and mouse grafts (right panels). (D) mRNA of transcription factors in mouse islets from NSG-HFD model (n=5/diet, ** p<0.01). (E, F) siRNA knockdown of NKX6.1 or MAFB in EndoC-BH1 cells. (E) Relative level of each gene after treatment with relevant siRNA. ** p< 0.01, *** p<0.001, relative to Ctrl siRNA for each gene (n=6/gene). (F) Static stimulation of insulin secretion with 5.5 mM or 15.5 mM glucose. ** p< 0.01, relative to Ctrl siRNA, (n=3/group).

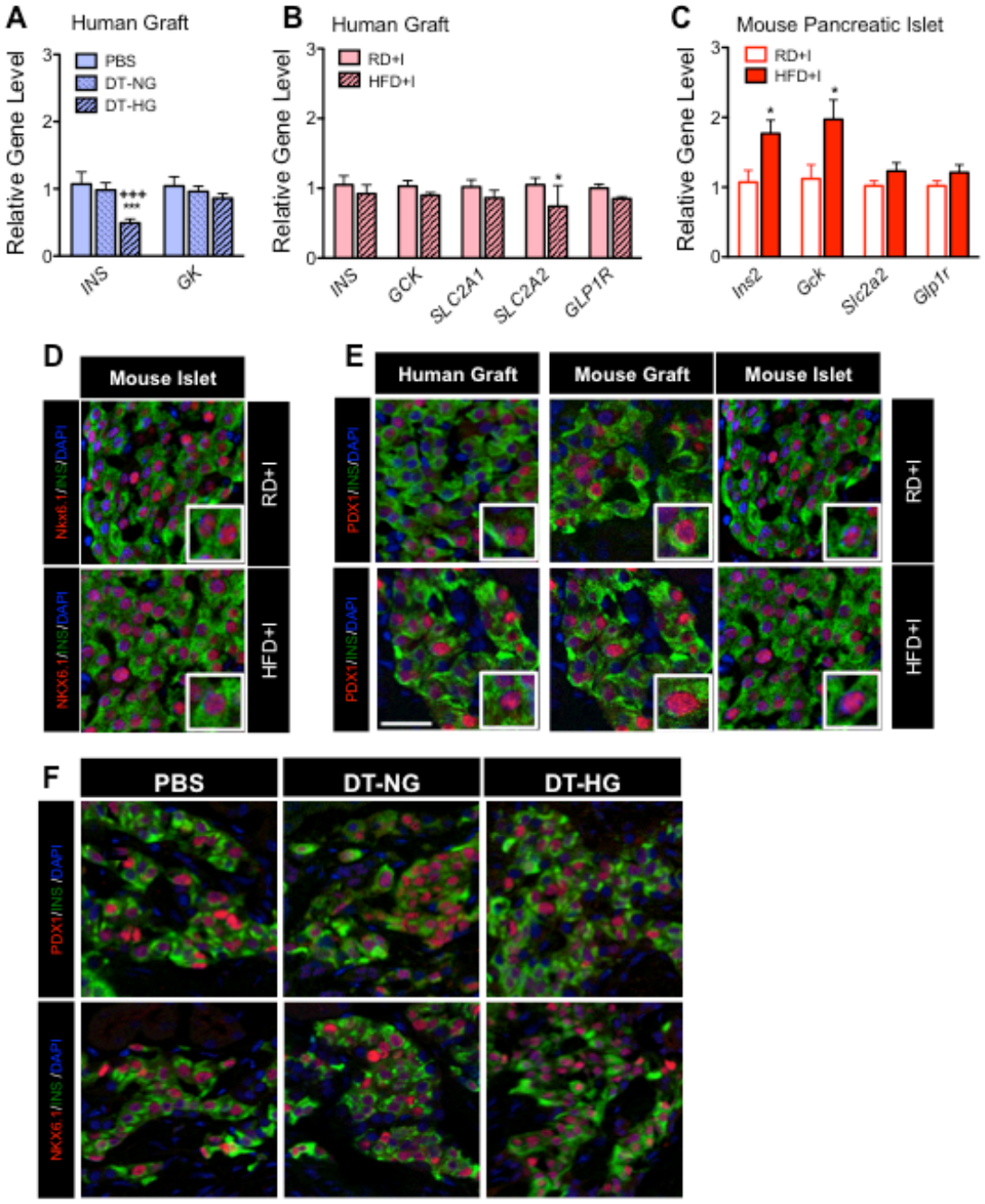

Figure 38. PDX1 protein level does not change in transplanted human β cells in NSG-HFD mice. (A-C) Expression of glucose metabolism genes in NSG-DTR human grafts (A), HFD human grafts (B), and HFD mouse islets (C). * p<0.05, *** p<0.001 vs PBS, ††† p<0.001 vs DT-NG. n=3/group. (D) Representative images of Nkx6.1 in mouse islets on HFD or RD. (E) Images of PDX1 in human grafts (left panels), mouse grafts (center panels), and mouse islets (right panels) in response to RD (top panels) or HFD (bottom panels). Green = insulin, red = PDX1 , blue = DAPI. Inserts are enlarged β cells. Scale bar = 50 μm and applies to (D) and (E). (F) Images of Pdx1 (top panels) and Nkx6.1 (bottom panels) in PBS (left panels), DT-HG (center panels), and DT-NG (right panels) human grafts.

and lipotoxic conditions reduce human insulin gene transcription. To ascertain if decreased NKX6.1 or MAFB affect glucose-stimulated insulin secretion in human β cells, we performed knockdown experiments in the EndoC-βH1 cell line.[160] Reduction of either *MAFB* or *NKX6.1* impaired glucose-stimulated insulin secretion (Figure 37E, F). The decrease observed upon knockdown of *MAFB* is consistent with the pattern recently reported.[274] Moreover, it is likely that the reduction in *NKX6.1* or *MAFB* also contributes to the decreased insulin gene transcription. These data strongly suggest that the glucotoxic and lipotoxic changes in human islet function *in vivo* were mediated by reduction in the level of *NKX6.1* or *MAFB* transcription factors (Figure 39).

Discussion

The terms glucotoxicity, lipotoxicity, and glucolipotoxicity are used frequently to describe a paradigm wherein excess glucose, lipid, or both result in islet dysfunction and pathology.[120,164,165] Based on studies in rodent β cell lines,[88,166,172] human or rodent islets *in vitro,*[92,121,196,205,206] and *in vivo* rodent models,[38,99,169] a range of molecular mechanisms, including oxidative stress, ER stress, β cell apoptosis, and increased amyloid deposition have been proposed[103,119,129,176,207] to contribute to these “toxicities”. However, there is limited information regarding whether these mechanisms are relevant to human islets *in vivo*. To address this gap in understanding, we generated and/or used three models of metabolic stress that enable the study of human islets *in vivo*. These studies demonstrate that chronic and acute hyperglycemia and/or excess lipid and insulin resistance impair stimulated insulin secretion by human islets *in vivo*. This impairment is similar to observations in human T2D[208] and is not explained by β cell death or loss. Chronic insulin resistance decreased human islet antioxidant enzymes, increased superoxide, and decreased the key β cell transcription factors *NKX6.1* and *MAFB*, while chronic hyperglycemia decreased *MAFB,* but not *NKX6.1*. Reducing either *NKX6.1* or *MAFB* in a human cell line

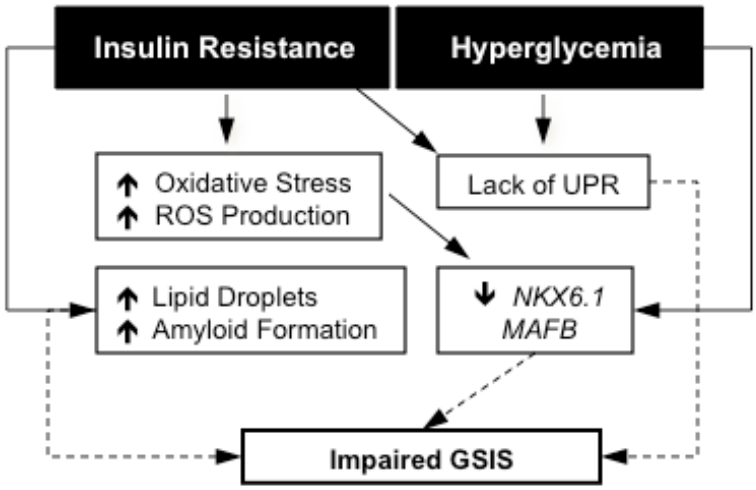

Figure 39. Proposed model of impaired insulin secretion in transplanted human islets under metabolic stress. Solid lines represent experimental relationships. Dotted lines represent possible relationships.

impaired stimulated insulin secretion, mimicking the functional human islet defects seen in the *in vivo* models and indicating that reduction of these transcription factors is likely central to the observed defect. Insulin resistance and hyperglycemia potently stimulated mouse β cell proliferation but not human β cell proliferation, In addition, HFD increased both peri-islet amyloid and intracellular lipid deposits in human islets. Interestingly, the UPR was not increased in response to either condition, despite increased demand for insulin secretion. Importantly, these studies found multiple differences in the response of human islets compared to mouse islets, as well as that some mechanisms noted in rodent models of T2D or *in vitro* studies of rodent or human islets were not operative in human islets challenged by chronic hyperglycemia or insulin resistance *in vivo*.

The presence of both human and mouse islets in the NSG-HFD and NSG-S961 models demonstrated fundamentally different responses of human islets to the same metabolic conditions. These included a lack of metabolic stress-induced β cell proliferation (Figure 32C and J), decreased insulin gene expression and unchanged insulin content (Figure 30B and C), prevalence of intracellular lipid droplets (Figure 32C, F, G, and J), lack of UPR induction (Figure 34I), levels of the reactive oxygen species superoxide (Figure 34F), and changes in transcription factor expression (Figure 37D) in the human islets. In support of our findings, previous studies have also demonstrated that basal human β cell proliferation rates are much lower than mouse,[53,54,209] that compensatory increases in human β cell mass are far smaller than those achieved in mouse,[210] and that human β cell transcription factor expression profiles are distinct from mouse and are not responsive to glucose.[46] A recent study proposes that human β cell proliferation has been systematically underestimated in postmortem studies, due to reduced Ki67 staining in postmortem tissues.[211] However, the functional, vascularized state of the transplanted human islets in our studies argues against Ki67-related underestimation of human β cell proliferation. In addition, we observed these differences in human and mouse islets across

multiple human islet donors. These results highlight the importance of studying human islets when possible and of assessing translational relevance of mouse islet studies.

As a result of these findings, we propose a paradigm of direct and indirect effects of insulin resistance (excess lipid) and hyperglycemia (excess glucose) on human islets *in vivo* (Figure 39). In this paradigm, insulin resistance increases the level of reactive oxygen species, which contributes to reduced expression of the transcription factors *NKX6.1* and *MAFB*. This reduction in transcription factors then impairs stimulated insulin secretion. In this paradigm, hyperglycemia reduces expression of *MAFB,* which impairs stimulated insulin secretion. Other consequences of insulin resistance and/or hyperglycemia, namely increased peri-islet amyloid formation, increased intracellular lipid droplets, and a lack of UPR stimulation may contribute to and exacerbate this secretion deficit in the insulin resistance and hyperglycemia models.

In the NSG-HFD model of excess lipid, the most highly reactive ROS, superoxide, is increased in HFD+I grafts. Reactive oxygen species have been proposed as the mechanism by which excess lipid and hyperglycemia exert many adverse cellular consequences.[196,212] ROS are important messengers required for insulin secretion,[111,112] but excess nutrients can elevate ROS levels and induce negative secondary consequences. Importantly, superoxide may work in conjunction with other ROS, such as hydrogen peroxide, to reduce *NKX6.1* and *MAFB* expression. In response to excess lipid, the dominant site of lipid oxidation shifts from mitochondria to peroxisomes. This shift is proposed to result in higher, toxic concentrations of hydrogen peroxide, against which insulin-producing cells have particularly low defenses.[115,116] Hydrogen peroxide can then directly reduce expression and/or protein function of Nkx6.1, Pdx1, and MafA,[38] defining a potential link between the excess lipid of insulin resistance and impaired stimulated insulin secretion. In our NSG-DTR model of chronic hyperglycemia, neither superoxide nor antioxidant expression changed in DT-HG grafts. However, in response to

hyperglycemia, increased glycolytic flux can directly lead to elevated ROS generation from the electron transport chain.[112] *MAFB*, but not *NKX6.1*, expression is reduced in this model, suggesting that the type of metabolic stress may influence which transcription factors are affected.

Our knockdown experiments in EndoC-βH1 cells demonstrate that reduced NKX6.1 or MAFB expression leads to impaired human islet β cell activity. Not only is Nkx6.1 fundamental to adult β cell identity and function,[29-31] but knockdown of Nkx6.1 in INS-1 cells and primary rat islets reduces stimulated insulin secretion without altering basal secretion or insulin content.[31] This effect is similar to that seen in the NSG-HFD model, in which Nkx6.1 expression is reduced. Contrary to human islets, mouse MafB is critical for β cell development but in adulthood is expressed only in mouse α cells.[33] Although comparatively little is known about MAFB function in the adult human β cell, the fact that it is reduced in both HFD+I and DT-HG islets indicates that reduced MAFB expression may be common to impaired insulin secretion in response to both insulin resistance and hyperglycemia. Interestingly, neither PDX1 nor MAFA, both of which are reduced in human T2D islets,[38] is reduced in HFD+I or DT-HG grafts, which may indicate that increased duration and/or severity of hyperglycemia and/or insulin resistance is required for loss of these particular factors.

In addition to oxidative stress, ER stress has been proposed as a mediator of gluco- and/or lipotoxicity. ER stress can be initiated by chronic activation of the unfolded protein response (UPR), which is critical for sustaining high levels of insulin production, processing, and packaging.[126] Neither DT-HG nor HFD+I grafts showed a change in expression of chaperones central to the UPR, but DT-NG grafts and mouse pancreatic islets in HFD+I mice, which had increased stimulated insulin secretion, increased expression of at least two of the three chaperones. Thus, in our models of insulin resistance or hyperglycemia, the ability to increase

stimulated insulin secretion in response to demand correlates with increased UPR-related gene expression. Lack of UPR induction may functionally compromise the DT-HG and HFD+I human grafts. However, this lack of UPR induction could also be an appropriate response, in which the need for increased human insulin secretion, specifically, is tempered by the shared contribution to secreted insulin by the transplanted HFD+I human β cells and the pancreatic mouse β cells.

Beyond cellular stress responses, peri-islet amyloid deposition, a pathologic hallmark of human T2D, has been suggested as a mechanism of β cell dysfunction and apoptosis.[134,142,143,145,213,214] However, studying the development of amyloid in human islets is difficult. The majority of prior data comes either from autopsy studies that do not permit time course studies, or from mouse models that transgenically express human amyloid. Using our models, we found that HFD+I grafts had both more and larger amyloid deposits (Figure 35B and C). Importantly, this increase in amyloid deposition did not lead to increased apoptosis, but could contribute to the impaired stimulated insulin secretion from human islets. Recent studies suggest that impaired autophagy increases susceptibility to amyloid-related toxicities,[140,215] a relationship that can now be examined in human islets using these models.

There was a striking lack of islet cell apoptosis in both DT-HG and HFD+I mice (Figure 33), which indicates that loss of β cells does not contribute to impaired stimulated insulin secretion. Some prior studies demonstrating lipid- and glucose-induced β cell death used high concentrations of lipid or glucose in culture.[103,176-178,216] Importantly, high-fat diet likely generates very different lipid species than the selected lipid moieties of infusion or islet culture studies. Low levels of β cell apoptosis and a modest reduction in β cell mass are observed in human cadaveric T2D studies.[107,217] The duration of metabolic stress experienced by human patients (years or decades) may be required for β cell death to occur *in vivo*, or it may require the

coexistence of hyperglycemia and insulin resistance that is present in those patients but not in our chronic models.

Glucose has been proposed as a mouse β cell mitogen.[191,192] Both by infusing glucose into human islet graft-containing mice[218] and by using the hyperglycemia of the Akita mouse model,[193] modest changes in human β cell proliferation rate were noted. However, in our models, neither 7 days nor one month of hyperglycemia stimulated human β cell proliferation. Importantly, by co-transplanting mouse islets, we confirmed that mouse β cells under the kidney capsule proliferate in response to hyperglycemia or insulin resistance. The lack of increased human β cell proliferation in our models is consistent with human autopsy studies of lean, obese, pregnant, and diabetic patients,[51,52] although a caveat is that human β cells may not respond to *in vivo* murine stimuli. The relative age of mouse and human islets must also be considered. Human islets used were from healthy, non-diabetic, adult donors, in the age range that humans develop T2D. Mouse islets were also from adults, but it is not clear how to control for islet age between these species. Although the NSG genetic background is critical for successful islet engraftment, it also eliminates many islet-immune interactions, which may impact islet function and health.[219-222]

Using three models of metabolic stress on human islets *in vivo*, this work demonstrates that hyperglycemia and insulin resistance impair stimulated insulin secretion in human islets *in vivo*, and this is at least partly due to reduced expression of NKX6.1 and/or MAFB. In addition, insulin resistance has a broader set of negative consequences than hyperglycemia. Surprisingly, neither hyperglycemia nor insulin resistance stimulated β cell proliferation or apoptosis, and the responses of human and mouse islets were fundamentally different in many aspects. Future studies should focus on determining if these abnormalities that likely contribute to the decline in insulin secretion in T2D can be therapeutically addressed.

CHAPTER IV

HUMAN ISLET PREPARATIONS DISTRIBUTED FOR RESEARCH EXHIBIT A VARIETY OF INSULIN SECRETORY PROFILES

Introduction

The availability of human islets for basic and translational research has increased markedly over the last decade, fueling insights into human islet biology and diabetes. Studies of human islets have provided insight into human islet morphology, β cell proliferation,[45,84,184,223] epigenetics,[45,84,184,223-225] regulation of insulin secretion,[226-228] nutrient-induced toxicity,[46,168,229] transcription factor regulation,[38,46,230] and transplantation of human islet cells.[84,218,231] For example, human β cells proliferate at much lower frequency *in vivo* than mouse β cells[53,190] and respond to different regulators than mouse β cells.[195,223] Such advances in our understanding have spurred interest in research with human islets and the demand for human islet tissue.

In the United States, human islets are currently available for research via the NIDDK-supported Integrated Islet Distribution Program (IIDP), https://iidp.coh.org, which replaced the National Islet Cell Resource Center Consortium (ICR) in 2009. Human islets isolated at IIDP-affiliated isolation centers are shipped overnight to recipient laboratories.[232] Both the number of investigators applying to receive human islets and the total number of requested islets have risen dramatically.[81] Along with each islet preparation, the isolation center provides metrics of the isolation procedure, e.g. cold ischemic time, estimated culture time, purity, and viability of the islets, as well as de-identified donor information (age, sex, BMI, race) that is released by the organ procurement organization.

Currently, there are no accepted standards to uniformly evaluate and report the health and function of human islets prior to experiments, to present data from multiple islet preparations from different isolation centers, or to compare the human islet data from different laboratories. Human islet research uses islets from donors of different ages, gender, BMIs, and races, that are isolated at isolation centers with different personnel and then shipped to investigators across the U.S. Certain donor attributes and isolation conditions may correlate with higher or lower islet yield upon isolation,[233-235] but little is known about these potential relationships. Furthermore, how or whether to assess the health and function of health of islet preparations prior to study is not standardized. Some laboratories assess human islet health and/or function using methods such as measurement of oxygen consumption[236,237] or insulin release in response to stimuli,[46,238], among others.[230,239] Although studies have examined the relationship between donor attributes and insulin release in the context of a single isolation center,[226] little is known about insulin secretion compared among islet preparations from different isolation centers, which reflects how human islet research is currently being conducted in most research laboratories.

To define the functional variability in human islet preparations being used for research in the United States, we analyzed categorical and functional data from 202 human islet preparations distributed by the IIDP/ICR, many which were also used by other investigators. Functional data was obtained via islet perifusion, a method that assesses integrated β cell function with high temporal resolution and in sequential response to multiple secretagogues.[238] Our studies indicate that the majority of islet preparations from 15 centers are functional, appropriately secreting insulin in response to two stimuli. However, a sizeable minority of preparations was dysfunctional. These studies suggest necessary considerations for conducting, reporting, and interpreting research with human islets.

Results

Influence of donor and islet attributes

To characterize the influence of donor and islet attributes on human islet preparations used for studies in our laboratory, we assessed the insulin secretory profile of 202 human islet preparations from 15 islet isolation centers during the years 2002-2013, using a dynamic cell perifusion system. Islets from pancreas donors were isolated at one of 15 U.S. isolation centers, then shipped to Vanderbilt by overnight courier (Figure 40A). Upon arrival, we hand-picked islets to increased purity (Figure 40B) and perifused islets and plotted insulin secretion data for all preparations, to assess islet function (Figure 40A). Islets were then used for a variety of experimental purposes. We first grouped and examined attribute values (Table 5) by isolation center. In the 202 islet preparations, most donor (Table 6) and islet attributes (Table 7) had similar values and ranges among the majority of centers, with one or two centers contributing significant variation. To reduce bias from differences in sample size across centers, we chose for further analysis (beyond statistical summarization) only centers that provided 7 or more preparations, leaving 183 islet preparations from 11 centers (centers 1, 2, 3, 6, 7, 8, 9, 10, 11, 14, and 15) for subsequent analysis.

Grouping of islet preparations by in vitro response

The shape of the perifusion response (insulin secretion) curves varied among preparations, suggesting that combining all data sets could veil biologic differences and the contribution of other factors to islet secretion. Among 183 preparations, we noted five recurring, *in vitro* insulin secretion patterns, defined as follows (Figure 41). Group 1 preparations: stable baseline at 5.6 mM glucose, well-defined peaks in response to both 16.7 mM glucose and 16.7 mM glucose + IBMX (denoted by both Fold 1 and Fold 2 exceeding 1.5), and a $Peak2_{Max}$ that was higher than

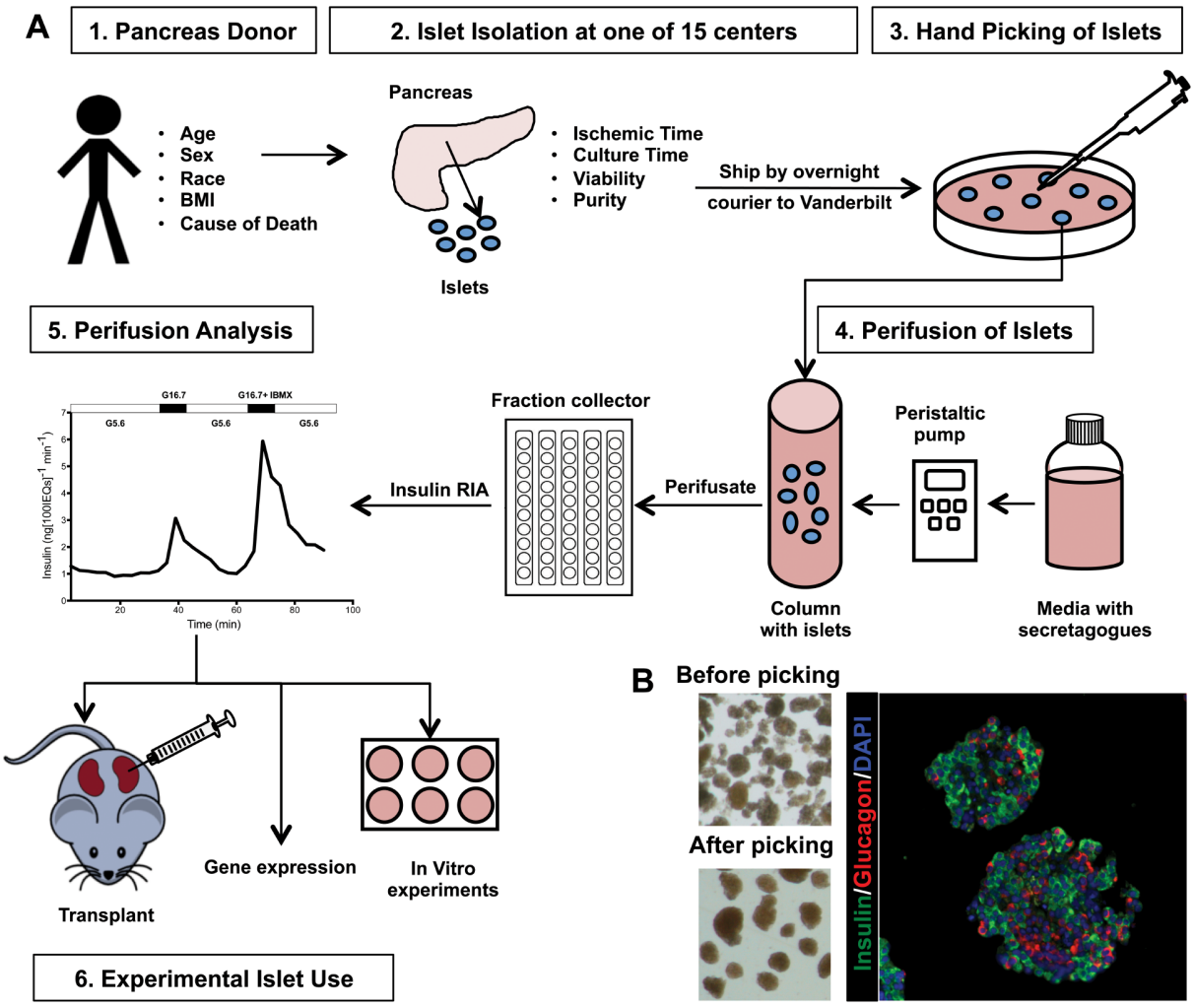

Figure 40. Order of events for assessing human pancreatic islets. A: Islets isolated from donor pancreata at isolation centers were shipped by overnight courier to Vanderbilt, where they were hand-picked for further purity and IEQ quantification. Islets were perifused to assess in vitro function. Islets were used for subsequent studies that are not part of the current report. B: Images showing a human islet preparation before (top left panel) and after (top right panel) hand picking. Immunolabeling of human islets for DAPI (blue), insulin (green), and glucagon (red) embedded in collagen gel (far right panel). Figure from Kayton et al. (2015)

Table 5. Donor and Islet Attributes and Possible Values		
Attribute	**Possible Values**	**Actual Value Range**
Center	#1-15	
Year	2002-2013	
Donor attributes		
Age (of donor)	Continuous (years)	7-74 years
Sex	Male/Female	
Race*	Caucasian, African American, Hispanic	
BMI	Continuous (kg/m^2)	15.2-53.2 kg/m^2
Cause of death	Categorical	
Islet attributes		
Ischemic Time †	Continuous (hours)	2-23 hours
Culture Time ‡	Continuous (days)	0-7 days
Viability §	Continuous, 1-100%	64-99%
Purity**	Continuous, 1-100%	40-99%

*Reported as Caucasian, African American, Hispanic, or Asian; †Time of cold eschemia. from time of aortic cross clamp to either pancreas trimmung, initial collagenase injection, or start of digestion; ‡ Estimated culture time prior to shipment; § Percent of viable cells in preparation; **Percent of dithizone-position cells in preparation. All information provided by islet isolation centers. Table adapted from Kayton et al. (2015).

Table 6. Summary of Donor Attributes

Center	Total N	Age (Years) *†	N	Sex (M / F) ‡	Race (C / A / H)§	BMI (kg/m^2)	N
1	15	54.0 ± 2.8 (52-56)	2	0 / 2	0 / 0 / 0	33	1
2	37	38.5 ± 12.6 (20-64)	35	19 / 16	25 / 3 / 3	28.8 ± 6.1 (16.9-46.6)	35
3	21	49.2 ± 10.9 (23-65)	12	4 / 8	6 / 0 / 2	26.6 ± 4.2 (18.0-34.2)	11
4	6	40.4 ± 13.4 (24-53)	5	3 / 2	4 / 0 / 1	31.4 ± 5.1 (24.1-37.9)	5
5	6	42.4 ± 12.3 (22-53)	5	2 / 1	2 / 0 / 0	33.2 ± 1.7 (31.4-34.6)	3
6	19	42.2 ± 13.4 (18-58)	18	10 / 8	2 / 0 / 0	28.5 ± 8.3 (16.1-45.0)	18
7	17	48.2 ± 12.4 (26-69)	17	9 / 7	9 / 0 / 1	29.6 ± 5.6 (22.3-40.9)	17
8	7	31.6 ± 14.1 (17-48)	6	2 / 3	4 / 1 / 0	33.4 ± 9.9 (23.3-48.4)	6
9	15	45.8 ± 16.2 (19-64)	12	6 / 6	10 / 0 / 2	36.1 ± 11.8 (21.6-52.4)	12
10	21	40.2 ± 14.7 (11-56)	19	10 / 9	15 / 1 / 2	27.0 ± 4.9 (18.3-37.8)	19
11	16	50.4 ± 15.4 (20-74)	16	6 / 6	4 / 0 / 1	28.5 ± 5.1 (20.3-39.3)	16
12	3	53.0 ± 5.6 (48-59)	3	1 / 2	1 / 2 / 0	25.2 ± 4.2 (21.4-29.8)	3
13	4	18.0 ± 9.6 (7-25)	3	3 / 1	0 / 2 / 0	21.0 ± 8.2 (15.2-26.8)	2
14	8	43.7 ± 15.7 (26-60)	7	4 / 3	7 / 0 / 0	35.7 ± 8.5 (28.7-53.2)	7
15	7	39.8 ± 6.9 (28-46)	4	3 / 1	1 / 0 / 0	31.6 ± 4.2 (26.0-37.4)	4
Total	202	42.9 ± 14.1 (7-74)	163	82 / 74	90 / 9 / 12	29.6 ± 7.1 (15.2-53.2)	158

* Mean ± standard deviation. † Range (max-min). ‡ Sex. Male (M), Female (F). N= number of preparations with that attribute reported, used to calculate mean, standard deviation, and range for that attribute. § Race. Caucasian (C), African American (A), Hispanic (H). Data was not available from all preparations. Figure from Kayton et al. (2015).

Table 7. Summary of Islet Attributes

Center	Total N	Cold Ischemic Time(Hours) *†	N‡	Est. Culture Time (Days)	N‡	Viability (%)	N‡	Purity (%)	N‡
1	15	13.0 ± 1.4 (12-14)	2	N.R.§	0	N.R.	0	N.R.	0
2	37	12.9 ± 5.2 (3-23)	34	2.2 ± 1.4 (1-7)	31	90.4 ± 6.0 (70-99)	27	87.3 ± 9.9 (40-97)	34
3	21	14.2 ± 3.2 (11-20)	10	2.1 ± 0.7 (1-3)	10	89.3 ± 8.1 (70-96)	10	84.5 ± 7.3 (70-95)	11
4	6	6.0 ± 2.8 (2-8)	4	3.0 ± 2.4 (1-7)	5	77.4 ± 12.1 (64-97)	5	60.6 ± 7.4 (55-73)	5
5	6	8.4 ± 4.4 (2-13)	5	2.5 ± 0.6 (2-3)	4	85.5 ± 5.8 (77-90)	4	72.5 ± 9.6 (60-80)	4
6	19	10.1 ± 3.2 (5-15)	17	1.5 ± 0.6 (1-2)	4	88.5 ± 8.8 (70-98)	8	72.2 ± 7.1 (60-85)	9
7	17	4.0 ± 2.8 (2-6)	2	1.8 ± 1.6 (0-6)	11	92.8 ± 6.2 (75-98)	13	77.5 ± 13.1 (40-90)	15
8	7	9.3 ± 1.3 (8-11)	5	4.6 ± 0.9 (4-6)	6	97.7 ± 2.3 (95-99)	4	75.0 ± 12.3 (60-90)	6
9	15	6.8 ± 2.5 (3-11)	11	2.4 ± 1.7 (1-7)	12	97.1 ± 2.9 (91-99)	8	80.8 ± 19.7 (40-99)	12
10	21	8.6 ± 2.9 (3-16)	19	1.6 ± 1.1 (1-5)	18	90.9 ± 4.7 (79-97)	17	85.6 ± 6.0 (70-95)	19
11	16	10.4 ± 2.7 (4-14)	15	3.2 ± 1.5 (2-7)	10	93.0 ± 3.3 (86-96)	15	74.5 ± 16.5 (43-95)	15
12	3	5.7 ± 3.1 (3-9)	3	4.0 ± 1.0 (3-5)	3	91.3 ± 6.5 (85-98)	3	82.5 ± 17.7 (70-95)	2
13	4	10.0	1	2.7 ± 3.1 (0-6)	3	96.0 ± 14.1 (95-97)	2	95.0	2
14	8	6.7 ± 1.9 (3-9)	7	1.8 ± 1.8 (1-6)	8	93.4 ± 4.0 (88-98)	7	92.1 ± 5.7 (80-95)	7
15	7	10.3 ± 1.9 (9-13)	3	1.6 ± 0.6 (1-2)	4	94.0 ± 1.2 (92-95)	4	89.2 ± 2.4 (85-91)	4
Total	202	10.1 ± 4.3 (2-23)	137	2.3 ± 1.5 (0-7)	128	91.2 ± 6.8 (64-99)	126	81.6 ± 13.0 (40-99)	144

* Mean ± standard deviation. † Range (max-min). ‡ N= number of preparations with that attribute reported, used to calculate mean, standard deviation, and range for that attribute. § N.R. = not reported. Figure from Kayton et al. (2015).

Peak1$_{Max}$ (Figure 41A). Group 2: Peak1$_{Max}$ that higher than Peak2$_{Max}$ (Figure 41B). Group 3: no peak in response to 16.7 mM glucose (Fold 1 of less than 1.5) but a peak in response to 16.7 mM glucose + IBMX (Fold 2 of greater than 1.5) (Figure 41C). Group 4: unstable baseline at 5.6 mM glucose (Figure 41D). Group 5: no response to either stimulus (Fold 1 and Fold 2 of less than 1.5) (Figure 41E). The majority of preparations (72%) were in Group 1 (Figure 42C and D), despite representing a variety of centers, years, donor attributes, and islet attributes. However, 12% of preparations were in Group 5, and the remaining 16% were in Groups 2, 3, or 4 (Figure 42C and D). Thus, caution is appropriate when making assumptions about performance of a specific human islet preparation.

Distribution of islet response groups

We next examined potential reasons for the variability in stimulated insulin secretion. The distribution of preparations among response Groups 1-5 was not influenced by Center (Figure 42A) or Year (Figure 42B). To determine whether donor or islet attributes correlate with a particular response Group, we compared Group 1 to Group 5, then searched for attributes associated with an increased probability of any Group. Race was the only factor that influenced probability of Group 1 versus Group 5 ($p=0.007$), which was demonstrated by polytomous regression analysis (Figure 44D). No other donor or islet attributes influenced Group.

Univariate analysis of donor and islet variables

To assess whether donor and islet attributes affected *in vitro* secretion, we focused on Group 1 islet preparations, because attributes of Groups 2-5 (uneven Baseline or lack of Peak 1, Peak 2, or both) might obscure an association between donor or islet attributes and secretion response. Within Group 1 preparations specifically, both Center and Year influenced Baseline (Figure 43A and D, respectively), and Center influenced Fold 1 (Figure 43B). The relationship between

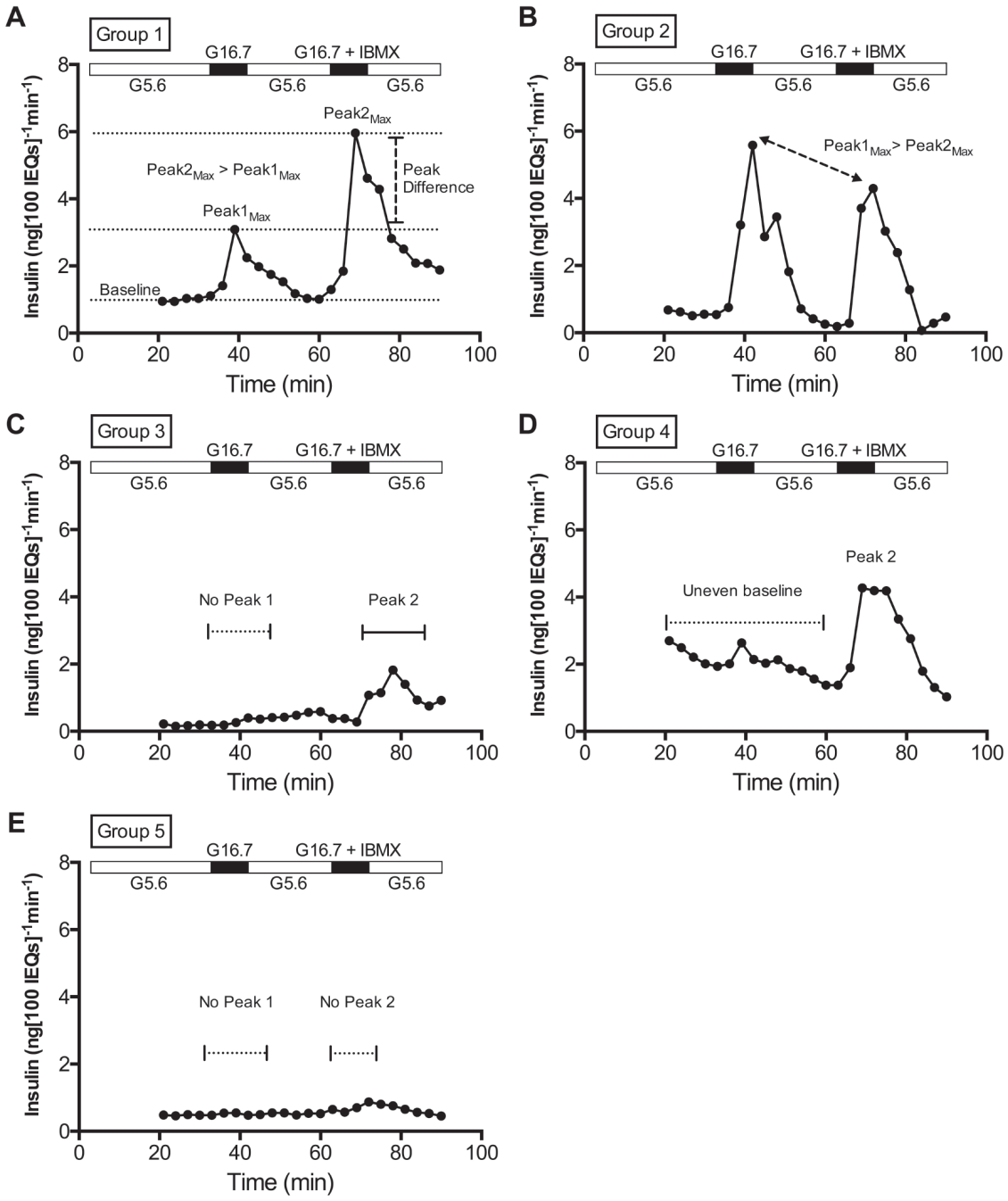

Figure 41. Definitions of *in vitro* response Groups. Perifusion of human islets with the following order of stimuli in media: 5.6 mM glucose to 16.7 mM glucose, back to 5.6 mM glucose, then to 16.7mM glucose with IBMX. From the entire body of perifusion data, five general response groups emerged. A-E: real curves from representative preparations, illustrating characteristics of each Group. A: Group 1 had two stimulation peaks (16.7 mM glucose + IBMX induces a higher $Peak_{max}$ than 16.7 mM glucose alone) and a stable baseline. B: Group 2 differed from Group 1 by having a higher $Peak1_{max}$ (in response to 16.7 mM glucose) than $Peak2_{max}$ (in response to 16.7mM glucose + IBMX). C: Group 3 had no Peak 1 but did have a Peak 2. D: Group 4 had an uneven baseline, but has one or both Peaks. E: Group 5 was considered non-responsive, because it had neither Peak1 nor Peak2. Figure from Kayton et al. (2015).

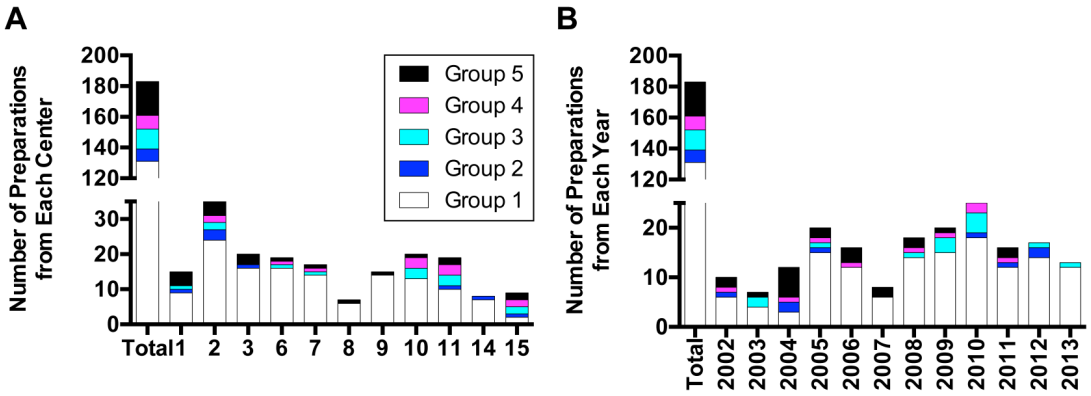

C **Response Groups by Center**

Center	N	#1 [N(%)]	#2 [N(%)]	#3 [N(%)]	#4 [N(%)]	#5 [N(%)]
1	15	9 (60)	1 (7)	1 (7)	0 (0)	4 (27)
2	37	24 (65)	3 (8)	2 (5)	2 (5)	6 (16)
3	21	16 (76)	1 (5)	0 (0)	1 (5)	3 (14)
6	19	16 (84)	0 (0)	1 (5)	1 (5)	1 (5)
7	17	14 (82)	0 (0)	1 (6)	1 (6)	1 (6)
8	7	6 (86)	0 (0)	0 (0)	0 (0)	1 (14)
9	15	14 (93)	0 (0)	0 (0)	0 (0)	1 (7)
10	21	13 (62)	0 (0)	3 (14)	4 (19)	1 (5)
11	16	10 (63)	1 (6)	3 (19)	0 (0)	2 (13)
14	8	7 (88)	1 (13)	0 (0)	0 (0)	0 (0)
15	7	2 (29)	1 (14)	2 (29)	0 (0)	2 (29)
Total	183	131 (72)	8 (4)	13 (7)	9 (5)	22 (12)

D **Response Groups by Year**

Year	N	#1 [N(%)]	#2 [N(%)]	#3 [N(%)]	#4[N(%)]	#5 [N(%)]
2002	10	6 (60)	1 (10)	0 (0)	1 (10)	2 (20)
2003	7	4 (57)	0 (0)	2 (29)	0 (0)	1 (14)
2004	12	3 (25)	2 (17)	0 (0)	1 (8)	6 (50)
2005	20	15 (75)	1 (5)	1 (5)	1 (5)	2 (10)
2006	16	12 (75)	0 (0)	0 (0)	1 (6)	3 (19)
2007	8	6 (75)	0 (0)	0 (0)	0 (0)	2 (25)
2008	18	14 (78)	0 (0)	1 (6)	1 (6)	2 (11)
2009	20	15 (75)	0 (0)	3 (15)	1 (5)	1 (5)
2010	26	18 (69)	1 (4)	4 (15)	2 (8)	1 (4)
2011	16	12 (75)	1 (6)	0 (0)	1 (6)	2 (13)
2012	17	14 (82)	2 (12)	1 (6)	0 (0)	0 (0)
2013	13	12 (92)	0 (0)	1 (8)	0 (0)	0 (0)
Total	**183**	**131 (72)**	**8 (4)**	**13 (7)**	**9 (5)**	**22 (12)**

Fiure 42. Distribution of response Groups among isolation Centers and across Year of isolation. Distribution of response groups by Center (A) or Year (B), and actual values for Center (C) and Year (D). Figure from Kayton et al (2015).

Center and Fold 2 suggested a trend but did not meet statistical significance (Figure 43C, p=0.06). There was a linear relationship of decreasing Baseline and increasing Fold 1 and Fold 2 as Year increased (Figure 43D-F). Linear regression analysis revealed that these relationships were significant (p=0.008, 0.001, and 0.005, respectively).

We adjusted all subsequent analyses for Center or Year, removing the contribution of each variable (adjusting for both Center and Year simultaneously was not possible due to loss of statistical power). When adjusted for Center, Baseline was influenced by Purity (p=0.048) and Year (p=0.005), Fold 1 was marginally influenced by Year (p=0.051), and Fold 2 was influenced by Cause of Death (0.016). When adjusted for Year, Fold 2 was influenced by BMI (p=0.045). These results indicate that (1) Baseline and Fold 2 may be influenced by separate variables, (2) Baseline decreases and Fold changes increase linearly with increasing Year, and (3) when Center or Year is controlled for, only Purity, Cause of Death, and BMI influenced any measure of the *in vitro* response. This suggests that *in vitro* responses of islet preparations available for research are improving over time (becoming more similar to a Group 1 curve, with low Baseline and large Fold increases).

In vitro stimulated insulin secretion does not correlate with in vivo function of responsive islet preparations

To address whether *in vitro* stimulated insulin secretion predicts *in vivo* function, we assessed 12 Group 1 preparations that were transplanted as part of other projects. For the 12 transplanted preparations, the average *in vivo* fold change from basal to stimulated insulin was 2.46 ± 0.38. There was a poor linear relationship between Fold 1 (derived from perifusion) and *in vivo* Fold change (derived from *in vivo* glucose-arginine stimulation) (Figure 43G) among

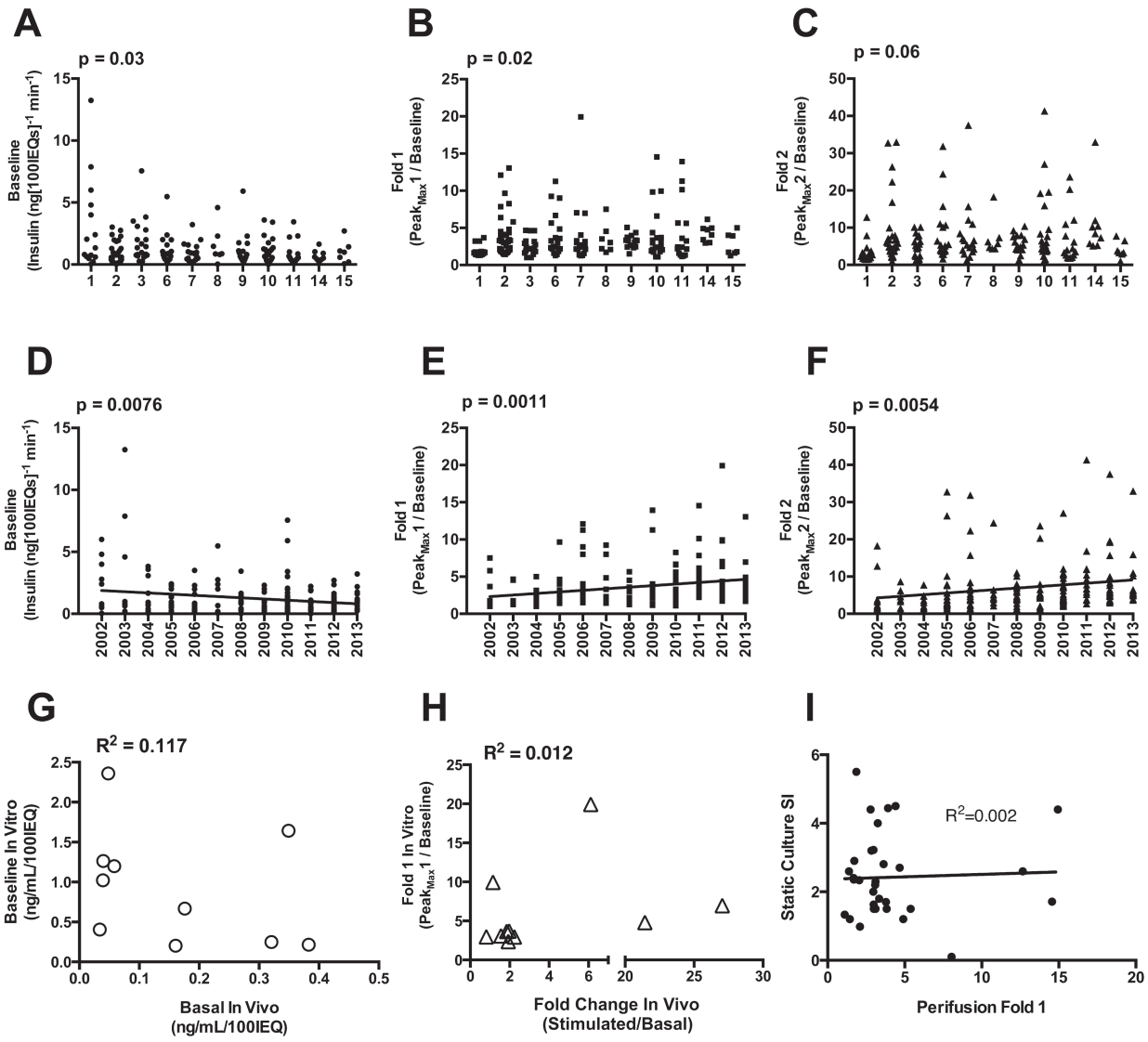

Figure 43. Effects of isolation Year and Center on in vitro and in vivo responsiveness. A-C: Univariate analyses of Center versus Baseline (A), Fold 1 (B), and Fold 2 (C). D-F: Linear regression analysis of Year versus Baseline (D), Fold 1 (E), and Fold 2 (F). G: Plot of Fold 1 values from perifusion (Perifusion Fold 1) against In Vivo Fold change, measured via glucose-arginine stimulation. Basal human insulin values measured in mouse plasma after 6-hour fast. Stimulated insulin values measured 15 minutes after injection of glucose-arginine; n=12. H: Perifusion Fold 1 values graphed against Static Culture Stimulation Index (SI), the ratio of insulin secretion at high glucose to secretion at low glucose, as reported by isolation centers to the IIDP; n=30. I: Plot of Perifusion Fold 1 versus Static Culture SI from static culture performed in our laboratory. Previously published data points are represented by open squares; newly procured data points are closed squares. Figure from Kayton et al. (2015).

these 12 preparations. Twelve transplanted islet preparations did not provide sufficient statistical power to detect an effect of donor or islet attributes on measures of *in vivo* insulin secretion.

Comparison of static culture and perifusion measures of stimulated insulin release

To compare perifusion and static culture as methods for functional islet assessment, we plotted static culture stimulation indices (reported by the isolation centers) against Perifusion Fold 1 responses (measured in our laboratory) of 30 human islets preparations. We observed no linear correlation between the two measures (Figure 43H), indicating that static culture does not predict stimulated insulin secretion from islet perifusion. We then analyzed 7 preparations for which both assays were conducted in our laboratory, on the same day (Figure 43I). This analysis yielded the same result, namely that stimulated insulin values do not correlate well between perifusion and static culture.

Modeling of insulin secretion as assessed by perifusion

To graphically represent the effects of significant attributes uncovered in our univariate analyses, we fit splines (curves) of the raw combined perifusion data for all preparations using nonlinear mixed effect models, which produce representative curves separated by different attributes of interest, such as Center, Year, and Cause of Death. Splines are defined by the full complement of *in vitro* data points, but they have smoothed shapes that ease visual interpretation and reduce degrees of freedom. Differences in secretion correlated with Center (Figure 44A) and Year (Figure 44B), in that two centers had a higher Baseline and Peak Max values than the majority. However, centers had similar average curve shapes. Baseline and $Peak_{Max}$ values generally decreased with Year, but Fold changes increased, as observed in our linear regression analyses (Figure 43D-F). Cause of Death (Figure 44C) is the single attribute that affected Baseline, $Peak1_{Max}$ and $Peak2_{Max}$ values, as well as the shape of the curve (such as the width of Peak 2

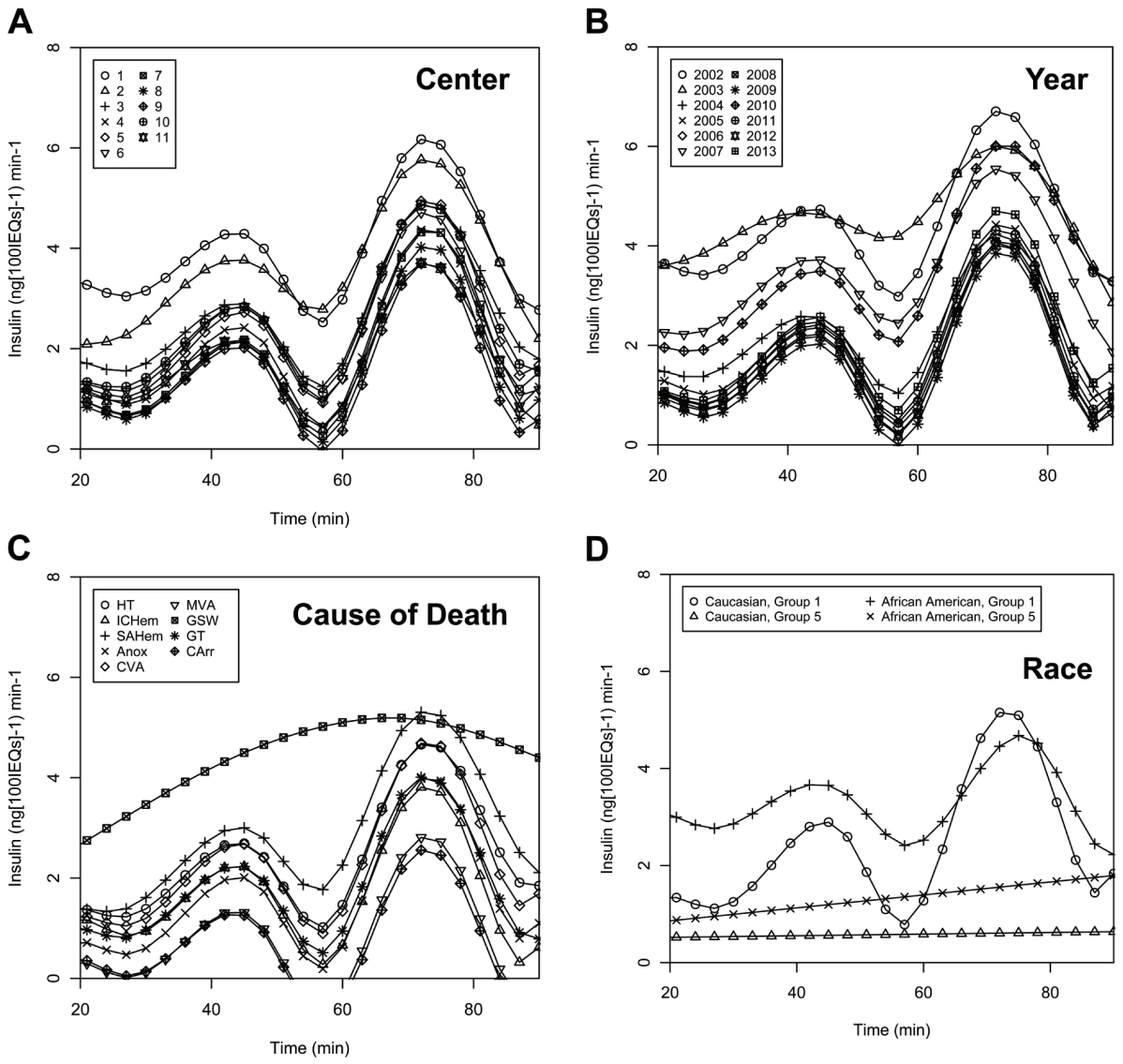

Figure 44. Fitted spline analysis of perifusion data. A-C: Smoothed average curve fits for response by (A) Center, (B) Year, and (C) Cause of Death. D: Fitted differences between Group 1 and Group 5 islet preparations by race (Caucasian and African American). HT = head trauma, ICHem = intracerebral hemorrhage, SAHem = subarachnoid hemorrhage, Anox = anoxia, CVA = cerebrovascular accident, MVA = motor vehicle accident, GSW = gunshot wound, GT = general trauma, CArr = cardiac arrest. Figure from Kayton et al. (2015).

and the consistency of the Baseline), by way of fitted spline modeling. Cardiac arrest (CArr) and intracerebral hemorrhage (ICHem) were associated with lower Baseline, $Peak1_{Max}$ and $Peak2_{Max}$ than other causes of death, and subarachnoid hemorrhage with the highest. It remained unclear whether Cause of Death biologically impacts islets or is associated with an attribute that does. The relationship between Race and response Group (Figure 44D) revealed that, within Group 1 preparations, African American preparations had smaller average Fold changes than Caucasian preparations and that Baseline of Group 5 preparations was higher if from African American donors. Race did not significantly influence any individual *in vitro* measures but was clearly related to the response Group and the shape of the curve in both Group 1 and Group 5 islet preparations. Collectively, these analyses both confirm our polytomous regression results that Race impacted likelihood of Group 1 versus Group 5 response type and revealed the influence of Cause of Death on *in vitro* response (on Baseline, Peak Max values, and curve shape).

Gene expression differences between Group 1 and Group 5 islets

To investigate the reason for functional differences between Group 1 and Group 5 preparations, we compared expression of key islet-enriched genes in preparations matched for age, sex, and BMI (Figure 45A-B). Transcript levels of GLUT-2 (*SLC2A2*), glucokinase (*GCK*), and MafA (*MAFA)* were significantly lower in Group 5 islets (Figure 45C), but insulin was similar (Figure 45C), highlighting alterations in glucose sensing, rather than in insulin production. Notably, there was no difference in the expression of apoptosis markers Chop, Bid, and Bad (Figure 45D), indicating that a lack of response to stimuli is not simply due to apoptosis or β cell death. We assessed insulin content from 30 human islets preparations (Figure 45E) to address whether insulin content differed among the response Groups,. The values and amount of variation appear similar among the 5 Groups, with the two values for Group 5 (unresponsive) preparations calling within the range of values for Group 1 preparations. We were unable to

A

Donor Information

	Group 1 n=6	Group 5 n=6
Sex	3M / 3F	3M / 3F
Age	37.0 ± 6.7	39.0 ± 5.4
BMI	24.6 ± 1.5	23.5 ± 2.7

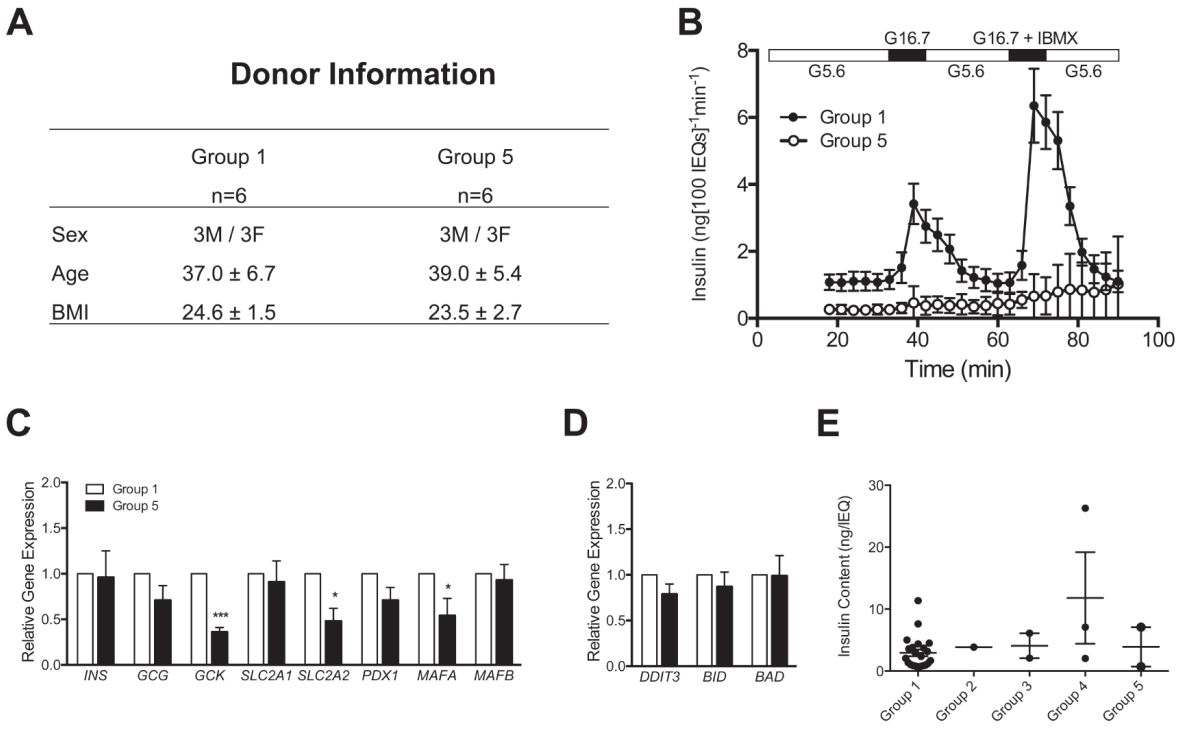

Figure 45. Gene expression in Group 1 and Group 5 islets. A: Islets from six Group 1 and six Group 5 preparations were matched for sex, age, and BMI. B: Perifusion results. Plotted insulin concentration (ng/100 IEQ/ min) values for all collected media fractions. n=6 for each group. These Group 1 preparations were a subset of a previously published data set (10). C-D: Expression of islet-enriched (C) and apoptosis (D) genes quantified by RT-PCR. Gene transcript levels expressed relative to Group 1 values. n=6 for each group. E: Insulin content (ng/IEQ) of aliquots from 30 human islet preparations, separated by response Group (1-5) (not same 30 islet preparations as in Fig. 43H). Figure from Kayton et al. (2015).

perform an ANOVA due to the low frequency of Group 2-5 preparations in the 30 preparations analyzed.

Discussion

Research using human islets is providing new insight into human islet biology and diabetes. The fact that human islet preparations for research are isolated at multiple centers from donors with varying characteristics presents a challenge to understanding, interpreting, and integrating research findings that arise from multiple laboratories using these islets, as little is known about the variation among preparations. We report the first comprehensive, standardized assessment of human islet function using preparations from multiple isolation centers. We used islet perifusion to assess human islet health and function, because it is more informative than static incubation, by allowing measurement of a sequential and temporal response to multiple secretagogues. We assessed insulin secretion from 202 human islet preparations from 15 centers over an 11-year period, and examined whether the variation among islet preparations related to biological differences or variability in islet isolation procedures.

We noted five recurring insulin secretion patterns (Groups), defined by the degree and nature of responsiveness to two stimuli (16.7 mM glucose with or without IBMX). The five insulin secretion patterns (Groups) suggest differences in the underlying biology of the preparations. For example, Group 2 preparations differed from Group 1 by having a lower $Peak2_{Max}$ than $Peak1_{Max}$, potentially indicating that insulin stores were depleted after stimulation with 16.7 mM glucose, or that elevation of cAMP via the phosphodiesterase inhibitor IBMX is not a contributory mechanism for insulin secretion in these islets. Group 3 preparations lacked a Peak 1 but maintained a modest Peak 2, which suggests that cAMP may be the sole signaling mechanism for stimulated insulin secretion in these islets. Group 4 preparations had inconsistent basal secretion, evidencing unregulated release. Lastly, Group 5 preparations lacked both peaks, but

these islets were not apoptotic, meaning that because they may have normal insulin content, they may be able to recover functionality. The expression of genes encoding proteins in the glucose-sensing pathway is reduced in Group 5 islets, suggesting that these preparations are unhealthy in other ways, which requires further investigation. Although the retrospective nature of our study did not permit comparison of protein levels of these glucose-sensing genes between Group 1 and Group 5 islets, we note that, in prior work,[38,46] mRNA levels of human islet transcription factors correlated well with their respective protein levels.

Interestingly, neither islet attributes nor information from the islet isolation center predicted the likelihood of a preparation being in a particular response Group. However, within Group 1 (highly responsive) human islet preparations specifically, both Center and Year did influence individual measures of insulin secretion (Baseline, Fold 1, and Fold 2). Overall, the pattern of insulin secretion in these preparations was remarkably similar among centers and across the years studied.

To limit the potential interrelatedness of Center and Year as variables, we controlled for either Center or Year and examined the effect of donor and islet attributes on Baseline, Fold 1, and Fold 2. In these controlled analyses, Cause of Death, Purity, and BMI influenced individual measures of insulin secretion (Fold 1, Baseline, and Fold 2, respectively). Each of these variables influenced only one of the three measures, which may simply highlight that basal, glucose-stimulated, and cAMP-mediated insulin secretion work via distinct mechanisms, or it may suggest that no attribute is potent enough to impact all three measures.

The influence of Center on individual measures *of in vitro* function may be partly procedural, or it may reflect the donor pool seen by that center (e.g. perhaps one center receives more organs from donors dying in motor vehicle accidents). Year of isolation is of interest for both procedural and practical reasons: not only because an influence of Year could stem from changes in

personnel at isolation centers, standards of practice, or adherence to protocol among centers, but also because practical aspects of isolation have changed with time, such as changes in the lot number or provider of digestive enzymes. Our linear regression and spline modeling results indicate that *in vitro* insulin secretion from human islet preparations has improved over the years studied.

The assessment of 12 transplanted preparations with Group 1 response profiles demonstrated a poor correlation between *in vitro* and *in vivo* stimulation-induced changes in insulin secretion (Figure 43G). It has previously been suggested that *in vitro* stimulated insulin secretion does not well predict *in vivo* graft function,[240,241] although these studies did not use perifusion as the *in vitro* assay. Conversely, a comparison of multiple quality control assessment methods, which did not include perifusion, found that only static islet stimulation identified preparations as being "Good" or "Poor," based on their *in vivo* function.[230] A limitation of our analysis is the lack of in vivo data from Group 5 preparations, because we deemed these not suitable for transplantation. A study directly comparing the relationship between *in vitro* and *in vivo* function of Group 1 and Group 5 preparations is needed to further address whether perifusion data can be useful for predicting *in vivo* function.

We used perifusion to assess *in vitro* islet function because it integrates β cell function with high temporal resolution and allows sequential responses to multiple secretagogues. Static incubation is widely used to assess glucose-stimulated insulin secretion. However, our analyses (Figure 43H and I) indicate that stimulation of insulin secretion in static islet culture does not correlate with stimulated insulin secretion via perifusion. Other approaches used to assess islet health have included glucose-induced changes in oxygen consumption rate,[236,237,241,242] glucose-induced preproinsulin mRNA expression,[243] and mitochondrial integrity.[230] Given that these approaches, including islet perifusion, are not widely available and pre-experimental human

islet assessment is critical, a new approach for islet distribution programs is necessary. Perhaps every islet preparation should be perifused or assessed by the islet isolation center and this functional information provided to investigators receiving the islets for research.

We noted a significant relationship between human islet responsiveness and Cause of Death, observed by spline modeling, but this interpretation is complicated by interrelated variables. Despite the fact that Cause of Death is reported by the institution where the organ was procured, using nationally-standardized phrases, some causes of death can have multiple appropriate definitions, such as “anoxia” encompassing multiple types of hemorrhage or “motor vehicle accident” causing “head trauma.” The mechanism by which Cause of Death influences islet response remains unclear, but it is known that events immediately preceding death can impact islet health, such as oxidative stress impairing islet function and islets from brain-dead donor rats being functionally inferior (both *in vitro* and *in vivo*).[244,245] However, the fact that our data suggest various types of anoxic events affect islet function differently suggests that Cause of Death is acting as a surrogate for more than one variable.

The implications of our findings for human islet research are both encouraging and cautionary. The majority of islet preparations from each center and year (with the exception of center 15 and the year 2004) have a responsive profile (Group 1). However, dysfunctional islet preparations are being shipped from all centers and are being used in studies where islet responsiveness is assumed. The information currently provided to researchers is insufficient to predict the functional profile of a human islet preparation.

The insulin secretion profiles of islet preparations should guide the way investigators represent collected data. For example, if two of six human islet preparations in a study had a pattern like Groups 2-5, it may confound interpretation to combine gene expression data. In a study with only 3-4 human islet preparations, there would be an even greater impact of including

a dysfunctional preparation, which would be statistically likely. Likewise, a study examining the contribution of cAMP-mediated insulin release, Group 2 preparations should perhaps be treated separately from Group 1 preparations. Thus, combining data from islet preparations with different health and functional statuses may confound interpretation, leading to inappropriate conclusions. It is advisable that researchers perform pre-experimental functional assessment to select appropriate islet preparations for experimental purposes.

CHAPTER V

INVESTIGATING THE ROLE OF EGFR SIGNALING IN ADULT β CELL PHYSIOLOGY

Introduction

Central to the pathogenesis of both Type 1 and Type 2 diabetes is an inadequate amount of circulating insulin to effectively regulate blood glucose levels. Increasing the availability of endogenous insulin requires either an enhancement of the secretory capacity of individual β-cells or an increase in the total number of rodent β-cells. Thus, there is great interest in stimulating β-cell proliferation and increasing β-cell mass. Multiple growth factors have a mitogenic effect on β-cells, including hepatocyte growth factor (HGF), parathyroid hormone-related protein, prolactin, and insulin itself.[246] Recently, the members of another family of growth factors, the epidermal growth factor (EGF) family, which signal through the ErbB receptor family, have been shown to impact pancreas development, β-cell proliferation, and insulin secretion.[247,248] Since the Nobel Prize-winning discovery of EGF by Stanley Cohen at Vanderbilt, the role of EGF has been implicated in the development and physiology of many tissues. More recently, interest has arisen in defining the influence of the EGF family ligands and their receptors, called ErbB receptors, on β-cell mass and insulin secretion.

The ErbB (**er**ythro**b**lastic leukemia viral oncogene analog) family of receptor tyrosine kinases is fundamentally important for development, cell proliferation, and cell survival in many tissues of neuronal, mesenchymal, and epithelial origin.[249] The proliferative influence of these receptors is highlighted by the fact that they were originally identified as viral oncogenes[250] and that they are the targets of many cancer therapies.[251,252] These receptors can transduce signal via two

distinct mechanisms. The first and arguably more frequent mechanism is initiated by the binding of an extracellular ligand from the EGF-like growth factor family.[249,253,254] Ligand-activated ErbB receptors signal in homo- or heterodimers with other members of the ErbB family (Figure 46).[253-255] This receptor dimerization is required because, in an activated dimer, the kinase domain of each receptor monomer transphosphorylates tyrosines in the dimer partner's cytoplasmic tail. The resultant phosphotyrosines on the cytoplasmic tail can then interact with and activate a panel of "mediator" proteins that initiate a variety of intracellular signaling cascades, namely the Akt, PLC-γ, MAPK/ERK1/2, and JAK/STAT pathways (Figure 47).[254,256,257] The second mechanism of ErbB activation is ligand-independent, beginning with tyrosine phosphorylation on the cytoplasmic tail by an intracellular kinase, such as Src kinase.[256]

The four members of the ErbB receptor tyrosine kinase family, ErbB1-4, bind the EGF-like family of growth factors (Figure 48). Of the four, the EGF receptor (also known as ErbB1 or EGFR) seems particularly involved in modulating multiple aspects of islet development and physiology.[258,259] The EGF-like growth factors include the epidermal growth factor (EGF), transforming growth factor-α (TGF-α), amphiregulin, heparin-binding EGF-like growth factor (HB-EGF), betacellulin, epiregulin, epigen, and multiple isoforms of neuregulin (NRG) (Figure 48). These ligands initially exist in pro-ligand form, anchored in the plasma membrane, until their extracellular signaling domains are

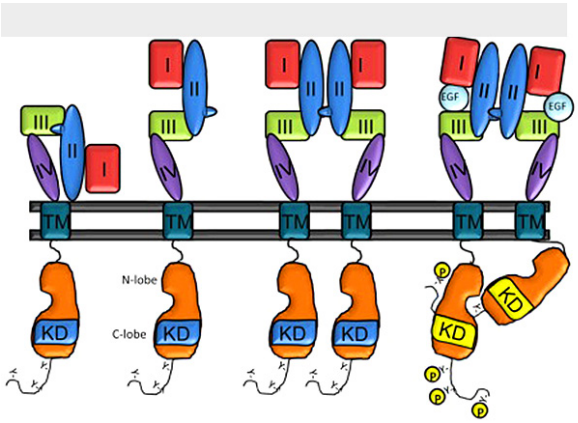

Figure 46. Structure of EGFR in closed, open, dimerized, and activated forms. Domains labeled I and III are ligand-binding. II=dimerization domain. IV=juxtamembrane domain. TM=transmembrane domain. KD=kinase domain. Domains I and III must be in open conformation for ligand binding, upon which the kinase domain of one receptor transphosphorylates tyrosine residues on the intracellular portion of the dimerized partner receptor. Image from Ceresa and Peterson (2014).

cleaved and released by members of the ADAM (**a** **d**isintegrin **a**nd **m**etalloproteinase) family of metalloproteinases (Figure 49).[260] The subsequently soluble ligands can then interact with one or more of the ErbB receptor tyrosine kinases, membrane-bound receptors that mediate a complex web of intracellular signaling programs.[256]

Importantly, each ligand of the EGF-like family has a different degree of binding specificity across the four ErbB receptors. For example, EGF itself binds only to ErbB1, the EGFR, but other ligands, such as epiregulin, HB-EGF, and NRG1 can bind two different ErbB receptors (Figure 48). Notably, ErbB2 binds no known ligand, as it lacks a ligand-binding domain in its extracellular region. For this reason, ErbB2 is unable to signal in homodimers, requiring a different ErbB receptor (1, 3, or 4) to transphosphorylate its cytoplasmic tail after ligand binding. ErbB3 is similarly impotent in homodimers, due to its inherent lack of tyrosine kinase activity in its intracellular tail. Thus, ErbB2 and ErbB3 signal only in heterodimers.

Upon phosphorylation of the intracellular tail, EGFR transduces signal through multiple pathways. The identity of the specific phosphorylated tyrosine residue largely determines which specific signaling cascade is initiated. These associations between individual phosphotyrosines and signaling pathways have been collectively dubbed “phosphomaps” (Figure 50). The most commonly activated pathways by EGFR phosphorylation are the PLC γ / PKC, PI3K/AKT, and MAPK pathways. Importantly, however, there are also

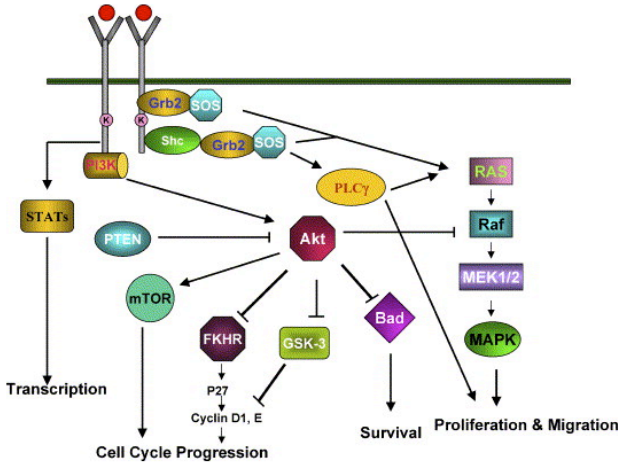

Figure 47. EGFR signaling cascades. Diversity of signaling pathways downstream of activated EGFR dimers, promoting cell growth, proliferation, survival, and motility. Image from Singh and Harris (2005).

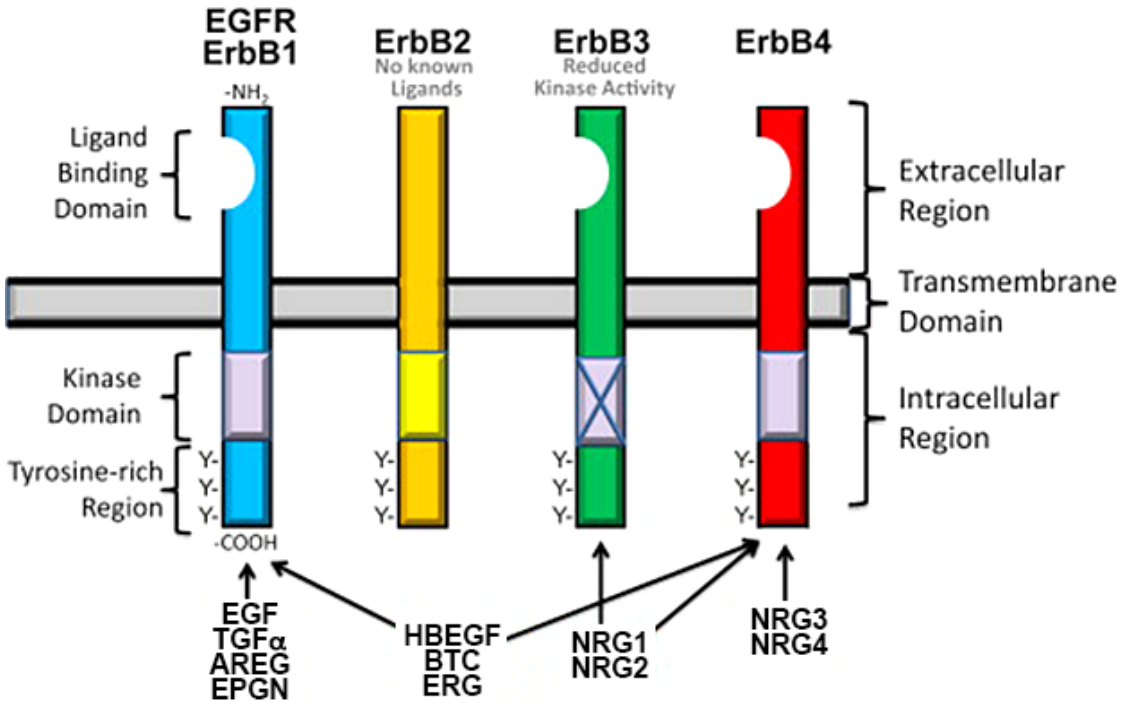

Figure 48. Members of the EGF-like ligand family and ErbB specificity. Shown are the known endogenous ligands for the ErbB receptor family, with indications of which receptor(s) each ligand is capable of binding. EGF = epidermal growth factor; TGFα = transforming growth factor-α; AREG = amphiregulin; EPGN = epigen; HBEGF = heparin-binding EGF; BTC = betacellulin; EREG = epiregulin; NRG1/2/3/4 = neuregulin 1/2/3/4. Image adapted from Ceresa and Peterson (2014).

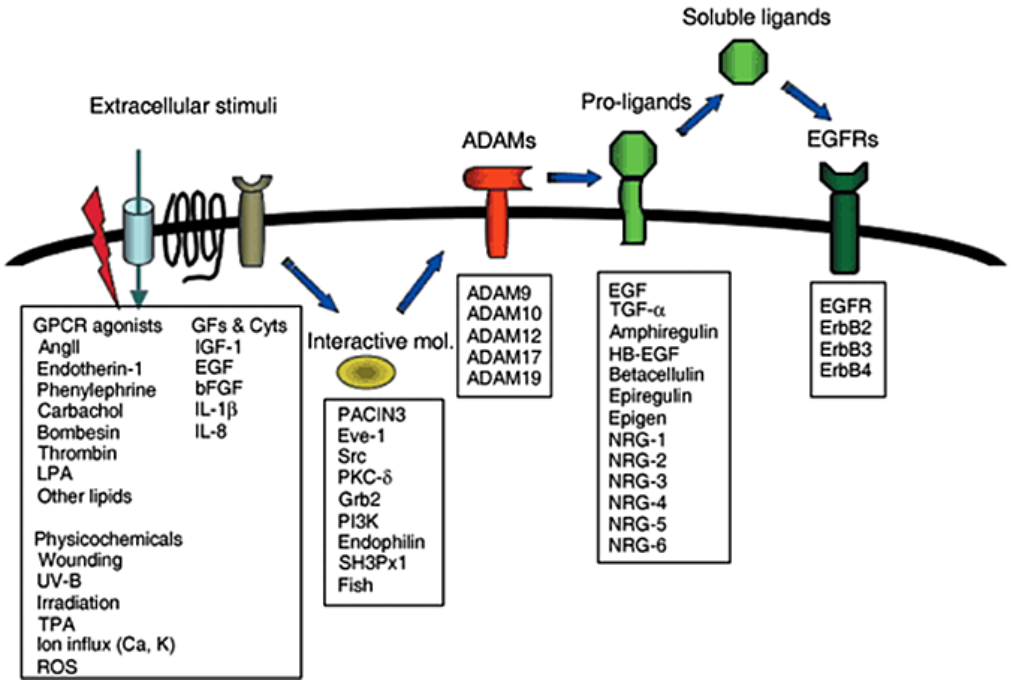

Figure 49. Events leading to cleavage of pro-ligands. In response to a multitude of initiating stimuli and mediated by multiple signaling molecules, members of the ADAM family of metalloproteinases cleave and release the extracellular portion of the EGF-like ligand family members, allowing them to, in soluble form, bind members of the ErbB receptor family. This process of pro-ligand cleavage is also called ligand shedding. Image from Higashiyama et al. (2008).

phospho-tyrosines that promote of receptor internalization and ubiquitylation/degradation (Figure 50). ErbB receptors are highly recycled, and the rate of internalization and degradation tightly regulate this process.[261] The consequences of the main signaling cascades above are multitudinous, but central are gene expression changes that promote cell growth, differentiation, and survival.

An initial association between EGF levels and diabetes was made with the observation that production of EGF by the submandibular gland was dramatically lower in diabetic mice.[262] This was true of both genetically diabetic mice (*db/db*) and of mice made diabetic with injection of the β cell toxin streptozotocin (STZ) (Figure 51). However, STZ-treated mice that then received exogenous insulin were able to partially recover both glandular and plasma EGF levels (Figure 51). Given the binding specificity of EGF for the EGFR, a correlation was thus made between diabetes and reduced EGFR signaling.

Previous studies have implicated EGFR signaling in proper pancreatic and islet development. In a mouse model of global EGFR knockout,[263] formation of normal islet architecture is delayed postnatally, and islets abnormally remain associated or even in contact with the pancreatic ducts (Figure 52A and B). In addition, β cell proliferation is lower in islets from EGFR -/- mice (Figure 52C and D), the percent of insulin+ cells per pancreas area is uniquely reduced, and the entire pancreatic area is reduced at E12.5 and E16.5. A subsequent study used a Pdx1-driven dominant-negative transgene of EGFR (E1-DN) to reduce EGFR signaling in the pancreas, specifically.[248] Although this model only reduced EGFR signaling by 40%, mice heterozygous for the transgene had more than an 80% loss of insulin-positive pancreas area (Figure 53A) and were glucose intolerant (Figure 53B and C). More recently, the E1-DN model was used to suggest that increases in β cell proliferation and expansion of β cell mass in response to high-fat diet feeding and to pregnancy are mitigated by reduced EGFR signaling.[264,265]

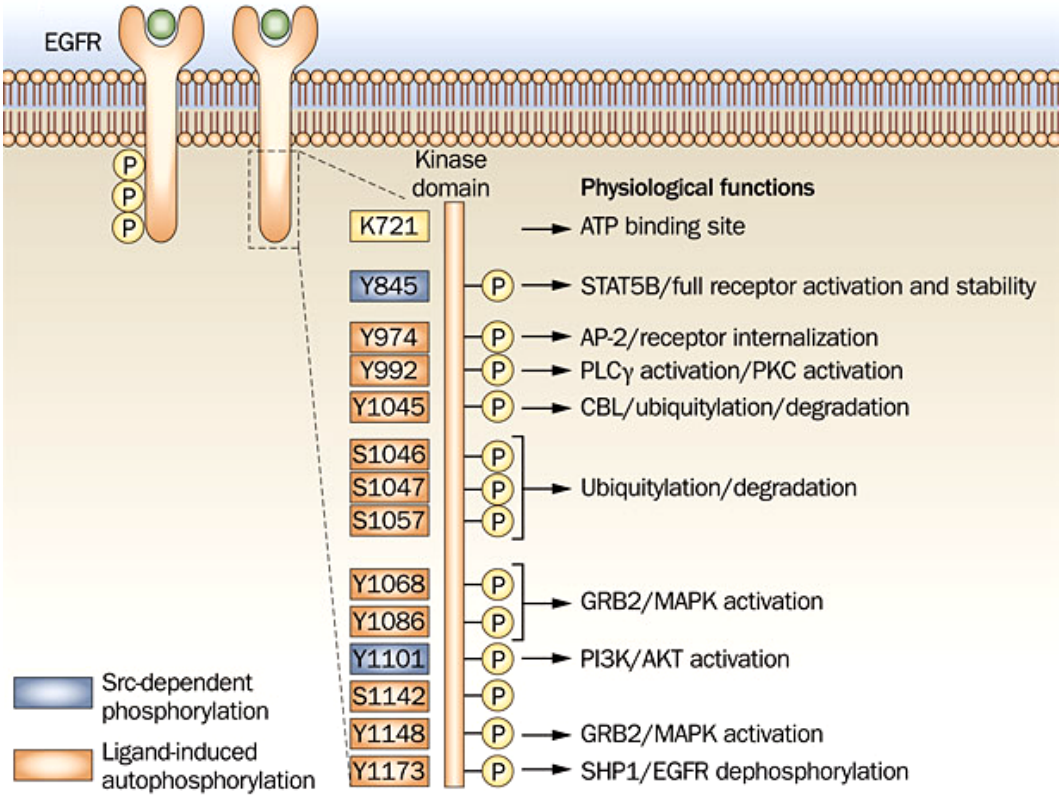

Figure 50. Phosphomap of EGFR. The identity of the signaling pathway initiated by EGFR signaling is determined by the specific phosphotyrosine. Various known phosphotyrosines on the EGFR cytoplasmic tail are depicted, with arrows indicating the respective signaling consequence for each. Importantly, dephosphorylation, internalization, and degradation of EGFR are also initiated by specific phosphotyrosine residues. Image from Wheeler et al. (2010).

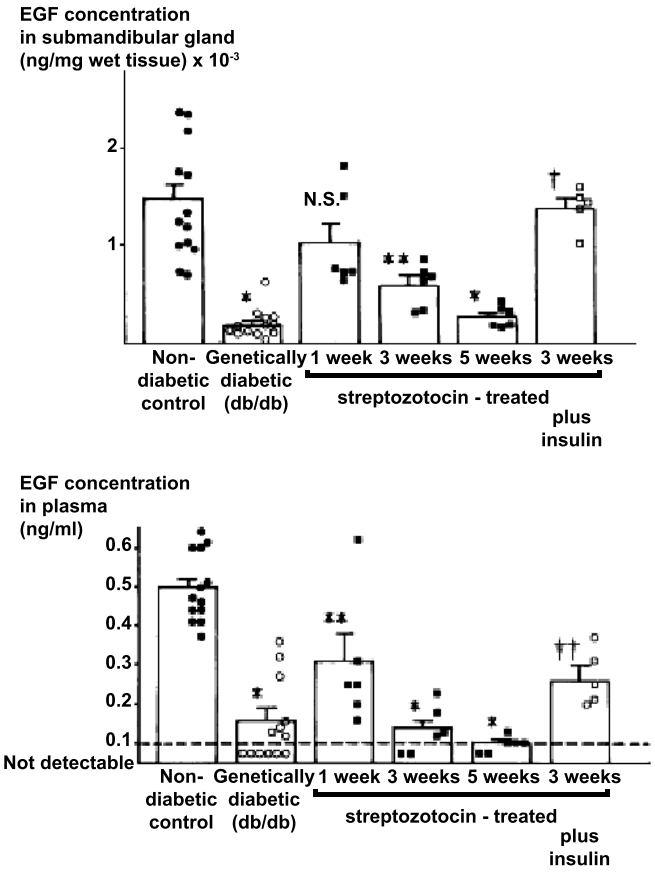

Figure 51. EGF deficiency is associated with diabetes. (A) EGF content in submandibular gland and (B) EGF concentration in plasma of control mice, genetically diabetic mice, streptozotocin-treated diabetic mice, and diabetic mice given exogenous insulin ("plus insulin"). Image from Kasayama et al. (1989).

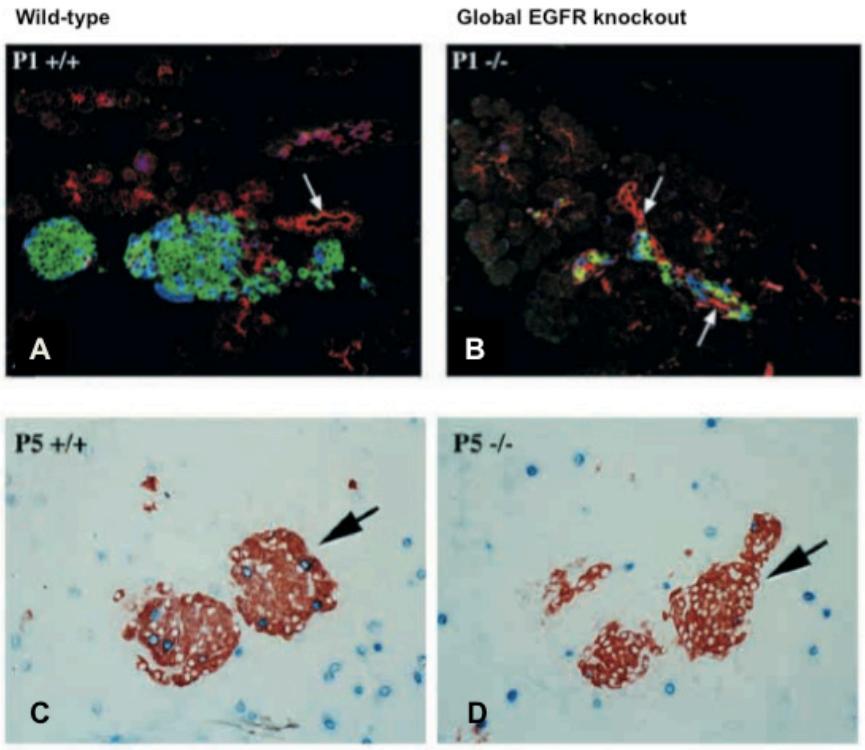

Figure 52. Global deletion of EGFR. A, B: Morphology of islets in wild-type and global EGFR knockout mice at postnatal day 1. Insulin=green; glucagon=blue; cytokeratin=red. C, D: Staining for Brdu in blue, insulin in red, showing proliferating β cells at postnatal day 5. Image from Miettinen, et al. 2000.

In addition to potential involvement in islet development and β cell mass, there is previous

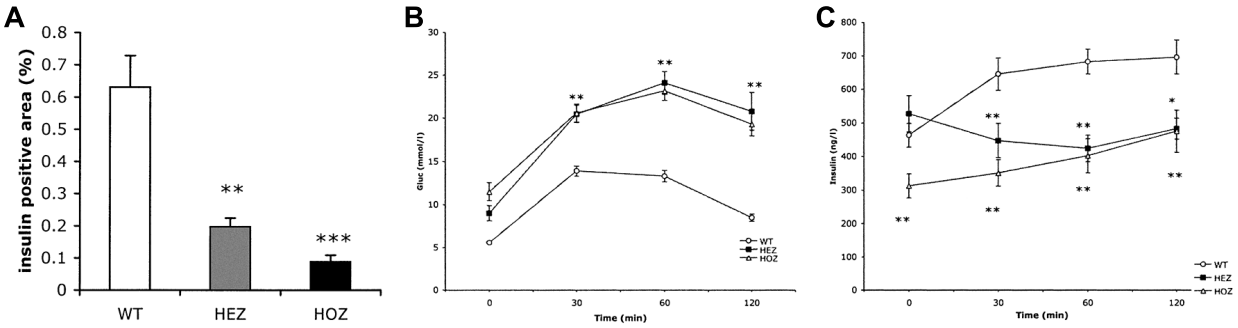

Figure 53. Pdx-E1-DN knockdown of EGFR. A: Insulin positive area in mice either heterozygous (HEZ or homozygous (HOZ) for a dominant-negative EGFR transgene driven by the Pdx-1 promoter. B: Glucose tolerance test. C: Insulin concentration in plasma during glucose tolerance test. Miettinen et al (2006).

evidence that EGFR signaling impacts β cell function. Treatment of isolated murine islets or a β-cell line with EGF increased insulin secretion in a low-glucose condition. Both wild-type and leptin receptor-deficient (*db/db*) mice, when given intravenous EGF injections, exhibited elevated plasma insulin levels and decreased blood glucose levels.[266] Given that EGFR is the unique receptor for EGF, this implicates EGFR activity in modulating levels of insulin secretion under both normal and diabetic conditions. In addition, the known signaling of EGFR through PI(3)K/AKT suggests a potential mechanism for EGF-mediated enhancement of insulin secretion, as PI(3)K/AKT is known to promote insulin secretion.[267-269]

Our objective in the following studies was to assess the potential involvement of EGFR signaling in the function and proliferation of adult β cells, specifically. To that end, we generated a model of β cell-specific removal of EGFR, in contrast to the global EGFR knockout and the pdx1-driven dominant-negative receptor that have previously been used. This allowed us to eliminate multiple confounding factors associated with previous models.

Results

We measured gene transcription of all ErbB receptors in wildtype C57Bl/6 mouse islets and in human islets. We found that the relative expression of the four ErbBs differed between the two species. In control mouse islets, EGFR levels were significantly higher than those of the other receptors, and ErbB4 was barely expressed at all (Figure 54A). In contrast, human islets had very similar levels of EGFR, ErbB2, and ErbB3, although lower overall than mouse EGFR (Figure 54B). Human ErbB4 expression was lowest of the four, but its levels were higher than in mouse islets.

To generate a model of EGFR loss in β cells only, we crossed a mouse with a floxed EGFR transgene,[149] here called the $EGFR^{fl/fl}$ mouse, with the Ins2-Cre transgenic mouse,[150] hereafter called InsCre. The resultant mouse lacks functional EGFR in insulin-producing cells. To determine the degree of EGFR knockdown in this model, we measured mRNA levels of EGFR, which is reduced by approximately 90% in $InsCre^{pos}$ $EGFR^{fl/fl}$ islets (Figure 54C). Beta cells make up approximately 80% of mouse islets, which suggests an efficiency of the transgene that is consistent with prior reports.[270] Given the ubiquity of ErbB heterodimers and the complexity of downstream ErbB-mediated signaling cascades, it was important to address whether expression of other ErbB receptors was increased in response to EGFR loss. ErbB2, ErbB3, and ErbB4 mRNA levels were unchanged in this model (Figure 54C), arguing against this phenomenon occurring at the transcriptional level.

To examine the metabolic consequences of EGFR loss in β cells, we performed glucose tolerance tests on male and female mice. There was no change in glucose tolerance nor in fasting blood glucose level between the groups (Figure 55). Insulin tolerance tests demonstrated similar insulin sensitivity between the two groups (Figure 56). Islet morphology was normal in $InsCre^{pos}EGFR^{fl/fl}$ mice, characterized by appropriate hormone expression, cell-type ratios, and

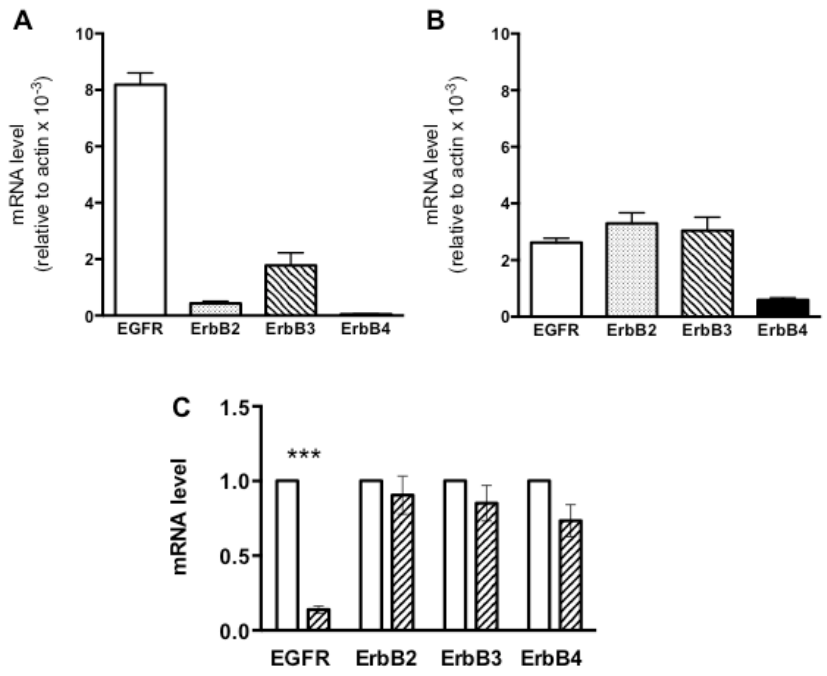

Figure 54. EGFR expression is dramatically reduced in the InsCre^{pos}EGFR$^{fl/fl}$ mouse. ErbB receptors are expressed in mouse and human islets. A-B. Relative gene expression of ErbB receptors in isolated mouse (A) and human (B) islets. n=8 (human), n=5 (mouse). C. Gene expression of ErbB receptors in isolated islets from InsCre^{pos}EGFR$^{fl/fl}$ (lined bars) and InsCre^{neg}EGFR$^{fl/fl}$ (white bars) mice. n=5 (knockout), n=3 (controls). *** p<0.001.

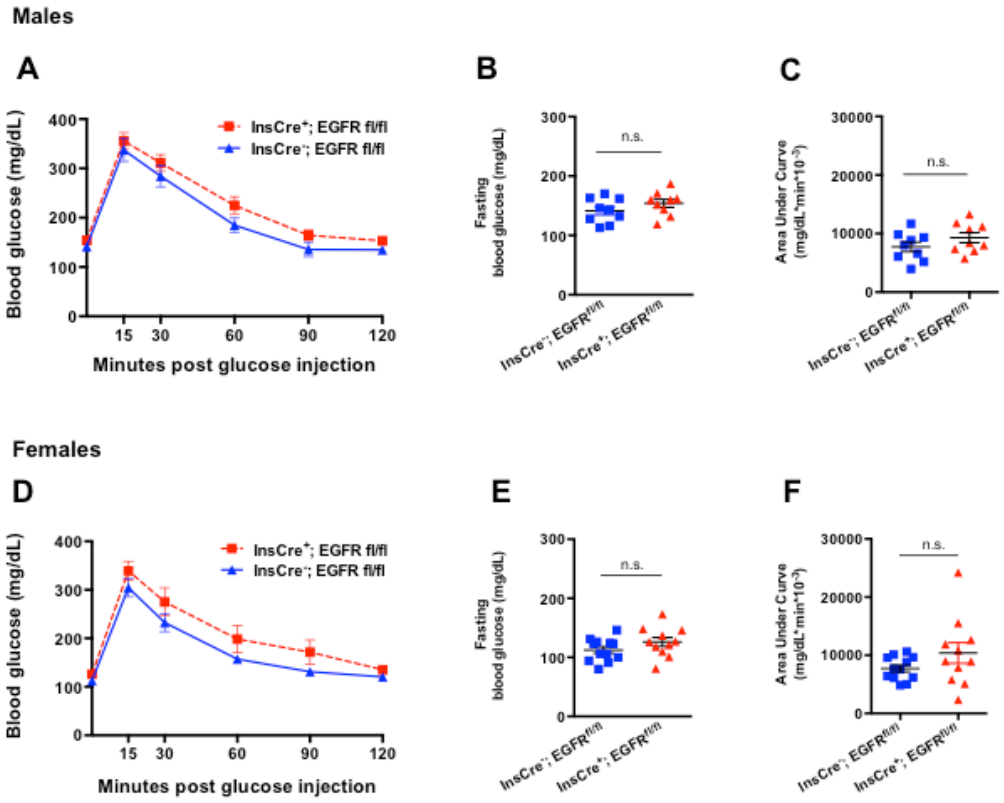

Figure 55. InsCre^{pos}EGFR$^{fl/fl}$ mice are glucose tolerant. Glucose tolerance test of male (A) and female (D) InsCre^{pos}EGFR$^{fl/fl}$ (red points) and InsCre^{neg}EGFR$^{fl/fl}$ (blue points) mice. Fasting blood glucose values of male (B) and female (E) mice. Glucose tolerance test area under the curve (AUC) calculations for male (C) and female (F) mice. n=9.

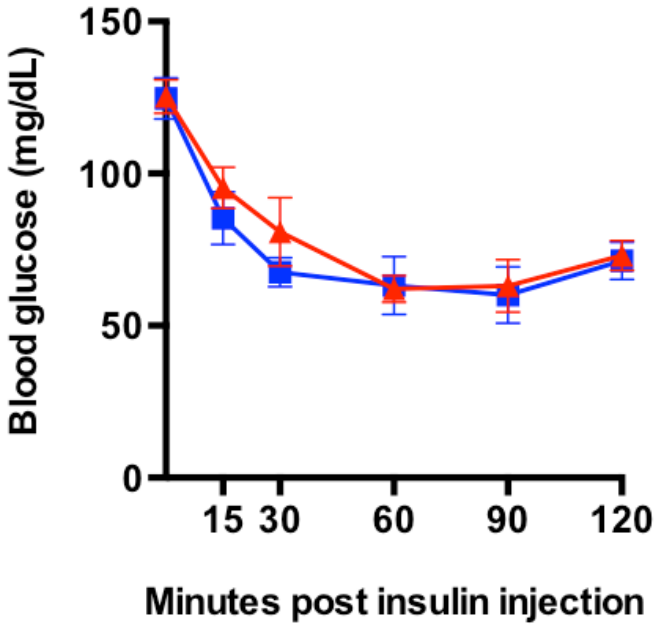

Figure 56. InsCre^{pos}EGFR$^{fl/fl}$ mice are insulin sensitive. Insulin tolerance test of InsCre^{pos}EGFR$^{fl/fl}$ (red points) and InsCre^{neg}EGFR$^{fl/fl}$ (blue points) mice. n=4-6.

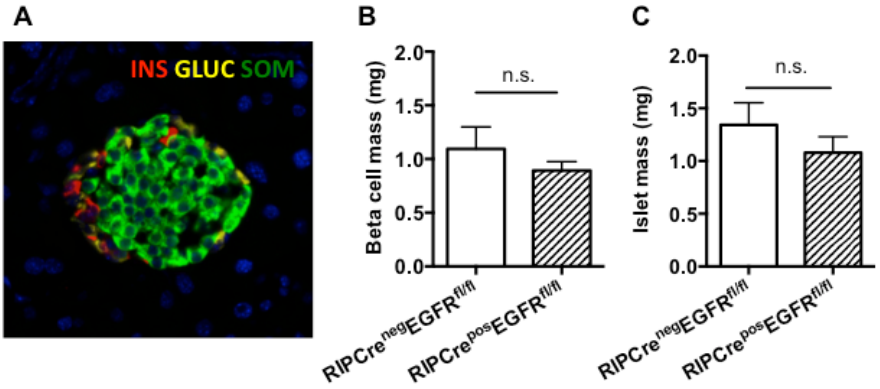

Figure 57. Loss of EGFR in β cells does not alter β cell or islet mass. A. Representative image of normal islet morphology in InsCre^{pos}EGFR$^{fl/fl}$ mice, stained for insulin (green), glucagon (yellow), somatostatin (red). β cell mass (B) and islet mass (C) of RIPCre^{pos}EGFR$^{fl/fl}$ (hashed bar) and RIPCre^{neg}EGFR$^{fl/fl}$ (white bar) mice.

overall islet architecture (Figure 57A). To examine whether β cell mass is altered by EGFR loss in β cells, we examined previously collected samples from a related model of EGFR loss, the rat insulin promoter (RIP)-driven Cre,[271] $EGFR^{fl/fl}$ model. There was no difference in islet mass or β cell mass between $RIPCre^{pos}EGFR^{fl/fl}$ and $RIPCre^{neg}EGFR^{fl/fl}$ mice (Figure 57B and C), demonstrating that loss of EGFR in β cells did not impair establishment or maintenance of β cell mass.

To assess islet function and address a potential effect on insulin secretion, we perifused isolated islets with a sequence of low and high glucose, as well as a maximal stimulation condition, using the phosphodiesterase inhibitor IBMX. Insulin secretion was similar under basal glucose, but $InsCre^{pos}EGFR^{fl/fl}$ islets secreted significantly less insulin in response to stimulatory glucose levels (Figure 58A and B). Upon maximal stimulation, however the difference between the groups was not significant (Figure 58A and C).

To address whether EGFR ligands promote insulin secretion, we cultured isolated islets from control, C57Bl/6 mice in low or high glucose, with or without the addition of EGF. Although insulin secretion was potently stimulated in response to high glucose, EGF did not alter insulin secretion at either glucose concentration (Figure 59).

Discussion

Our results jointly show that removal of EGFR signaling specifically from β cells has little, if any, consequence for β cell mass regulation, glucose metabolism, and that EGF does not stimulate insulin secretion from isolated islets. The primary consideration in interpreting how these data differ from previous studies is that this model is more specific than any previously used to address EGFR's role in islet physiology. Given the ubiquitous importance of EGFR signaling throughout many organ systems, the pancreatic and islet phenotypes of the global knockout

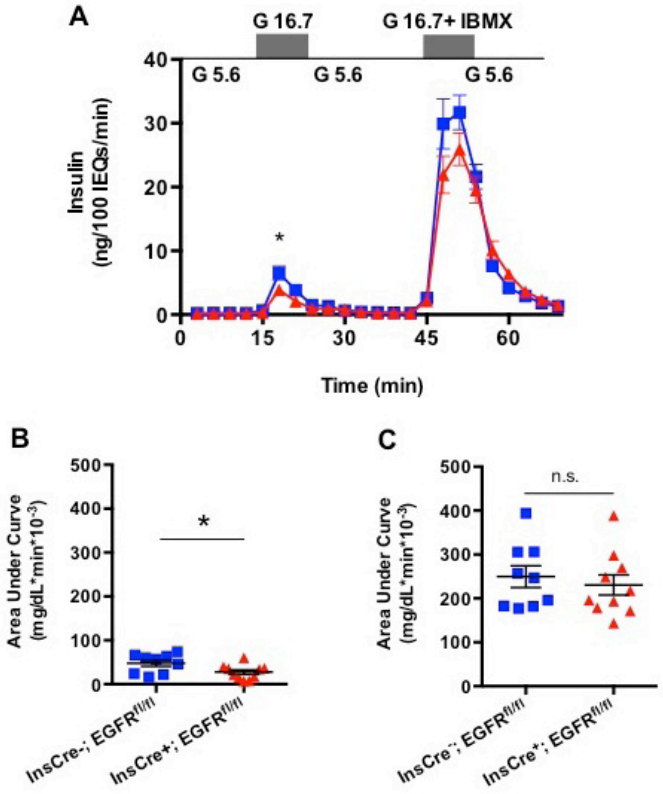

Figure 58. Stimulated insulin secretion is reduced in isolated InsCre^{pos}EGFR$^{fl/fl}$ islets. A. Perifusion of isolated islets from InsCre^{pos}EGFR$^{fl/fl}$ (red points) and InsCre^{neg}EGFR$^{fl/fl}$ (blue points) mice. *p<0.05. n=9 (control), n=10 (knockout). B-C. Area under the curve calculation for 16.7mM glucose (B) and 16.7mM glucose + IBMX (C) stimulation. *p<0.05.

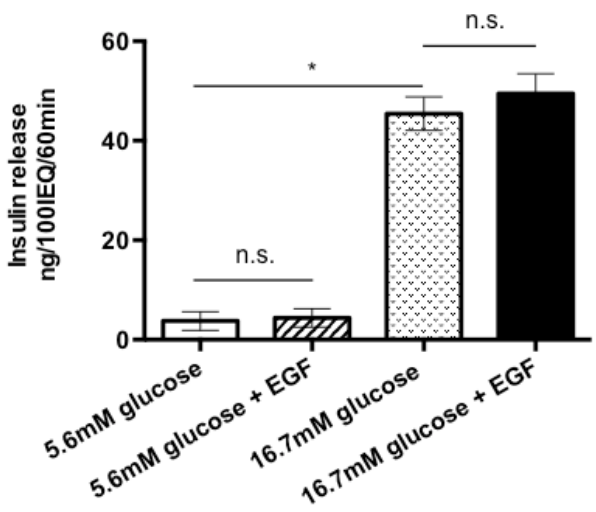

Figure 59. EGF does not augment basal or stimulated insulin secretion. Insulin release from C57Bl/6 islets in static culture in response to basal (5.6mM) or stimulatory (16.7mM) glucose concentrations, with or without EGF. *p<0.05. n=3.

are almost certainly influenced by EGFR loss in other tissues. The E1-DN transgenic model, although pdx1-restricted, is complicated by the possibility that dominant negative EGFRs are affecting signaling of other ErbB receptors in heterodimers. This may thus be expanding the negative consequence of the E1-DN, despite the fact that only 40% of intracellular signaling attributed to EGFR is lost. One rationale for this work was to address the role of EGFR in *adult* islet physiology. For this reason, this work does not address whether the InsCre^{pos}EGFR$^{fl/fl}$ model has transient developmental abnormalities along the lines of those observed in other studies. Importantly, the insulin gene used to drive Cre recombinase in this model is turned on at E10.5, compared to pdx-1, which is transcribed beginning at E8.5.[8] Thus this model initiates EGFR deletion slightly later than the pdx1-E1-DN model initiates expression of the dominant negative receptor.

The reduced insulin secretion observed in response to stimulatory glucose in InsCre^{pos}EGFR$^{fl/l}$ islets suggests that some downstream consequence of EGFR signaling supports insulin release. The mitigation of this effect upon maximal stimulation with IBMX, however, hints that the mechanism of EGFR involvement is likely not related to cAMP-based potentiation of the secretion signal, which is being stimulated by IBMX.

EGF signaling does not seem to play an important role in normal islet physiology, making future work in this area a challenging proposition. However, little is known about the role of ErbB signaling in human islets. The differences in gene expression of ErbB1-4 in mouse and human islets suggest that there may be different roles and levels of involvement for EGFR and/or the other ErbBs in human islets. Some studies have examined the use of EGF for improving human islet graft survival and performance, although most required combined treatment with gastrin or another factor,[272,273] making it uncertain what the therapeutic potential may be.

CHAPTER VI

CONCLUSION

Summary of findings

Glucotoxicity and Lipotoxicity in Human Islets

The objectives of this Dissertation were to advance our understanding of human islet physiology, which was accomplished by two projects. The first project, presented in Chapter III, examined and defined the consequences of excess glucose and excess lipid, two central components of T2DM pathology, for human islets *in vivo*. Using three complementary models of metabolic stress, we examined function of transplanted human islets in response to hyperglycemia, insulin resistance, or combined hyperglycemia and insulin resistance. Importantly, the first two models represented multiple weeks of chronic exposure to metabolic stress, but the combined model was much more acute, examining only 7 or 14 days of exposure. A second project, presented in Chapter IV, analyzed the degree of functional variation among human islet preparations used for research, correlated the greatest functional differences to islet gene expression changes, and addressed whether *in vitro* islet function correlated to *in vivo* islet function.

Our results in the NSG-DTR, NSG-HFD, and NSG-S961 models demonstrate that stimulated human insulin secretion is impaired in ways very similar to diabetic patients. The mechanisms behind these functional changes are of great importance. Much interest has developed in a mechanistic paradigm to explain the establishment of glucotoxicity and lipotoxicity, namely that increases in glucose and lipid metabolism in the β cell enhances the generation of reactive oxygen species, which then, among other deleterious effects, alter expression and function of critical β cell transcription factors.

Our results indicate that superoxide levels are increased in human islets from our NSG-HFD model, and MAFB and/or NKX6.1 expression is reduced in our chronic models of metabolic stress. However, and of great potential importance, MAFA and PDX1, were not significantly reduced in either model, but they were dramatically reduced in islets from T2DM patients.[38] This suggests that either a longer exposure to hyperglycemia or insulin resistance is required before expression of other transcription factors is affected, or the combination of the two may be required. Conversely, it may be that function of MAFA and PDX1 (or also the remaining NKX6.1 and MAFB) are impaired, in the absence of expression changes, a possibility that was beyond the scope of these studies. This effect of hydrogen peroxide has been demonstrated in human islets vitro,[38] and future studies to determine whether this occurs *in vivo*, or in response to other ROS would be valuable. Interestingly, the decrease in MAFB expression in the NSG-DTR model is not accompanied by changes in superoxide, introducing the ideas that another reactive oxygen species is elevated, such as hydrogen peroxide, or that the MAFB reduction is not downstream of elevated ROS at all.

Functional assessment of human islet preparations

Our comprehensive analyses of human islet preparations for research yielded a new and informative system for classifying *in vitro* insulin secretion profiles. Islets were categorized as Group 1-5, based on characteristics of their perifusion patterns (Figure 41). Importantly, Groups 2-5 have varying functional attributes that suggest dysfunction, reduced function, or lack of function. This categorization system allowed us to then assess whether the islet isolation center impacted the probability of a particular functional profile and whether the distribution of Groups changed over recent years. These analyses demonstrated that, overall, the function of human islet preparations has improved over time, suggesting better isolation and handling techniques. We also demonstrated that the distribution of Groups 1-5 was not significantly different at

any of the isolation centers, and that most centers supply a similar percent of Group 1 islets. Importantly, however, clear gene expression changes may contribute to or even explain the difference between Group 1 and Group 5 function. Two genes critical to glucose sensing, the GLUT2 glucose transporter and the enzyme glucokinase are both significantly reduced in Group 5 islets. MAFA, which has a plethora of downstream targets, was also reduced.

Many attributes of the islet donor and of the islet isolation experience seem to be potential influencers of islet function, such as donor age, donor BMI, cold ischemic time, or culture time. Our analyses show, however, that no donor or islet isolation attributes are associated with a particular functional Group, indicating that preferences among investigators for islets preparations with particular attributes, such as cold ischemic time less than a certain number of hours, may not translate to more highly functioning islets.

Both to better inform decisions preceding human islet transplantation studies and to address general aspects of human islet biology, we were interested in whether *in vitro* function correlated with *in vivo* function. Our comparison of stimulated fold changes in insulin secretion by perifusion *in vitro* and by glucose-arginine stimulation *in vivo* revealed no significant correlation between the two, indicating that *in vitro* function may be a poor predictor of *in vivo* performance.

Significance and future directions

Glucotoxicity and lipotoxicity in human islets

The NSG-DTR model is, in itself, a new, important, powerful tool, as well as a significant advancement in the study of human islets *in vivo*. The ability to generate endogenous hyperglycemia without accompanying insulin resistance or dyslipidemia is an advantage over mouse models of T2DM. To that effect, the NSG-DTR mouse is not, in fact, a model of T2DM,

but rather of hyperglycemia. Compared to other methods of toxin-induced β cell death, such as streptozotocin or Alloxan, the DTR model is incredibly specific. No mouse cells can possibly be affected unless they express the insulin gene, as mouse cells do not inherently express the diphtheria toxin receptor. This essentially eliminates the general or off-target toxicity seen in response to other toxins but generates a mouse with only human β cells. This last aspect is hugely attractive, as the co-existence of mouse and human β cells, secreting mouse and human insulin into the blood stream, has potential confounding effects that are not defined. Important to our study of human islets is the ability that the NSG-DTR model gives to establish hyperglycemia *after* human islet transplantation, reducing the barrier to successful human islet engraftment. Similarly, the toxic specificity mentioned above allows transplantation of mouse islets from mice without the RIP-DTR transgene, before DT administration. The potential future applications of this model are multitudinous and can provide additional critical insight to the interaction into the relationship between hyperglycemia and human islet function that has never before been possible.

There is ample *in vitro* evidence that lipid species have varied effects on islet function and survival. For example, it appears that saturated fatty acids, such as palmitate, are more toxic than mono- or poly-unsaturated fatty acids, such as oleic acid or arachidonic acid. Importantly, there is a category of “essential fatty acids” that cannot be synthesized by the body and must be ingested in the diet. This raises an important larger question regarding HFD-induced insulin resistance: whether it is chronic exposure to the lipids in the diet that is causing islet dysfunction, or is it HFD-induced insulin resistance, and its resulting lipid profile, that is responsible. In our model of HFD-induced insulin resistance, there is no easy way to address this question. Thus, although the HFD model is, in many ways, a more clinically relevant model of insulin resistance induction, future studies examining the phenomena and mechanisms in Chapter III using a genetic model would address whether lipid changes purely downstream

of insulin resistance can replicate our current findings. Unfortunately, a model of purely HFD-associated lipid exposure is more elusive. Long-term culture of human islets introduces gene expression changes and functional changes that confound data interpretation, and given the complexity of lipid metabolism, *in vivo* infusion of specific lipids cannot guarantee exposure of islets to certain species of lipids or specific concentrations.

For patients with T2DM and the clinicians that manage their disease, there is great interest in how reversible islet dysfunction may be. Although elegant *in vitro* studies have suggested that “resting” β cells by temporarily reducing or stopping insulin production and secretion can ameliorate subsequent β cell performance, it is unclear whether glucotoxic and lipotoxic consequences are reversible in human islets. Future studies can address this by adding a period of “rest” after the initial metabolic stress. In the NSG-DTR model, exogenous insulin therapy by osmotic pump or treatment with renal sodium channel blockers could reestablish normoglycemia. Then, many aspects of islet function and health could be re-evaluated at various timepoints, to determine if/when islet function normalizes. In the HFD model of insulin resistance, a simple change to Chow diet would remove the initial metabolic stress. However, normalization of insulin resistance indicators, such as glucose intolerance, triglyceride levels, and hepatic fat content may be required for islet function to improve. There is evidence that insulin resistance is reversible, depending on degree and duration, but it presumably would take time for those features to return to normal physiological levels. This period between diet change and resolution of frank insulin resistance could provide a valuable scenario in which to address the question mentioned above, regarding the differences between the effect of HFD-derived lipid versus lipid downstream of insulin resistance. Importantly, the duration of metabolic stress (hyperglycemia or HFD) may be the main determinant of reversibility. Thus, hyperglycemia for more and less than 4 weeks and HFD for more and less than 12 weeks should be examined, depending on initial results.

Results of these studies could provide very useful lessons for clinicians and patients. For example, if the dietary lipid that induces insulin resistance is largely responsible for lipotoxicity, changing a patient's diet would be critically important, even if it takes much longer to address their insulin resistance with weight loss or other interventions. And if glucotoxicity is reversible after some durations of hyperglycemia, therapeutic options that directly normalize glycemia, such as exogenous insulin, may become even more appealing. Conversely, if glucotoxicity is not reversible, then the importance of prevention increases many-fold. Importantly, any temporal aspect of experiment design does not directly correlate to the average duration of hyperglycemia or insulin resistance in human T2DM patients, which is years or decades, rather than weeks or months. Thus, data from the above proposed experiments can only inform further clinical studies.

One of the most stark findings from our studies was the specific lack of human β cell proliferation, compared to both transplanted and pancreatic mouse β cells. Although it is commonly agreed that human β cells do proliferate less readily than mouse, the reasons for this are unclear, and human β cell proliferation is still an observed phenomenon in cadaveric samples. Given the inherent difficulty in proving any phenomenon does not happen, some questions from our studies are whether (i) there was truly no human β cell proliferation induced by the metabolic stresses in our models, (ii) aspects of metabolic stress suppressed or prevented proliferation that would otherwise occur when the demand for insulin is increased, (iii) the mitogens that influence human β cell proliferation in humans are absent, or (iv) mouse β cell mitogens do not signal in human β cells the same way. An interesting way to address these questions may be to culture human islets in human versus mouse plasma, or even to infuse human plasma into our *in vivo* models. Caveats accompany each approach, in that culture would optimally be restricted to approximately 72 hours, which may not be sufficient, and infusion of whole plasma may induce a number of unanticipated, systemic or "off-target"

consequences. However, if increased proliferation were observed in either scenario, it would be clear not only that our model of human islet transplantation has an important caveat, but also that human β cells have greater proliferative potential *in vivo* than previously thought. This last message would be incredibly welcome to the many patients and researchers that place hope in the promise of therapeutic induction of human β cell proliferation. It would also encourage continued investment of time and money into defining human β cell mitogens. However, a negative result, showing that human β cells simply are not highly proliferative, would be equally important in directing research toward strategies that enable β cell secretion under stress.

Functional assessment of human islet preparations

The fundamental nature of human islet preparations and human islet transplantation in the above studies furthered our practical and scientific interest in defining the functional variation in human islet preparations and in examining the potential for predicting *in vivo* performance based on in vitro secretory profiles.

Our comparison of *in vitro* to *in vivo* function was limited by the fact that our laboratory has, historically, predominantly transplanted islet preparations that fit the Group 1 functional profile. Thus, we were not equipped to analyze whether dysfunctional or underfunctioning islet preparations can recover function after transplantation. Future studies should include purposeful selection of islet preparations from every Group, to assess this possibility. Some ways in which islets differ *in vivo* from *in vitro* are clear, such as vascularization, innervation, and interaction with the extracellular matrix. However, other potential differences have not been as well examined. Expanding the gene expression studies from Figure 45 to (i) compare all 5 Groups and (ii) compare expression before transplant, *in vitro*, to engrafted islets, *in vivo*, could provide valuable insight into the changes islets undergo upon transplantation.

The significance of our work lies partly in demonstrating that human islet preparations distributed for research are not all appropriately functional. We hope that our findings serve as motivation for investigators to perform pre-experimental assessment of islet function before making decisions about how or whether to use a particular preparation. In addition, our results have retrospective implications for interpreting previously-published human islet data from laboratories that do not perform any such baseline functional analysis. As a result, we propose that the NIDDK and IIDP adopt a standardize method of functional assessment for each human islet preparation that is shipped to investigators. Specifically, every preparation must be evaluated using the same method, in the same laboratory, and the resulting data must be made available to the entire research community. In addition, there should be a specific identifier, alphanumeric or otherwise, for each islet preparation. Investigators should publish these identifiers in all manuscripts, so that readers can associate the IIDP-published functional assessment data with the specific preparation in the published manuscript.

REFERENCES

1 In't Veld P, Marichal M. Microscopic anatomy of the human islet of Langerhans. *Adv Exp Med Biol* 2010; **654**: 1–19.

2 Lifson N, Lassa CV, Dixit PK. Relation between blood flow and morphology in islet organ of rat pancreas. *Am J Physiol* 1985; **249**: E43–8.

3 Lammert E, Gu G, McLaughlin M, Brown D, Brekken R, Murtaugh LC *et al.* Role of VEGF-A in vascularization of pancreatic islets. *Curr Biol* 2003; **13**: 1070–1074.

4 Ahrén B. Autonomic regulation of islet hormone secretion--implications for health and disease. *Diabetologia* 2000; **43**: 393–410.

5 Tang S-C, Peng S-J, Chien H-J. Imaging of the islet neural network. *Diabetes Obes Metab* 2014; **16 Suppl 1**: 77–86.

6 Rodriguez-Diaz R, Speier S, Molano RD, Formoso A, Gans I, Abdulreda MH *et al.* Noninvasive in vivo model demonstrating the effects of autonomic innervation on pancreatic islet function. *Proceedings of the National Academy of Sciences of the United States of America* 2012; **109**: 21456–21461.

7 Reinert RB, Cai Q, Hong J-Y, Plank JL, Aamodt K, Prasad N *et al.* Vascular endothelial growth factor coordinates islet innervation via vascular scaffolding. *Development* 2014; **141**: 1480–1491.

8 Habener JF, Kemp DM, Thomas MK. Minireview: transcriptional regulation in pancreatic development. *Endocrinology* 2005; **146**: 1025–1034.

9 Burlison JS, Long Q, Fujitani Y, Wright CVE, Magnuson MA. Pdx-1 and Ptf1a concurrently determine fate specification of pancreatic multipotent progenitor cells. *Developmental Biology* 2008; **316**: 74–86.

10 Gittes GK. Developmental biology of the pancreas: a comprehensive review. *Developmental Biology* 2009; **326**: 4–35.

11 Pan FC, Wright C. Pancreas organogenesis: from bud to plexus to gland. *Dev Dyn* 2011; **240**: 530–565.

12 Chakrabarti SK, Mirmira RG. Transcription factors direct the development and function of pancreatic β cells. *Trends in Endocrinology & Metabolism* 2003; **14**: 78–84.

13 Murtaugh LC. Pancreas and β-cell development: from the actual to the possible. *Development* 2006; **134**: 427–438.

14 Rukstalis JM, Habener JF. Neurogenin3: A master regulator of pancreatic islet differentiation and regeneration. *Islets* 2014; **1**: 177–184.

15 Kaneto H, Matsuoka T-A. Role of pancreatic transcription factors in maintenance of mature β-cell function. 2015; **16**: 6281–6297.

16 Gu G, Dubauskaite J, Melton DA. Direct evidence for the pancreatic lineage: NGN3+ cells are islet progenitors and are distinct from duct progenitors. *Development* 2002; **129**: 2447–2457.

17 Wang S, Yan J, Anderson DA, Xu Y, Kanal MC, Cao Z *et al.* Neurog3 gene dosage regulates allocation of endocrine and exocrine cell fates in the developing mouse pancreas. *Developmental Biology* 2010; **339**: 26–37.

18 Gradwohl G, Dierich A, LeMeur M, Guillemot F. neurogenin3 is required for the development of the four endocrine cell lineages of the pancreas. *Proceedings of the National Academy of Sciences of the United States of America* 2000; **97**: 1607–1611.

19 Conrad E, Stein R, Hunter CS. Revealing transcription factors during human pancreatic. *Trends in Endocrinology & Metabolism* 2014; **25**: 407–414.

20 Nair G, Hebrok M. ScienceDirectIslet formation in mice and men: lessons for the generation of functional insulin-producing. *Current Opinion in Genetics & Development* 2015; **32**: 171–180.

21 Artner I, Blanchi B, Raum JC, Guo M, Kaneko T, Cordes S *et al.* MafB is required for islet β cell maturation. *Proceedings of the National Academy of Sciences of the United States of America* 2007; **104**: 3853–3858.

22 Goodyer WR, Gu X, Liu Y, Bottino R, Crabtree GR, Kim SK. Neonatal β cell development in mice and humans is regulated by calcineurin/NFAT. *Dev Cell* 2012; **23**: 21–34.

23 Benitez CM, Goodyer WR, Kim SK. Deconstructing Pancreas Developmental Biology. *Cold Spring Harbor Perspectives in Biology* 2012; **4**: a012401–a012401.

24 Babu DA, Deering TG, Mirmira RG. A feat of metabolic proportions: Pdx1 orchestrates islet development and function in the maintenance of glucose homeostasis. *Mol Genet Metab* 2007; **92**: 43–55.

25 Gannon M, Tweedie Ables E, Crawford L, Lowe D, Offield MF, Magnuson MA *et al.* pdx-1 function is specifically required in embryonic β cells to generate appropriate numbers of endocrine cell types and maintain glucose homeostasis. *Developmental Biology* 2008; **314**: 406–417.

26 Brissova M, Blaha M, Spear C, Nicholson W, Radhika A, Shiota M *et al.* Reduced PDX-1 expression impairs islet response to insulin resistance and worsens glucose homeostasis. *Am J Physiol Endocrinol Metab* 2005; **288**: E707–14.

27 Brissova M, Shiota M, Nicholson WE, Gannon M, Knobel SM, Piston DW *et al.* Reduction in pancreatic transcription factor PDX-1 impairs glucose-stimulated insulin secretion. *J Biol Chem* 2002; **277**: 11225–11232.

28 Mirmira RG, Watada H, German MS. B-cell differentiation factor Nkx6.1 contains distinct DNA binding interference and transcriptional repression domains. *J Biol Chem* 2000; **275**: 14743–14751.

29 Schaffer AE, Taylor BL, Benthuysen JR, Liu J, Thorel F, Yuan W *et al.* Nkx6.1 controls a gene regulatory network required for establishing and maintaining pancreatic B cell identity. *PLoS Genet* 2013; **9**: e1003274.

30 Taylor BL, Liu F-F, Sander M. Nkx6.1 is essential for maintaining the functional state of pancreatic β cells. *Cell Rep* 2013; **4**: 1262–1275.

31 Schisler JC, Jensen PB, Taylor DG, Becker TC, Knop FK, Takekawa S *et al.* The Nkx6.1 homeodomain transcription factor suppresses glucagon expression and regulates glucose-stimulated insulin secretion in islet β cells. *Proceedings of the National Academy of Sciences of the United States of America* 2005; **102**: 7297–7302.

32 Hang Y, Stein R. MafA and MafB activity in pancreatic β cells. *Trends Endocrinol Metab* 2011; **22**: 364–373.

33 Artner I, Hang Y, Mazur M, Yamamoto T, Guo M, Lindner J *et al.* MafA and MafB regulate genes critical to β-cells in a unique temporal manner. *Diabetes* 2010; **59**: 2530–2539.

34 Artner I, Hang Y, Guo M, Gu G, Stein R. MafA is a dedicated activator of the insulin gene in vivo. *J Endocrinol* 2008; **198**: 271–279.

35 Kataoka K, Han S-I, Shioda S, Hirai M, Nishizawa M, Handa H. MafA is a glucose-regulated and pancreatic β-cell-specific transcriptional activator for the insulin gene. *J Biol Chem* 2002; **277**: 49903–49910.

36 Zhang C, Moriguchi T, Kajihara M, Esaki R, Harada A, Shimohata H *et al.* MafA is a key regulator of glucose-stimulated insulin secretion. *Mol Cell Biol* 2005; **25**: 4969–4976.

37 Matsuoka T-A, Zhao L, Artner I, Jarrett HW, Friedman D, Means A *et al.* Members of the large Maf transcription family regulate insulin gene transcription in islet β cells. *Mol Cell Biol* 2003; **23**: 6049–6062.

38 Guo S, Dai C, Guo M, Taylor B, Harmon JS, Sander M *et al.* Inactivation of specific β cell transcription factors in type 2 diabetes. *J Clin Invest* 2013.

39 Torres N, Noriega L, Tovar AR. *Nutrient Modulation of Insulin Secretion*. 1st ed. Elsevier Inc., 2009.

40 De León DD, Stanley CA. Mechanisms of Disease: advances in diagnosis and treatment of hyperinsulinism in neonates. *Nat Clin Pract Endocrinol Metab* 2007; **3**: 57–68.

41 Corkey BE, Deeney JT, Yaney GC, Tornheim K, Prentki M. The role of long-chain fatty acyl-CoA esters in β-cell signal transduction. *J Nutr* 2000; **130**: 299S–304S.

42 Prentki M, Matschinsky FM, Madiraju SRM. Metabolic Signaling in Fuel-Induced Insulin Secretion. *Cell Metabolism* 2013. doi:10.1016/j.cmet.2013.05.018.

43 Levetan CS, Pierce SM. Distinctions between the islets of mice and men: implications for new therapies for type 1 and 2 diabetes. *Endocr Pract* 2013; **19**: 301–312.

44 Cabrera O, Sorkin A, Berman DM, Goh LK, Kenyon NS, Ricordi C *et al.* The unique cytoarchitecture of human pancreatic islets has implications for islet cell function.

Proceedings of the National Academy of Sciences of the United States of America 2009; **315**: 683–696.

45 Brissova M, Fowler MJ, Nicholson WE, Chu A, Hirshberg B, Harlan DM *et al.* Assessment of human pancreatic islet architecture and composition by laser scanning confocal microscopy. *J Histochem Cytochem* 2005; **53**: 1087–1097.

46 Dai C, Brissova M, Hang Y, Thompson C, Poffenberger G, Shostak A *et al.* Islet-enriched gene expression and glucose-induced insulin secretion in human and mouse islets. *Diabetologia* 2012; **55**: 707–718.

47 Ackermann AM, Gannon M. Molecular regulation of pancreatic beta-cell mass development, maintenance, and expansion. *J Mol Endocrinol* 2007; **38**: 193–206.

48 Chen G, Liu C, Xue Y, Mao X, Xu K, Liu C. Molecular mechanism of pancreatic β-cell adaptive proliferation: studies during pregnancy in rats and in vitro. *Endocrine* 2011; **39**: 118–127.

49 Nir T, Melton DA, Dor Y. Recovery from diabetes in mice by β cell regeneration. *J Clin Invest* 2007; **117**: 2553–2561.

50 Gregg BE, Moore PC, Demozay D, Hall BA, Li M, Husain A *et al.* Formation of a human β-cell population within pancreatic islets is set early in life. *J Clin Endocrinol Metab* 2012; **97**: 3197–3206.

51 Saisho Y, Butler AE, Manesso E, Elashoff D, Rizza RA, Butler PC. β-cell mass and turnover in humans: effects of obesity and aging. *Diabetes Care* 2013; **36**: 111–117.

52 Butler AE, Cao-Minh L, Galasso R, Rizza RA, Corradin A, Cobelli C *et al.* Adaptive changes in pancreatic β cell fractional area and β cell turnover in human pregnancy. *Diabetologia* 2010; **53**: 2167–2176.

53 Kulkarni RN, Mizrachi E-B, Ocana AG, Stewart AF. Human β-cell proliferation and intracellular signaling: driving in the dark without a road map. *Diabetes* 2012; **61**: 2205–2213.

54 Stewart AF, Hussain MA, Garcia-Ocaña A, Vasavada RC, Bhushan A, Bernal-Mizrachi E *et al.* Human β-Cell Proliferation and Intracellular Signaling: Part 3. *Diabetes* 2015; **64**: 1872–1885.

55 Hanley NA, Hanley NA, Hanley KP, Hanley KP, Miettinen PJ, Miettinen PJ *et al.* Weighing up β-cell mass in mice and humans: self-renewal, progenitors or stem cells? *Molecular and Cellular Endocrinology* 2008; **288**: 79–85.

56 Kitabchi AE. Proinsulin and C-peptide: a review. *Metabolism* 1977; **26**: 547–587.

57 Miranda PJ, DeFronzo RA, Califf RM, Guyton JR. Metabolic syndrome: definition, pathophysiology, and mechanisms. 2005, pp 33–45.

58 Becker AB, Roth RA. Insulin receptor structure and function in normal and pathological conditions. *Annu Rev Med* 1990; **41**: 99–115.

59 Saltiel AR, Kahn CR. Insulin signalling and the regulation of glucose and lipid metabolism. *Nature* 2001; **414**: 799–806.

60 Watanabe M, Hayasaki H, Tamayama T, Shimada M. Histologic distribution of insulin and glucagon receptors. *Braz J Med Biol Res* 1998; **31**: 243–256.

61 Boucher J, Kleinridders A, Kahn CR. Insulin Receptor Signaling in Normal and Insulin-Resistant States. *Cold Spring Harbor Perspectives in Biology* 2014; **6**: a009191–a009191.

62 Guo S. Insulin signaling, resistance, and the metabolic syndrome: insights from mouse models into disease mechanisms. *J Endocrinol* 2014; **220**: T1–T23.

63 Stumvoll M, Goldstein BJ, van Haeften TW. Type 2 diabetes: principles of pathogenesis and therapy. *Lancet* 2005; **365**: 1333–1346.

64 Nolan CJ, Damm P, Prentki M. Type 2 diabetes across generations: from pathophysiology to prevention and management. *Lancet* 2011; **378**: 169–181.

65 Atkinson MA, Eisenbarth GS, Michels AW. Type 1 diabetes. *The Lancet* 2014; **383**: 69–82.

66 Simmons KM. Type 1 diabetes: A predictable disease. *WJD* 2015; **6**: 380.

67 Egro FM. Why is type 1 diabetes increasing? *J Mol Endocrinol* 2013; **51**: R1–R13.

68 Shapiro AM, Lakey JR, Ryan EA, Korbutt GS, Toth E, Warnock GL *et al.* Islet transplantation in seven patients with type 1 diabetes mellitus using a glucocorticoid-free immunosuppressive regimen. *N Engl J Med* 2000; **343**: 230–238.

69 Barton FB, Rickels MR, Alejandro R, Hering BJ, Wease S, Naziruddin B *et al.* Improvement in outcomes of clinical islet transplantation: 1999-2010. *Diabetes Care* 2012; **35**: 1436–1445.

70 Shapiro J, Bruni A, Pepper AR, Gala-Lopez B, Abualhassan NS. Islet cell transplantation for the treatment of type 1 diabetes: recent advances and future challenges. *DMSO* 2014; : 211.

71 Fajans SS, Bell GI. MODY: History, genetics, pathophysiology, and clinical decision making. *Diabetes Care* 2011; **34**: 1878–1884.

72 Velho G, Robert J-J. Maturity-onset diabetes of the young (MODY): genetic and clinical characteristics. *Horm Res* 2002; **57 Suppl 1**: 29–33.

73 Schofield CJ, Sutherland C. Disordered insulin secretion in the development of insulin resistance and Type 2 diabetes. *Diabet Med* 2012; **29**: 972–979.

74 Brownlee M. Biochemistry and molecular cell biology of diabetic complications. *Nature* 2001; **414**: 813–820.

75 Paneni F, Beckman JA, Creager MA, Cosentino F. Diabetes and vascular disease: pathophysiology, clinical consequences, and medical therapy: part I. *Eur Heart J* 2013; **34**: 2436–2443.

76 Hara K, Fujita H, Johnson TA, Yamauchi T, Yasuda K, Horikoshi M *et al.* Genome-wide association study identifies three novel loci for type 2 diabetes. *Hum Mol Genet* 2014; **23**: 239–246.

77 Strawbridge RJ, Dupuis J, Prokopenko I, Barker A, Ahlqvist E, Rybin D *et al.* Genome-wide association identifies nine common variants associated with fasting proinsulin levels and provides new insights into the pathophysiology of type 2 diabetes. *Diabetes* 2011; **60**: 2624–2634.

78 Torres JM, Bose R, Cox NJ, Zhang X, Philipson LH. Genome wide association studies for diabetes: perspective on results and challenges. *Pediatr Diabetes* 2013; **14**: 90–96.

79 Brietzke SA. Oral antihyperglycemic treatment options for type 2 diabetes mellitus. *Med Clin North Am* 2015; **99**: 87–106.

80 Alejandro R, Singh AB, Barton FB, Harris RC, Hering BJ, Wease S *et al.* 2008 Update from the Collaborative Islet Transplant Registry. *Transplantation* 2008; **86**: 1783–1788.

81 Kaddis JS, Olack BJ, Sowinski J, Cravens J, Contreras JL, Niland JC. Human pancreatic islets and diabetes research. *JAMA* 2009; **301**: 1580–1587.

82 Kulkarni RN, Stewart AF. Summary of the Keystone islet workshop (April 2014): the increasing demand for human islet availability in diabetes research. *Diabetes* 2014; **63**: 3979–3981.

83 Brissova M, Fowler M, Wiebe P, Shostak A, Shiota M, Radhika A *et al.* Intraislet endothelial cells contribute to revascularization of transplanted pancreatic islets. *Diabetes* 2004; **53**: 1318–1325.

84 Brissova M, Aamodt K, Brahmachary P, Prasad N, Hong J-Y, Dai C *et al.* Islet Microenvironment, Modulated by Vascular Endothelial Growth Factor-A Signaling, Promotes β Cell Regeneration. *Cell Metabolism* 2014; **19**: 498–511.

85 Greiner DL, Brehm MA, Hosur V, Harlan DM, Powers AC, Shultz LD. Humanized mice for the study of type 1 and type 2 diabetes. *Ann N Y Acad Sci* 2011; **1245**: 55–58.

86 Brehm MA, Powers AC, Shultz LD, Greiner DL. Advancing animal models of human type 1 diabetes by engraftment of functional human tissues in immunodeficient mice. *Cold Spring Harb Perspect Med* 2012; **2**: a007757.

87 Robertson RP, Zhang HJ, Pyzdrowski KL, Walseth TF. Preservation of insulin mRNA levels and insulin secretion in HIT cells by avoidance of chronic exposure to high glucose concentrations. *J Clin Invest* 1992; **90**: 320–325.

88 Pino MF, Ye DZ, Linning KD, Green CD, Wicksteed B, Poitout V *et al.* Elevated glucose attenuates human insulin gene promoter activity in INS-1 pancreatic β-cells via reduced nuclear factor binding to the A5/core and Z element. *Mol Endocrinol* 2005; **19**: 1343–1360.

89 Dubois M, Vacher P, Roger B, Huyghe D, Vandewalle B, Kerr-Conte J *et al.* Glucotoxicity inhibits late steps of insulin exocytosis. *Endocrinology* 2007; **148**: 1605–1614.

90 Somanath S, Barg S, Marshall C, Silwood CJ, Turner MD. High extracellular glucose inhibits exocytosis through disruption of syntaxin 1A-containing lipid rafts. *Biochemical and Biophysical Research Communications* 2009; **389**: 241–246.

91 Somesh BP, Verma MK, Sadasivuni MK, Mammen-Oommen A, Biswas S, Shilpa PC *et al.* Chronic glucolipotoxic conditions in pancreatic islets impair insulin secretion due to dysregulated calcium dynamics, glucose responsiveness and mitochondrial activity. *BMC Cell Biol* 2013; **14**: 31.

92 Olofsson CS, Collins S, Bengtsson M, Eliasson L, Salehi A, Shimomura K *et al.* Long-term exposure to glucose and lipids inhibits glucose-induced insulin secretion downstream of granule fusion with plasma membrane. *Diabetes* 2007; **56**: 1888–1897.

93 El-Assaad W, Buteau J, Peyot M-L, Nolan C, Roduit R, Hardy S *et al.* Saturated fatty acids synergize with elevated glucose to cause pancreatic β-cell death. *Endocrinology* 2003; **144**: 4154–4163.

94 Briaud I, Kelpe CL, Johnson LM, Tran POT, Poitout V. Differential effects of hyperlipidemia on insulin secretion in islets of langerhans from hyperglycemic versus normoglycemic rats. *Diabetes* 2002; **51**: 662–668.

95 Jacqueminet S, Briaud I, Rouault C, Reach G, Poitout V. Inhibition of insulin gene expression by long-term exposure of pancreatic β cells to palmitate is dependent on the presence of a stimulatory glucose concentration. *Metabolism* 2000; **49**: 532–536.

96 Lupi R, Del Guerra S, Fierabracci V, Marselli L, Novelli M, Patané G *et al.* Lipotoxicity in human pancreatic islets and the protective effect of metformin. *Diabetes* 2002; **51 Suppl 1**: S134–7.

97 Zhou YP, Grill VE. Long-term exposure of rat pancreatic islets to fatty acids inhibits glucose-induced insulin secretion and biosynthesis through a glucose fatty acid cycle. *J Clin Invest* 1994; **93**: 870–876.

98 Mason TM, Goh T, Tchipashvili V, Sandhu H, Gupta N, Lewis GF *et al.* Prolonged elevation of plasma free fatty acids desensitizes the insulin secretory response to glucose in vivo in rats. *Diabetes* 1999; **48**: 524–530.

99 Goh TT, Mason TM, Gupta N, So A, Lam TKT, Lam L *et al.* Lipid-induced β-cell dysfunction in vivo in models of progressive β-cell failure. *Am J Physiol Endocrinol Metab* 2007; **292**: E549–60.

100 Gremlich S, Bonny C, Waeber G, Thorens B. Fatty acids decrease IDX-1 expression in rat pancreatic islets and reduce GLUT2, glucokinase, insulin, and somatostatin levels. *J Biol Chem* 1997; **272**: 30261–30269.

101 Ritz-Laser B, Meda P, Constant I, Klages N, Charollais A, Morales A *et al.* Glucose-induced preproinsulin gene expression is inhibited by the free fatty acid palmitate. *Endocrinology* 1999; **140**: 4005–4014.

102 Kelpe CL, Moore PC, Parazzoli SD, Wicksteed B, Rhodes CJ, Poitout V. Palmitate inhibition of insulin gene expression is mediated at the transcriptional level via ceramide synthesis. *J Biol Chem* 2003; **278**: 30015–30021.

103 Federici M, Hribal M, Perego L, Ranalli M, Caradonna Z, Perego C *et al.* High glucose causes apoptosis in cultured human pancreatic islets of Langerhans: a potential role for regulation of specific Bcl family genes toward an apoptotic cell death program. *Diabetes* 2001; **50**: 1290–1301.

104 Maedler K, Spinas GA, Lehmann R, Sergeev P, Weber M, Fontana A *et al.* Glucose induces β-cell apoptosis via upregulation of the Fas receptor in human islets. *Diabetes* 2001; **50**: 1683–1690.

105 Maedler K, Oberholzer J, Bucher P, Spinas GA, Donath MY. Monounsaturated fatty acids prevent the deleterious effects of palmitate and high glucose on human pancreatic β-cell turnover and function. *Diabetes* 2003; **52**: 726–733.

106 Matveyenko AV, Butler PC. B-cell deficit due to increased apoptosis in the human islet amyloid polypeptide transgenic (HIP) rat recapitulates the metabolic defects present in type 2 diabetes. *Diabetes* 2006; **55**: 2106–2114.

107 Butler AE, Janson J, Bonner-Weir S, Ritzel R, Rizza RA, Butler PC. B-cell deficit and increased β-cell apoptosis in humans with type 2 diabetes. *Diabetes* 2003; **52**: 102–110.

108 Cnop M, Hannaert JC, Hoorens A, Eizirik DL, Pipeleers DG. Inverse relationship between cytotoxicity of free fatty acids in pancreatic islet cells and cellular triglyceride accumulation. *Diabetes* 2001; **50**: 1771–1777.

109 Maedler K, Spinas GA, Dyntar D, Moritz W, Kaiser N, Donath MY. Distinct effects of saturated and monounsaturated fatty acids on β-cell turnover and function. *Diabetes* 2001; **50**: 69–76.

110 Yu EPK, Bennett MR. Mitochondrial DNA damage and atherosclerosis. *Trends Endocrinol Metab* 2014; **25**: 481–487.

111 Pi J, Bai Y, Zhang Q, Wong V, Floering LM, Daniel K *et al.* Reactive oxygen species as a signal in glucose-stimulated insulin secretion. *Diabetes* 2007; **56**: 1783–1791.

112 Leloup C, Tourrel-Cuzin C, Magnan C, Karaca M, Castel J, Carneiro L *et al.* Mitochondrial reactive oxygen species are obligatory signals for glucose-induced insulin secretion. *Diabetes* 2009; **58**: 673–681.

113 Melov S. Mitochondrial oxidative stress. Physiologic consequences and potential for a role in aging. *Ann N Y Acad Sci* 2000; **908**: 219–225.

114 Grankvist K, Marklund SL, Täljedal IB. CuZn-superoxide dismutase, Mn-superoxide dismutase, catalase and glutathione peroxidase in pancreatic islets and other tissues in the mouse. *Biochem J* 1981; **199**: 393–398.

115 Lenzen S, Drinkgern J, Tiedge M. Low antioxidant enzyme gene expression in pancreatic islets compared with various other mouse tissues. *Free Radic Biol Med* 1996; **20**: 463–466.

116 Tiedge M, Lortz S, Drinkgern J, Lenzen S. Relation between antioxidant enzyme gene expression and antioxidative defense status of insulin-producing cells. *Diabetes* 1997; **46**: 1733–1742.

117 Robertson RP, Harmon JS. Diabetes, glucose toxicity, and oxidative stress: A case of double jeopardy for the pancreatic islet β cell. *Free Radic Biol Med* 2006; **41**: 177–184.

118 Gehrmann W, Elsner M, Lenzen S. Role of metabolically generated reactive oxygen species for lipotoxicity in pancreatic β-cells. *Diabetes Obes Metab* 2010; **12 Suppl 2**: 149–158.

119 Elsner M, Gehrmann W, Lenzen S. Peroxisome-generated hydrogen peroxide as important mediator of lipotoxicity in insulin-producing cells. *Diabetes* 2011; **60**: 200–208.

120 Poitout V, Robertson RP. Glucolipotoxicity: fuel excess and β-cell dysfunction. *Endocr Rev* 2008; **29**: 351–366.

121 Harmon JS, Stein R, Robertson RP. Oxidative stress-mediated, post-translational loss of MafA protein as a contributing mechanism to loss of insulin gene expression in glucotoxic β cells. *J Biol Chem* 2005; **280**: 11107–11113.

122 Kim M-H, Kawamori D, Kino-oka M, Kajimoto Y, Kawase M, Kaneto H *et al.* Oxidative stress induces nucleo-cytoplasmic translocation of pancreatic transcription factor PDX-1 through activation of c-Jun NH(2)-terminal kinase. *Diabetes* 2003; **52**: 2896–2904.

123 Mahadevan J, Parazzoli S, Oseid E, Hertzel AV, Bernlohr DA, Vallerie SN *et al.* Ebselen treatment prevents islet apoptosis, maintains intranuclear Pdx-1 and MafA levels, and preserves β-cell mass and function in ZDF rats. *Diabetes* 2013. doi:10.2337/db13-0357.

124 Tanaka Y, Tran POT, Harmon J, Robertson RP. A role for glutathione peroxidase in protecting pancreatic β cells against oxidative stress in a model of glucose toxicity. *Proceedings of the National Academy of Sciences of the United States of America* 2002; **99**: 12363–12368.

125 Haataja L, Gurlo T, Huang CJ, Butler PC. Islet amyloid in type 2 diabetes, and the toxic oligomer hypothesis. *Endocr Rev* 2008; **29**: 303–316.

126 Papa FR. Endoplasmic reticulum stress, pancreatic β-cell degeneration, and diabetes. *Cold Spring Harb Perspect Med* 2012; **2**: a007666.

127 Dufey E, Sepúlveda D, Rojas-Rivera D, Hetz C. Cellular mechanisms of endoplasmic reticulum stress signaling in health and disease. 1. An overview. *Am J Physiol, Cell Physiol* 2014; **307**: C582–94.

128 Back SH, Kaufman RJ. Endoplasmic Reticulum Stress and Type 2 Diabetes. *Annu Rev Biochem* 2012; **81**: 767–793.

129 Laybutt DR, Preston AM, Akerfeldt MC, Kench JG, Busch AK, Biankin AV *et al.* Endoplasmic reticulum stress contributes to β cell apoptosis in type 2 diabetes. *Diabetologia* 2007; **50**: 752–763.

130 Chan JY, Luzuriaga J, Bensellam M, Biden TJ, Laybutt DR. Failure of the adaptive unfolded protein response in islets of obese mice is linked with abnormalities in β-cell gene expression and progression to diabetes. *Diabetes* 2013; **62**: 1557–1568.

131 Biden TJ, Boslem E, Chu KY, Sue N. Lipotoxic endoplasmic reticulum stress. *Trends in Endocrinology & Metabolism* 2014; **25**: 389–398.

132 Höppener JW, Ahrén B, Lips CJ. Islet amyloid and type 2 diabetes mellitus. *N Engl J Med* 2000; **343**: 411–419.

133 Citri A, Zhao H-L, Zhao H-L, Sui Y, Sui Y, Guan J *et al.* Amyloid oligomers in diabetic and nondiabetic human pancreas. *Transl Res* 2009; **153**: 24–32.

134 Abedini A, Schmidt AM. Mechanisms of islet amyloidosis toxicity in type 2 diabetes. *FEBS Lett* 2013; **587**: 1119–1127.

135 Kahn SE, Andrikopoulos S, Verchere CB. Islet amyloid: a long-recognized but underappreciated pathological feature of type 2 diabetes. *Diabetes* 1999; **48**: 241–253.

136 Westermark P, Andersson A, Westermark GT. Islet Amyloid Polypeptide, Islet Amyloid, and Diabetes Mellitus. *Physiological Reviews* 2011; **91**: 795–826.

137 Lin C-Y, Gurlo T, Kayed R, Butler AE, Haataja L, Glabe CG *et al.* Toxic human islet amyloid polypeptide (h-IAPP) oligomers are intracellular, and vaccination to induce anti-toxic oligomer antibodies does not prevent h-IAPP-induced β-cell apoptosis in h-IAPP transgenic mice. *Diabetes* 2007; **56**: 1324–1332.

138 Janson J, Ashley RH, Harrison D, McIntyre S, Butler PC. The mechanism of islet amyloid polypeptide toxicity is membrane disruption by intermediate-sized toxic amyloid particles. *Diabetes* 1999; **48**: 491–498.

139 Westermark P, Engström U, Johnson KH, Westermark GT, Betsholtz C. Islet amyloid polypeptide: pinpointing amino acid residues linked to amyloid fibril formation. *Proceedings of the National Academy of Sciences of the United States of America* 1990; **87**: 5036–5040.

140 Shigihara N, Fukunaka A, Hara A, Komiya K, Honda A, Uchida T *et al.* Human IAPP-induced pancreatic β cell toxicity and its regulation by autophagy. *J Clin Invest* 2014; **124**: 3634–3644.

141 Zraika S, Hull RL, Verchere CB, Clark A, Potter KJ, Fraser PE *et al.* Toxic oligomers and islet β cell death: guilty by association or convicted by circumstantial evidence? *Diabetologia* 2010; **53**: 1046–1056.

142 Park YJ, Woo M, Kieffer TJ, Hakem R, Safikhan N, Yang F *et al.* The role of caspase-8 in amyloid-induced β cell death in human and mouse islets. *Diabetologia* 2014; **57**: 765–775.

143 Poojari C, Xiao D, Batista VS, Strodel B. Membrane permeation induced by aggregates of human islet amyloid polypeptides. *Biophys J* 2013; **105**: 2323–2332.

144 Engel MFM, Khemtémourian L, Kleijer CC, Meeldijk HJD, Jacobs J, Verkleij AJ *et al.* Membrane damage by human islet amyloid polypeptide through fibril growth at the membrane. *Proceedings of the National Academy of Sciences of the United States of America* 2008; **105**: 6033–6038.

145 Potter KJ, Abedini A, Marek P, Klimek AM, Butterworth S, Driscoll M *et al.* Islet amyloid deposition limits the viability of human islet grafts but not porcine islet grafts. *Proceedings of the National Academy of Sciences of the United States of America* 2010; **107**: 4305–4310.

146 Kayton NS, Poffenberger G, Henske J, Dai C, Thompson C, Aramandla R *et al.* Human Islet Preparations Distributed for Research Exhibit a Variety of Insulin Secretory Profiles. *Am J Physiol Endocrinol Metab* 2015; : ajpendo.00437.2014.

147 Shultz LD, Ishikawa F, Greiner DL. Humanized mice in translational biomedical research. *Nat Rev Immunol* 2007; **7**: 118–130.

148 Thorel F, Népote V, Avril I, Kohno K, Desgraz R, Chera S *et al.* Conversion of adult pancreatic [agr]-cells to [bgr]-cells after extreme [bgr]-cell loss. *Nature* 2010; **464**: 1149–1154.

149 Threadgill DW, Dlugosz AA, Hansen LA, Tennenbaum T, Lichti U, Yee D *et al.* Targeted disruption of mouse EGF receptor: effect of genetic background on mutant phenotype. *Science* 1995; **269**: 230–234.

150 Herrera PL. Adult insulin- and glucagon-producing cells differentiate from two independent cell lineages. *Development* 2000; **127**: 2317–2322.

151 Wang T, Lacík I, Brissova M, Anilkumar AV, Prokop A, Hunkeler D *et al.* An encapsulation system for the immunoisolation of pancreatic islets. *Nat Biotechnol* 1997; **15**: 358–362.

152 Schäffer L, Brand CL, Hansen BF, Ribel U, Shaw AC, Slaaby R *et al.* A novel high-affinity peptide antagonist to the insulin receptor. *Biochemical and Biophysical Research Communications* 2008; **376**: 380–383.

153 Vikram A, Jena G. S961, an insulin receptor antagonist causes hyperinsulinemia, insulin-resistance and depletion of energy stores in rats. *Biochemical and Biophysical Research Communications* 2010; **398**: 260–265.

154 Reinert RB, Brissova M, Shostak A, Pan FC, Poffenberger G, Cai Q *et al.* Vascular Endothelial Growth Factor-A and Islet Vascularization are Necessary in Developing, but not Adult, Pancreatic Islets. *Diabetes* 2013. doi:10.2337/db13-0071.

155 Cai Q, Brissova M, Reinert RB, Pan FC, Brahmachary P, Jeansson M *et al.* Enhanced expression of VEGF-A in β cells increases endothelial cell number but impairs islet morphogenesis and β cell proliferation. *Developmental Biology* 2012; **367**: 40–54.

156 Brissova M, Shostak A, Shiota M, Wiebe PO, Poffenberger G, Kantz J *et al.* Pancreatic islet production of vascular endothelial growth factor--a is essential for islet vascularization, revascularization, and function. *Diabetes* 2006; **55**: 2974–2985.

157 Dai C, Brissova M, Reinert RB, Nyman L, Liu EH, Thompson C *et al.* Pancreatic islet vasculature adapts to insulin resistance through dilation and not angiogenesis. *Diabetes* 2013; **62**: 4144–4153.

158 Kang L, Dai C, Lustig ME, Bonner JS, Mayes WH, Mokshagundam S *et al.* Heterozygous SOD2 deletion impairs glucose-stimulated insulin secretion, but not insulin action, in high-fat-fed mice. *Diabetes* 2014; **63**: 3699–3710.

159 Huggett JF, Foy CA, Benes V, Emslie K, Garson JA, Haynes R *et al.* The digital MIQE guidelines: Minimum Information for Publication of Quantitative Digital PCR Experiments. *Clin Chem* 2013; **59**: 892–902.

160 Ravassard P, Hazhouz Y, Pechberty S, Bricout-Neveu E, Armanet M, Czernichow P *et al.* A genetically engineered human pancreatic β cell line exhibiting glucose-inducible insulin secretion. *J Clin Invest* 2011; **121**: 3589–3597.

161 Kashyap S, Belfort R, Gastaldelli A, Pratipanawatr T, Berria R, Pratipanawatr W *et al.* A sustained increase in plasma free fatty acids impairs insulin secretion in nondiabetic subjects genetically predisposed to develop type 2 diabetes. *Diabetes* 2003; **52**: 2461–2474.

162 Stefan N, Wahl HG, Fritsche A, Häring H, Stumvoll M. Effect of the pattern of elevated free fatty acids on insulin sensitivity and insulin secretion in healthy humans. *Horm Metab Res* 2001; **33**: 432–438.

163 Unger RH. Lipotoxicity in the pathogenesis of obesity-dependent NIDDM. Genetic and clinical implications. *Diabetes* 1995; **44**: 863–870.

164 Unger RH, Zhou YT. Lipotoxicity of β-cells in obesity and in other causes of fatty acid spillover. *Diabetes* 2001; **50 Suppl 1**: S118–21.

165 Poitout V, Amyot J, Semache M, Zarrouki B, Hagman D, Fontés G. Glucolipotoxicity of the pancreatic β cell. *Biochim Biophys Acta* 2010; **1801**: 289–298.

166 Gleason CE, Gonzalez M, Harmon JS, Robertson RP. Determinants of glucose toxicity and its reversibility in the pancreatic islet β-cell line, HIT-T15. *Am J Physiol Endocrinol Metab* 2000; **279**: E997–1002.

167 Göhring I, Sharoyko VV, Malmgren S, Andersson LE, Spégel P, Nicholls DG *et al.* Chronic high glucose and pyruvate levels differentially affect mitochondrial bioenergetics and fuel-stimulated insulin secretion from clonal INS-1 832/13 cells. *Journal of Biological Chemistry* 2014; **289**: 3786–3798.

168 Vernier S, Chiu A, Schober J, Weber T, Nguyen P, Luer M *et al.* β-cell metabolic alterations under chronic nutrient overload in rat and human islets. *Islets* 2012; **4**: 379–392.

169 Tang C, Naassan AE, Chamson-Reig A, Koulajian K, Goh TT, Yoon F *et al.* Susceptibility to fatty acid-induced β-cell dysfunction is enhanced in prediabetic diabetes-prone biobreeding rats: a potential link between β-cell lipotoxicity and islet inflammation. *Endocrinology* 2013; **154**: 89–101.

170 Andrali SS, Sampley ML, Vanderford NL, Özcan S. Glucose regulation of insulin gene expression in pancreatic β-cells. *Biochem J* 2008; **415**: 1.

171 Poitout V, Hagman D, Stein R, Artner I, Robertson RP, Harmon JS. Regulation of the insulin gene by glucose and fatty acids. *J Nutr* 2006; **136**: 873–876.

172 Moran A, Zhang HJ, Olson LK, Harmon JS, Poitout V, Robertson RP. Differentiation of glucose toxicity from β cell exhaustion during the evolution of defective insulin gene expression in the pancreatic islet cell line, HIT-T15. *J Clin Invest* 1997; **99**: 534–539.

173 Cao P, Marek P, Noor H, Patsalo V, Tu L-H, Wang H *et al.* Islet amyloid: from fundamental biophysics to mechanisms of cytotoxicity. *FEBS Lett* 2013; **587**: 1106–1118.

174 Hull RL, Andrikopoulos S, Verchere CB, Vidal J, Wang F, Cnop M *et al.* Increased dietary fat promotes islet amyloid formation and β-cell secretory dysfunction in a transgenic mouse model of islet amyloid. *Diabetes* 2003; **52**: 372–379.

175 Verchere CB, D'Alessio DA, Palmiter RD, Weir GC, Bonner-Weir S, Baskin DG *et al.* Islet amyloid formation associated with hyperglycemia in transgenic mice with pancreatic β cell expression of human islet amyloid polypeptide. *Proceedings of the National Academy of Sciences of the United States of America* 1996; **93**: 3492–3496.

176 Shimabukuro M, Higa M, Zhou YT, Wang MY, Newgard CB, Unger RH. Lipoapoptosis in β-cells of obese prediabetic fa/fa rats. Role of serine palmitoyltransferase overexpression. *J Biol Chem* 1998; **273**: 32487–32490.

177 Lupi R, Dotta F, Marselli L, Del Guerra S, Masini M, Santangelo C *et al.* Prolonged exposure to free fatty acids has cytostatic and pro-apoptotic effects on human pancreatic islets: evidence that β-cell death is caspase mediated, partially dependent on ceramide pathway, and Bcl-2 regulated. *Diabetes* 2002; **51**: 1437–1442.

178 Véret J, Coant N, Berdyshev EV, Skobeleva A, Therville N, Bailbé D *et al.* Ceramide synthase 4 and de novo production of ceramides with specific N-acyl chain lengths are involved in glucolipotoxicity-induced apoptosis of INS-1 β-cells. *Biochem J* 2011; **438**: 177–189.

179 Boslem E, Meikle PJ, Biden TJ. Roles of ceramide and sphingolipids in pancreatic β-cell function and dysfunction. *Islets* 2012; **4**: 177–187.

180 Prentki M, Joly E, El-Assaad W, Roduit R. Malonyl-CoA signaling, lipid partitioning, and glucolipotoxicity: role in β-cell adaptation and failure in the etiology of diabetes. *Diabetes* 2002; **51 Suppl 3**: S405–13.

181 El-Assaad W, Joly E, Barbeau A, Sladek R, Buteau J, Maestre I *et al.* Glucolipotoxicity alters lipid partitioning and causes mitochondrial dysfunction, cholesterol, and ceramide deposition and reactive oxygen species production in INS832/13 ss-cells. *Endocrinology* 2010; **151**: 3061–3073.

182 Matsuoka T-A, Kaneto H, Kawashima S, Miyatsuka T, Tochino Y, Yoshikawa A *et al.* Preserving Mafa expression in diabetic islet β-cells improves glycemic control in vivo. *Journal of Biological Chemistry* 2015; **290**: 7647–7657.

183 Fiaschi-Taesch NM, Salim F, Kleinberger J, Troxell R, Cozar-Castellano I, Selk K *et al.* Induction of human β-cell proliferation and engraftment using a single G1/S regulatory molecule, cdk6. *Diabetes* 2010; **59**: 1926–1936.

184 Fiaschi-Taesch NM, Kleinberger JW, Salim FG, Troxell R, Wills R, Tanwir M *et al.* Cytoplasmic-Nuclear Trafficking of G1/S Cell Cycle Molecules and Adult Human -Cell Replication: A Revised Model of Human -Cell G1/S Control. *Diabetes* 2013; **62**: 2460–2470.

185 Brehm MA, Bortell R, Diiorio P, Leif J, Laning J, Cuthbert A *et al.* Human immune system development and rejection of human islet allografts in spontaneously diabetic NOD-Rag1null IL2rgammanull Ins2Akita mice. *Diabetes* 2010; **59**: 2265–2270.

186 Brehm MA, Wiles MV, Greiner DL, Shultz LD. Journal of Immunological Methods. *Journal of Immunological Methods* 2014; **410**: 3–17.

187 Shultz LD, Pearson T, King M, Giassi L, Carney L, Gott B *et al.* Humanized NOD/LtSz-scid IL2 receptor common gamma chain knockout mice in diabetes research. *Ann N Y Acad Sci* 2007; **1103**: 77–89.

188 Mosser RE, Maulis MF, Moullé VS, Dunn JC, Carboneau BA, Arasi K *et al.* High Fat Diet-Induced B Cell Proliferation Occurs Prior to Insulin Resistance in C57Bl/6J Male Mice. *Am J Physiol Endocrinol Metab* 2015; : ajpendo.00460.2014.

189 Mezza T, Muscogiuri G, Sorice GP, Clemente G, Hu J, Pontecorvi A *et al.* Insulin resistance alters islet morphology in nondiabetic humans. *Diabetes* 2014; **63**: 994–1007.

190 Mezza T, Kulkarni RN. The regulation of pre- and post-maturational plasticity of mammalian islet cell mass. *Diabetologia* 2014; **57**: 1291–1303.

191 Porat S, Weinberg-Corem N, Tornovsky-Babaey S, Schyr-Ben-Haroush R, Hija A, Stolovich-Rain M *et al.* Control of pancreatic β cell regeneration by glucose metabolism. *Cell Metabolism* 2011; **13**: 440–449.

192 Alonso LC, Yokoe TT, Zhang PP, Scott DK, Kim SK, O'Donnell CP *et al.* Glucose infusion in mice: a new model to induce β-cell replication. *Diabetes* 2007; **56**: 1792–1801.

193 Diiorio P, Jurczyk A, Yang C, Racki WJ, Brehm MA, Atkinson MA *et al.* Hyperglycemia-induced proliferation of adult human β cells engrafted into

spontaneously diabetic immunodeficient NOD-Rag1null IL2rγnull Ins2Akita mice. *Pancreas* 2011; **40**: 1147–1149.

194 Yi P, Park J-S, Melton DA. Btrophin: a hormone that controls pancreatic β cell proliferation. *Cell* 2013; **153**: 747–758.

195 Jiao Y, Le Lay J, Yu M, Naji A, Kaestner KH. Elevated mouse hepatic βtrophin expression does not increase human β-cell replication in the transplant setting. *Diabetes* 2014; **63**: 1283–1288.

196 Robertson RP. Chronic oxidative stress as a central mechanism for glucose toxicity in pancreatic islet β cells in diabetes. *J Biol Chem* 2004; **279**: 42351–42354.

197 Welsh N, Margulis B, Borg LA, Wiklund HJ, Saldeen J, Flodström M *et al.* Differences in the expression of heat-shock proteins and antioxidant enzymes between human and rodent pancreatic islets: implications for the pathogenesis of insulin-dependent diabetes mellitus. *Mol Med* 1995; **1**: 806–820.

198 Gao Y, Sartori DJ, Li C, Yu Q-C, Kushner JA, Simon MC *et al.* PERK is required in the adult pancreas and is essential for maintenance of glucose homeostasis. *Mol Cell Biol* 2012; **32**: 5129–5139.

199 Elouil H, Bensellam M, Guiot Y, Vander Mierde D, Pascal SMA, Schuit FC *et al.* Acute nutrient regulation of the unfolded protein response and integrated stress response in cultured rat pancreatic islets. *Diabetologia* 2007; **50**: 1442–1452.

200 Cadavez L, Montane J, Alcarraz-Vizán G, Visa M, Vidal-Fàbrega L, Servitja J-M *et al.* Chaperones ameliorate β cell dysfunction associated with human islet amyloid polypeptide overexpression. *PLoS ONE* 2014; **9**: e101797.

201 Qi D, Cai K, Wang O, Li Z, Chen J, Deng B *et al.* Fatty acids induce amylin expression and secretion by pancreatic β-cells. *Am J Physiol Endocrinol Metab* 2010; **298**: E99–E107.

202 Tokuyama T, Yagui K, Yamaguchi T, Huang CI, Kuramoto N, Shimada F *et al.* Expression of human islet amyloid polypeptide/amylin impairs insulin secretion in mouse pancreatic β cells. *Metab Clin Exp* 1997; **46**: 1044–1051.

203 Trevino MB, Machida Y, Hallinger DR, Garcia E, Christensen A, Dutta S *et al.* Perilipin 5 regulates islet lipid metabolism and insulin secretion in a cyclic AMP dependent manner: Implication of its role in the postprandial insulin secretion. *Diabetes* 2014. doi:10.2337/db14-0559.

204 Dorrell C, Schug J, Lin CF, Canaday PS, Fox AJ, Smirnova O *et al.* Transcriptomes of the major human pancreatic cell types. *Diabetologia* 2011; **54**: 2832–2844.

205 Hosokawa H, Corkey BE, Leahy JL. B-cell hypersensitivity to glucose following 24-h exposure of rat islets to fatty acids. *Diabetologia* 1997; **40**: 392–397.

206 Hall E, Volkov P, Dayeh T, Bacos K, Rönn T, Nitert MD *et al.* Effects of palmitate on genome-wide mRNA expression and DNA methylation patterns in human pancreatic islets. *BMC Med* 2014; **12**: 103.

207 Ihara Y, Toyokuni S, Uchida K, Odaka H, Tanaka T, Ikeda H *et al.* Hyperglycemia causes oxidative stress in pancreatic β-cells of GK rats, a model of type 2 diabetes. *Diabetes* 1999; **48**: 927–932.

208 Elder DA, Prigeon RL, Wadwa RP, Dolan LM, D'Alessio DA. B-cell function, insulin sensitivity, and glucose tolerance in obese diabetic and nondiabetic adolescents and young adults. *J Clin Endocrinol Metab* 2006; **91**: 185–191.

209 Tyrberg B, Ustinov J, Otonkoski T, Andersson A. Stimulated endocrine cell proliferation and differentiation in transplanted human pancreatic islets: effects of the ob gene and compensatory growth of the implantation organ. *Diabetes* 2001; **50**: 301–307.

210 Rahier J, Guiot Y, Goebbels RM, Sempoux C, Henquin JC. Pancreatic β-cell mass in European subjects with type 2 diabetes. *Diabetes Obes Metab* 2008; **10 Suppl 4**: 32–42.

211 Sullivan BA, Hollister-Lock J, Bonner-Weir S, Weir GC. Reduced Ki67 Staining in the Postmortem State Calls Into Question Past Conclusions About the Lack of Turnover of Adult Human β-Cells. *Diabetes* 2015; **64**: 1698–1702.

212 Evans JL, Goldfine ID, Maddux BA, Grodsky GM. Oxidative stress and stress-activated signaling pathways: a unifying hypothesis of type 2 diabetes. *Endocr Rev* 2002; **23**: 599–622.

213 Butler AE, Janson J, Soeller WC, Butler PC. Increased β-cell apoptosis prevents adaptive increase in β-cell mass in mouse model of type 2 diabetes: evidence for role of islet amyloid formation rather than direct action of amyloid. *Diabetes* 2003; **52**: 2304–2314.

214 Alarcon C, Hughes WE, Verchere CB, Rhodes CJ. Translational control of glucose-induced islet amyloid polypeptide production in pancreatic islets. *Endocrinology* 2012; **153**: 2082–2087.

215 Rivera JF, Costes S, Gurlo T, Glabe CG, Butler PC. Autophagy defends pancreatic β cells from human islet amyloid polypeptide-induced toxicity. *J Clin Invest* 2014; **124**: 3489–3500.

216 Mir SUR, George NM, Zahoor L, Harms R, Guinn Z, Sarvetnick NE. Inhibition of Autophagic Turnover in β-Cells by Fatty Acids and Glucose Leads to Apoptotic Cell Death. *Journal of Biological Chemistry* 2015; **290**: 6071–6085.

217 Butler AE, Jang J, Gurlo T, Carty MD, Soeller WC, Butler PC. Diabetes due to a progressive defect in β-cell mass in rats transgenic for human islet amyloid polypeptide (HIP Rat): a new model for type 2 diabetes. *Diabetes* 2004; **53**: 1509–1516.

218 Levitt HE, Cyphert TJ, Pascoe JL, Hollern DA, Abraham N, Lundell RJ *et al.* Glucose stimulates human β cell replication in vivo in islets transplanted into NOD-severe combined immunodeficiency (SCID) mice. *Diabetologia* 2011; **54**: 572–582.

219 Imai Y, Dobrian AD, Weaver JR, Butcher MJ, Cole BK, Galkina EV *et al.* Interaction between cytokines and inflammatory cells in islet dysfunction, insulin resistance and vascular disease. *Diabetes Obes Metab* 2013; **15 Suppl 3**: 117–129.

220 O'Neill CM, Lu C, Corbin KL, Sharma PR, Dula SB, Carter JD *et al.* Circulating levels of IL-1B+IL-6 cause ER stress and dysfunction in islets from prediabetic male mice. *Endocrinology* 2013; **154**: 3077–3088.

221 Donath MY, Dalmas E, Sauter NS, Böni-Schnetzler M. Inflammation in obesity and diabetes: islet dysfunction and therapeutic opportunity. *Cell Metabolism* 2013; **17**: 860–872.

222 Wu Y, Wu T, Wu J, Zhao L, Li Q, Varghese Z *et al.* Chronic inflammation exacerbates glucose metabolism disorders in C57BL/6J mice fed with high-fat diet. *J Endocrinol* 2013; **219**: 195–204.

223 Avrahami D, Changhong L, Yu M, Jiao Y, Zhang J, Naji A *et al.* Targeting the cell cycle inhibitor p57Kip2 promotes adult human β cell replication. *The Journal of Clinical Investigation* 2014; **124**: 670.

224 Kameswaran V, Bramswig NC, McKenna LB, Penn M, Schug J, Hand NJ *et al.* Epigenetic regulation of the DLK1-MEG3 microRNA cluster in human type 2 diabetic islets. *Cell Metabolism* 2014; **19**: 135–145.

225 Bramswig NC, Everett LJ, Schug J, Dorrell C, Liu C, Luo Y *et al.* Epigenomic plasticity enables human pancreatic α to β cell reprogramming. *J Clin Invest* 2013; **123**: 1275–1284.

226 D'Aleo V, Del Guerra S, Gualtierotti G, Filipponi F, Boggi U, De Simone P *et al.* Functional and Survival Analysis of Isolated Human Islets. *Transplant Proc* 2014; **42**: 2250–2251.

227 Kyriazis GA, Soundarapandian MM, Tyrberg B. Sweet taste receptor signaling in β cells mediates fructose-induced potentiation of glucose-stimulated insulin secretion. *Proceedings of the National Academy of Sciences of the United States of America* 2012; : E524–E532.

228 Oh E, Kalwat MA, Kim MJ, Verhage M, Thurmond DC. Munc18-1 Regulates First-phase Insulin Release by Promoting Granule Docking to Multiple Syntaxin Isoforms. *Journal of Biological Chemistry* 2012; **287**: 25821–25833.

229 Kondegowda NG, Mozar A, Chin C, Otero A, Garcia-Ocana A, Vasavada RC. Lactogens protect rodent and human β cells against glucolipotoxicity-induced cell death through Janus kinase-2 (JAK2)/signal transducer and activator of transcription-5 (STAT5) signalling. *Diabetologia* 2012; **55**: 1721–1732.

230 Hanson MS, Park EE, Sears ML, Greenwood KK, Danobeitia JS, Hullett DA *et al.* A simplified approach to human islet quality assessment. *Transplantation* 2010; **89**: 1178–1188.

231 Andrali SS, Virostko J, Henske J, Vanderford NL, Vinet L, Özcan S *et al.* Multimodal image coregistration and inducible selective cell ablation to evaluate imaging ligands. *Proceedings of the National Academy of Sciences of the United States of America* 2011; **108**: 20719–20724.

232 Kaddis JS, Hanson MS, Cravens J, Qian D, Olack B, Antler M *et al.* Standardized transportation of human islets: an islet cell resource center study of more than 2,000 shipments. *Cell Transplant* 2013; **22**: 1101–1111.

233 Kaddis JS, Danobeitia JS, Niland JC, Stiller T, Fernandez LA. Multicenter analysis of novel and established variables associated with successful human islet isolation outcomes. *Am J Transplant* 2010; **10**: 646–656.

234 Wang Y, Danielson KK, Ropski A, Harvat T, Barbaro B, Paushter D *et al.* Systematic analysis of donor and isolation factor's impact on human islet yield and size distribution. *Cell Transplant* 2013; **22**: 2323–2333.

235 Sakuma Y, Ricordi C, Miki A, Yamamoto T, Pileggi A, Khan A *et al.* Factors that affect human islet isolation. *Transplant Proc* 2008; **40**: 343–345.

236 Buchwald P. A local glucose-and oxygen concentration-based insulin secretion model for pancreatic islets. *Theor Biol Med Model* 2011; **8**: 20.

237 Sweet IR, Gilbert M, Scott S, Todorov I, Jensen R, Nair I *et al.* Glucose-stimulated increment in oxygen consumption rate as a standardized test of human islet quality. *Am J Transplant* 2008; **8**: 183–192.

238 Bentsi-Barnes K, Doyle ME, Abad D, Kandeel F, Al-Abdullah IH. Detailed protocol for evaluation of dynamic perifusion of human islets to assess β-cell function. *Islets* 2011; **3**: 284.

239 Gurka MJ, Lilly CL, Oliver MN, DeBoer MD. An examination of sex and racial/ethnic differences in the metabolic syndrome among adults: A confirmatory factor analysis and a resulting continuous severity score. *Metabolism* 2014; **63**: 218–225.

240 Street CN, Lakey JRT, Shapiro AMJ, Imes S, Rajotte RV, Ryan EA *et al.* Islet graft assessment in the Edmonton Protocol: implications for predicting long-term clinical outcome. *Diabetes* 2004; **53**: 3107–3114.

241 Sweet IR, Gilbert M, Jensen R, Sabek O, Fraga DW, Gaber AO *et al.* Glucose stimulation of cytochrome C reduction and oxygen consumption as assessment of human islet quality. *Transplantation* 2005; **80**: 1003–1011.

242 Papas KK, Colton CK, Nelson RA, Rozak PR, Avgoustiniatos ES, Scott WE *et al.* Human islet oxygen consumption rate and DNA measurements predict diabetes reversal in nude mice. *Am J Transplant* 2007; **7**: 707–713.

243 Omori K, Mitsuhashi M, Todorov I, Rawson J, Shiang K-D, Kandeel F *et al.* Microassay for glucose-induced preproinsulin mRNA expression to assess islet functional potency for islet transplantation. *Transplantation* 2010; **89**: 146–154.

244 Contreras JL, Eckstein C, Smyth CA, Sellers MT, Vilatoba M, Bilbao G *et al.* Brain death significantly reduces isolated pancreatic islet yields and functionality in vitro and in vivo after transplantation in rats. *Diabetes* 2003; **52**: 2935–2942.

245 Eckhoff DE, Eckstein C, Smyth CA, Vilatoba M, Bilbao G, Rahemtulla FG *et al.* Enhanced isolated pancreatic islet recovery and functionality in rats by 17β-estradiol treatment of brain death donors. *Surgery* 2004; **136**: 336–345.

246 Vasavada RC, Gonzalez-Pertusa JA, Fujinaka Y, Fiaschi-Taesch N, Cozar-Castellano I, Garcia-Ocaña A. Growth factors and β cell replication. *The International Journal of Biochemistry & Cell Biology* 2006; **38**: 931–950.

247 Huotari M-A, Miettinen PJ, Palgi J, Koivisto T, Ustinov J, Harari D *et al.* ErbB signaling regulates lineage determination of developing pancreatic islet cells in embryonic organ culture. *Endocrinology* 2002; **143**: 4437–4446.

248 Miettinen PJ, Ustinov J, Ormio P, Gao R, Palgi J, Hakonen E *et al.* Downregulation of EGF receptor signaling in pancreatic islets causes diabetes due to impaired postnatal β-cell growth. *Diabetes* 2006; **55**: 3299–3308.

249 Leahy DJ. Structure and function of the epidermal growth factor (EGF/ErbB) family of receptors. *Adv Protein Chem* 2004; **68**: 1–27.

250 Raines MA, Maihle NJ, Moscovici C, Moscovici MG, Kung HJ. Molecular characterization of three erbB transducing viruses generated during avian leukosis virus-induced erythroleukemia: extensive internal deletion near the kinase domain activates the fibrosarcoma- and hemangioma-inducing potentials of erbB. *J Virol* 1988; **62**: 2444–2452.

251 Joshi M, Rizvi SM, Belani CP. Afatinib for the treatment of metastatic non-small cell lung cancer. *Cancer Manag Res* 2015; **7**: 75–82.

252 Fu X-H, Li J, Huang J-J, Zheng S, Zhang S-Z. Translational research of a novel humanized epidermal growth factor receptor-related protein: a putative inhibitor of pan-ErbB. *Cancer Chemother Pharmacol* 2011; **68**: 1373–1376.

253 Lemmon MA. Ligand-induced ErbB receptor dimerization. *Experimental Cell Research* 2009; **315**: 638–648.

254 Yarden Y, Sliwkowski MX. Untangling the ErbB signalling network. *Nat Rev Mol Cell Biol* 2001; **2**: 127–137.

255 Tao RH, Maruyama IN. All EGF(ErbB) receptors have preformed homo- and heterodimeric structures in living cells. *Journal of Cell Science* 2008; **121**: 3207–3217.

256 Singh AB, Harris RC. Autocrine, paracrine and juxtacrine signaling by EGFR ligands. *Cellular Signalling* 2005; **17**: 1183–1193.

257 Katz M, Amit I, Yarden Y. Regulation of MAPKs by growth factors and receptor tyrosine kinases. *Biochimica et Biophysica Acta (BBA) - Molecular Cell Research* 2007; **1773**: 1161–1176.

258 Miettinen P, Ormio P, Hakonen E, Banerjee M, Otonkoski T. EGF receptor in pancreatic β-cell mass regulation. *Biochem Soc Trans* 2008; **36**: 280–285.

259 Kuntz E, Broca C, Komurasaki T, Kaltenbacher M-C, Gross R, Pinget M *et al.* Effect of epiregulin on pancreatic β cell growth and insulin secretion. *Growth Factors* 2005; **23**: 285–293.

260 Higashiyama S, Buchanan R, Iwabuki H, Krause MA, Morimoto C, Zhang X *et al.* Membrane-anchored growth factors, the epidermal growth factor family: Beyond receptor ligands. *Cancer Science* 2008; **99**: 214–220.

261 Ceresa BP, Peterson JL. Cell and molecular biology of epidermal growth factor receptor. *Int Rev Cell Mol Biol* 2014; **313**: 145–178.

262 Kasayama S, Ohba Y, Oka T. Epidermal growth factor deficiency associated with diabetes mellitus. *Proceedings of the National Academy of Sciences of the United States of America* 1989; **86**: 7644–7648.

263 Miettinen PJ, Huotari M, Koivisto T, Ustinov J, Palgi J, Rasilainen S *et al.* Impaired migration and delayed differentiation of pancreatic islet cells in mice lacking EGF-receptors. *Development* 2000; **127**: 2617–2627.

264 Hakonen E, Ustinov J, Mathijs I, Palgi J, Bouwens L, Miettinen PJ *et al.* Epidermal growth factor (EGF)-receptor signalling is needed for murine β cell mass expansion in response to high-fat diet and pregnancy but not after pancreatic duct ligation. *Diabetologia* 2011; **54**: 1735–1743.

265 Hakonen E, Ustinov J, Palgi J, Miettinen PJ, Otonkoski T. EGFR Signaling Promotes β-Cell Proliferation and Survivin Expression during Pregnancy. *PLoS ONE* 2014; **9**: e93651.

266 Lee HY, Yea K, Kim J, Lee BD, Chae YC, Kim HS *et al.* Epidermal growth factor increases insulin secretion and lowers blood glucose in diabetic mice. *Journal of Cellular and Molecular Medicine* 2008; **12**: 1593–1604.

267 Wijesekara N, Krishnamurthy M, Bhattacharjee A, Suhail A, Sweeney G, Wheeler MB. Adiponectin-induced ERK and Akt phosphorylation protects against pancreatic β cell apoptosis and increases insulin gene expression and secretion. *Journal of Biological Chemistry* 2010; **285**: 33623–33631.

268 Kaneko K, Ueki K, Takahashi N, Hashimoto S, Okamoto M, Awazawa M *et al.* Class IA phosphatidylinositol 3-kinase in pancreatic β cells controls insulin secretion by multiple mechanisms. *Cell Metabolism* 2010; **12**: 619–632.

269 Leibiger B, Moede T, Uhles S, Barker CJ, Creveaux M, Domin J *et al.* Insulin-feedback via PI3K-C2alpha activated PKBalpha/Akt1 is required for glucose-stimulated insulin secretion. *FASEB J* 2010; **24**: 1824–1837.

270 Wicksteed B, Brissova M, Yan W, Opland DM, Plank JL, Reinert RB *et al.* Conditional gene targeting in mouse pancreatic ß-Cells: analysis of ectopic Cre transgene expression in the brain. *Diabetes* 2010; **59**: 3090–3098.

271 Ray MK, Fagan SP, Moldovan S, DeMayo FJ, Brunicardi FC. B cell-specific ablation of target gene using Cre-loxP system in transgenic mice. *J Surg Res* 1999; **84**: 199–203.

272 Suarez-Pinzon WL. Combination Therapy with Epidermal Growth Factor and Gastrin Induces Neogenesis of Human Islet -Cells from Pancreatic Duct Cells and an Increase in Functional -Cell Mass. *Journal of Clinical Endocrinology & Metabolism* 2005; **90**: 3401–3409.

273 Rooman I, Bouwens L. Combined gastrin and epidermal growth factor treatment induces islet regeneration and restores normoglycaemia in C57Bl6/J mice treated with alloxan. *Diabetologia* 2004; **47**: 259–265.

274 Scoville D, Cyphert HA, Liao L, Xu J, Reynolds A, Guo S, *et al.* MLL3 and MLL4 methyltransferases bind to the MAFA and MAFB transcription factors to regulate islet ß-cell function. *Diabetes* 2015; epub ahead of print.